NTNU
Norwegian University of
Science and Technology

Optimizing Emulsions for More Efficient Uptake of Lipophilic Compounds

Tuna Baydin

Preface and Acknowledgements

NTNU, Trondheim

August 15, 2018

Tuna Baydın

Abstract

Lipid based oral drug delivery systems provide a spectrum of formulations for the delivery of poorly water soluble compounds. When naturally occurring lipid molecules are utilized in these systems, in addition to being biodegradable and biocompatible, lipid based oral drug delivery systems may improve the solubility, absorption, bioavailability and pharmaceutical stability of the lipophilic molecules they carry. Pre-emulsified systems were shown to increase the bioavailability of lipophilic compounds, compared to bulk oil systems *in vivo*. This increase was suggested to be due to enhanced lipolysis/uptake of the emulsions compared to bulk oil carriers. In this study, we optimized emulsions regarding droplet size and oil type parameters. The aim of this optimization was to increase the bioavailability of lipophilic molecules such as nutraceuticals, biologics and pharmaceuticals.

A range of corn oil, olive oil and coconut oil emulsions, with $D[4,3]$ volume means ranging from 15.800 µm to 0.208 µm were prepared by combining different surfactant (T80) concentrations and homogenizing methods (High-speed mixing and high-pressure homogenizer Star Burst). Despite exceptions, the $D[4,3]$ volume means and the $D[3,2]$ surface means of emulsions prepared with different oil types were different when the T80 concentrations were kept constant. The long term stability of all prepared emulsions was tested upon storage at +4° C and room temperature. Starbursted (2%, 1%, 0.5% and 0.25% T80) corn oil emulsions and Vitamin D_3 – K_3 containing corn oil emulsions (2% and 1% T80) exhibited coalescing oil droplets on the surface when stored at +4°C but not at room temperature. Olive oil emulsions showed solid creaming on the surface or color change when stored at +4°C, but not at room temperature. Coconut oil emulsions crystallized and therefore, were less stable when stored at +4°C, compared to room temperature.

In vitro lipolysis of (starbursted 2%, 1%, 0.5%, 0.25% T80 and non-starbursted 2% T80) corn oil emulsions was enzyme limited with 0.4 mg/ml pancreatin. With 1.2 mg/ml pancreatin and lipase, among (starbursted 8%, 4%, 2%, 1%, 0.5%, 0.25% T80 and non-starbursted 2% T80) corn oil emulsions starbursted 2% T80 emulsion showed the highest *in vitro* lipolysis rate with 0.0708 mmol FA/min. When different oil type emulsions (starbursted 2% and 0.25% T80 and non-starbursted 2% T80) were subjected to *in vitro* lipolysis, coconut oil resulted in the highest lipolysis rate, compared to corn oil and olive oil. In the Back-Titration experiments, coconut oil required 21% and 25% more NaOH to be completely titrated at pH 10, compared to corn oil and olive oil, respectively. At pH 7, 74% of the fatty acids of coconut oil were deprotonated, whereas this number was 55% and 64% for corn oil and olive oil, respectively.

For the *in vivo* experiments, three corn oil emulsions containing vitamin D_3 and vitamin E with different droplet sizes (starbursted 2% and 0.25% T80 and non-starbursted 2% T80) and a non-pre-emulsified pure corn oil system were prepared. Vitamin D_3 – E containing starbursted corn oil emulsions were stable upon long term storage at +4°C. These systems were fed to rats in a single dose after being freshly prepared. The pharmacokinetics of vitamin D_3, 25-OH-vitamin D_3, *i.e.* the circulating form of vitamin D_3, and vitamin E were studied by collecting blood samples from rats at 7 time points (0h, 1h, 2h, 4h, 6h, 8h and 24h), isolating plasma from the blood samples and analyzing the plasma samples with UHPLC – MS/MS after solid phase extraction. Vitamin E could not be analyzed with the currently developed solid phase extraction method. Upon preliminary inspection of the vitamin D_3 concentration in rat plasma vs time, highest C_{max}, T_{max} and AUC_{24} values of vitamin D_3 were obtained with 0.25% T80 corn oil emulsion. However, ANOVA test revealed no significant difference between the C_{max} means of different feed systems. With the current experiment set up, T_{max} and C_{max} were not reached for 25-OH-vitamin D_3, suggesting that the enzymatic conversion of vitamin D_3 to 25-OH-vitamin D_3 form was the rate limiting step.

Table of Contents

Nomenclature

d	Droplet diameter
r	Droplet radius
g	Earth gravitational acceleration
γ	Interfacial tension
ρ	Density
η	Viscosity
ΔA	Change in area
ΔG	Gibbs free energy
ΔP_L	Laplace pressure

#	Number
(% wt)	Percentage by weight
(v/v)	Volume by volume
(w/w)	Weight by weight

List of Abbreviations

ANOVA	Analysis of Variance
API	Active Pharmaceutical Ingredient
CE	Collision Energies
CID	Collision Induced Dissociation
CMC	Critical Micellar Concentration
CoMed	Comparative Medicine Core Facility
CV	Cone Voltages
DAG	Diacylglycerol
DLS	Dynamic Light Scattering
ESI	Electrospray
FOTS	Forsøksdyrforvaltningens Tilsyns- og Søknadssystem
GI	Gastrointestinal
HLB	Hydrophilic-Lipophilic Balance
HPLC	High Performance Liquid Chromatography
IND	Investigational New Drug
IPA	Isopropanol
IS	Internal Standard
LALLS	Low Angle Laser Light Scattering
LBDD	Lipid-based Drug Delivery
LCFA	Long Chain Fatty Acid
LCMS	Liquid Chromatography Mass Spectrometry
LCT	Long Chain Triglyceride
LD	Laser Diffraction
LLE	Liquid/Liquid Extraction
MAG	Monoacylglycerol
MCFA	Medium Chain Fatty Acid
MCT	Medium Chain Triglyceride
MQ	Milli-Q
MS	Mass Spectrometry
MS/MS	Tandem Mass Spectrometry
No SB	Non-starbursted
O/W	Oil-in-water
O/W/O	Oil-in-water-in-oil
pKa	Logarithmic Acid Dissociation Constant
QC	Quality Control

QELS	Quasi-elastic Light Scattering
RT	Retention Time
SCFA	Short Chain Fatty Acid
SMEDDS	Self-Micro Emulsifying Drug Delivery Systems
SNEDDS	Self-Nano Emulsifying Drug Delivery Systems
SPE	Solid Phase Extraction
SRM	Single Reaction Monitoring
TAG	Triacylglycerol
TQMS	Triple Quadrupole Mass Spectrometer
T80	Polysorbate 80
UHPLC	Ultra-High Performance Liquid Chromatography
USP	United States Pharmacopeia
W/O	Water-in-oil
W/O/W	Water-in-oil-in-water
25-OH-vitamin D_3	25-hydroxyvitamin-D_3

1. Introduction

1.1. Motivation

The uptake of nutrient supplements, nutraceuticals, pharmaceuticals and biologics require optimized delivery systems to increase the bioavailability of such molecules. Lipid-based formulations for delivering lipophilic molecules may exploit naturally occurring lipid digestion and absorption mechanisms in the body (N'Goma *et al.*, 2012). Emulsions offer finely tunable and modifiable delivery systems. When compared to bulk oil, pre-emulsified oral delivery systems may improve the bioavailability of lipophilic molecules (McClements, 2018). This has been shown for omega-3 (Haug *et al.*, 2011), fat soluble vitamins (Öztürk, 2017) and bioactives (Salvia-Trujillo *et al.*, 2016). A possible reason for increased bioavailability was reported as more efficient lipolysis of the emulsified oil (Haug *et al.*, 2011). In emulsified delivery systems, the rate of digestion depends on emulsion parameters, *e.g.* droplet size and oil composition. Modifying these parameters to optimize emulsions would result in increased uptake and bioavailability of pre-emulsified systems, which are promising superior alternatives to commonly-used bulk oil systems.

1.2. Scope and Objectives of the Thesis

The main objective of this thesis is to optimize emulsions regarding droplet size and oil type parameters, in order to utilize emulsions as oral delivery vehicles of lipophilic compounds. The motivation behind this optimization is to improve the bioavailability of orally delivered lipophilic compounds such as nutraceuticals and pharmaceuticals. Systematically investigated droplet size and oil type parameters of emulsions are to be tested regarding emulsion stability, *in vitro* lipolysis and *in vivo* experiments on rats. The aim is to examine the link between emulsion parameters and digestion/uptake rate for different emulsion systems, *in vivo*. The findings from this study can be used to improve the oral delivery of lipophilic drugs with poor bioavailability as well as to enhance the absorption of food supplements, nutraceuticals and pharmaceuticals.

1.3. Thesis Layout

Chapter 1, Introduction covers several topics that were used to develop the methods and consequently the results obtained in this thesis. In Section 1.4, Lipid Based Oral Drug Delivery systems are introduced. In Section 1.5, Lipolysis is described, focusing on Physiology and *In vitro* Lipolysis. Section 1.6, reviews Emulsions majoring on their general properties, Stabilizers, Destabilizing Processes, Droplet Size and Laser Diffraction Particle Size Analysis, and Oil Types used in the emulsions. In Section 1.7, Animal Studies are introduced as a part of the drug delivery development process. Lastly, in Section 1.8, Liquid Chromatography/Mass Spectrometry and its underlying mechanisms are reviewed.

In Chapter 2, Materials and Methods, thorough descriptions of experimental protocols and required materials can be found. The chapter follows a practical sequence, starting with Preparation of the Emulsions, continuing with Droplet Size Measurements, Microscopy, *In vitro* Lipolysis and Animal Experiments. In Chapter 3, Results and Discussion, the results of each experiment are given in detail. After each presented result, the outcomes are discussed with the help of theoretical knowledge described

in Chapter 1. Finally, in Chapter 4, Conclusions and Future Perspectives, the thesis is summarized, main outcomes are presented and suggestions for future investigations are given.

1.4. Lipid Based Oral Drug Delivery

Oral delivery is the most popular route of administration (Roger *et al.*, 2011). Main reasons for that are convenience, affordability and large surface absorption area in the gastrointestinal (GI) tract. Disadvantages of oral delivery are metabolic and chemical instability, variable absorption due to poor solubility and individual variance, low permeability, and first-pass effect of the liver; all leading to poor bioavailability (Prabhu *et al.*, 2005).

Lipids offer a large variety of delivery systems for poorly water soluble small molecules, biologics and nutraceuticals (Pouton, 2006). Lipid-based drug delivery (LBDD) systems may be able to improve the solubility and absorption, as well as the bioavailability of such molecules. LBDD systems provide advantages such as controlled drug release, pharmaceutical stability such as protection from chemical degradation and interactions in the GI tract, and high and enhanced drug content, compared to other carriers (Souto *et al.*, 2007). Furthermore, these systems are biodegradable and biocompatible when they utilize naturally occurring lipid molecules (Shrestha *et al.*, 2014). The absorption of molecules from lipid based formulations depend on particle size, degree of emulsification, rate of dispersion and molecule precipitation upon dispersion (Porter *et al.*, 2001).

LBDD systems have three subtypes: (1) Emulsions, (2) Vesicular Systems and (3) Lipid Particulate Systems. Emulsions include normal emulsions, microemulsions such as self-micro or self-nano emulsifying drug delivery systems (SMEDDS/SNEDDS), and pickering emulsions. Vesicular systems include liposomes, niosomes, pharmacosomes etc. Lipid particulate systems comprise solid lipid micro/nanoparticles, liospheres and lipid drug conjugates (Kalepu *et al.*, 2013; Shrestha *et al.*, 2014).

1.5. Lipolysis

Lipolysis is the hydrolysis, *i.e.* breakdown, of triacylglycerols (TAGs, also known as triacyglycerides, fully acylated derivatives of glycerol) into glycerol and free fatty acids by the cleavage of ester bonds between the glycerol molecule and the free fatty acids. Depending on the fatty acid composition and time, intestinal lipolysis may only yield monoacylglycerols (MAGs, fatty acid monoesters of glycerol) and free fatty acids. TAG is the major form of energy storage in eukaryotic cells. When dietary fats are consumed, they are mostly in the form of TAGs (Silverthorn *et al.*, 2013). Therefore, understanding the mechanism behind digestion, absorption and distribution of fats in the human body is important in order to study the uptake of lipids.

1.5.1. Physiology

When dietary fats are consumed, lipolysis starts in the stomach. Even though humans have lingual lipases which are secreted along with saliva by serous lingual glands, they have little functional importance since they make little to no contribution to lipolysis (Feher, 2017). When fats reach the stomach, they are subjected to gastric lipases which are secreted by gastric mucosa. Gastric lipases break down TAGs into

diacylglycerols (DAGs, fatty acid diesters of glycerol) and free fatty acids (Phan *et al.*, 2001). Lingual and gastric lipases are called the acidic lipases since they exhibit highest enzymatic activity in acidic medium (pH approximately 3 to 6) and they do not require bile salts or colipase for optimal enzymatic activity (Carey *et al.*, 1983). 10 – 30% of total lipolysis in the GI tract takes place in the stomach (Hamosh *et al.*, 1973). Furthermore, muscle contractions of the stomach provide shear forces that contribute to emulsification (Carey *et al.*, 1983). Following the stomach, ingested lipids which are in the form of TAGs, DAGs and free fatty acids reach the duodenum, the first segment of the small intestine. In the duodenum, mechanical contractions result in size reduction of the emulsion droplets, leading to increased surface area (Senior, 1964). Surface area is relevant since pancreatic lipase can only work on the surface of a fat droplet. Pancreatic lipase hydrolyses TAG into DAG and a free fatty acid; subsequently a DAG is broken down into a MAG and a free fatty acid. Gastric lipolysis promotes immediate pancreatic lipase activity in the small intestine. Pancreatic lipase is classified as an alkaline lipase. However, it is active at neutral pH conditions. It requires bile salts or colipase for optimal enzymatic activity (Gargouri *et al.*, 1986; Liao *et al.*, 1984). After bile enters the duodenum, it mixes with the free fatty acids and MAGs. Bile salts are important for further emulsification and pancreatic lipase activity. Bile is synthesized from cholesterol in the liver and secreted from the gall bladder. Bile contains bile salts, which are amphipathic molecules, *i.e.* they contain both hydrophilic and hydrophobic regions, that act as the emulsifier of lipids (Silverthorn *et al.*, 2013).
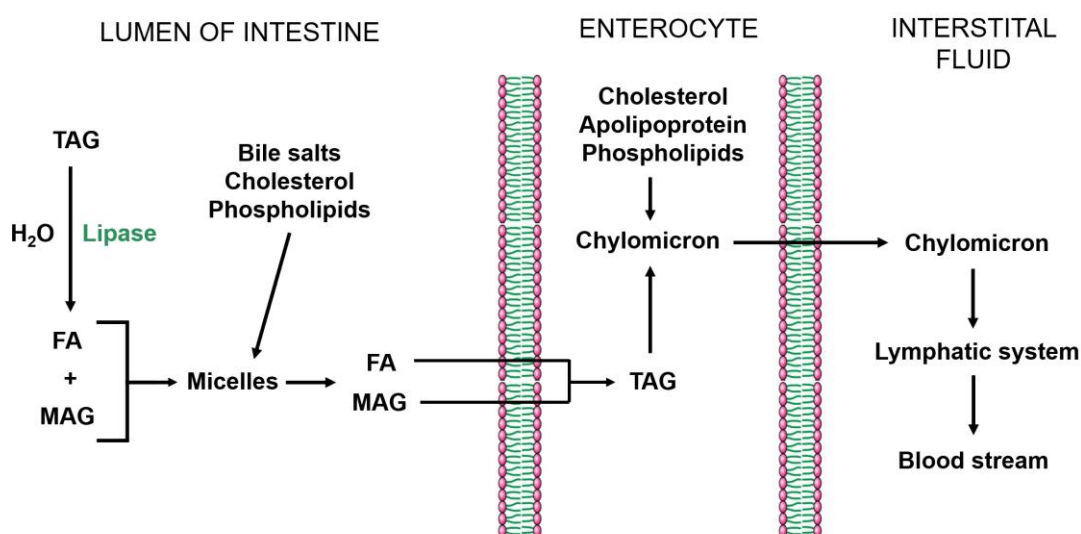
Figure 1: Lipolysis and transportation of lipid molecules from intestinal lumen to blood stream. Modified from Berg *et al.* (2012).

Bile salts and other surface active components, *e.g.* phospholipids, together with MAGs and free fatty acids form micelles in the intestinal lumen. Micelle formation takes place in aqueous bile salt solution above critical micellar concentration (CMC) (Hofmann, 1963). In micelles, the ester bonds of lipids are facing outside and therefore are more susceptible to cleavage by lipases (Berg *et al.*, 2012). The final digestive products of lipids, MAGs and free fatty acids, are carried in micelles towards the enterocytes (*i.e.* intestinal epithelial cells). Intestinal wall is covered with small microvilli structures which increase the total surface area of the small intestine, providing increased absorptive surface for the uptake of molecules (Caspary, 1992). Due to their small size, micelles can diffuse to the narrow areas between the microvilli through the mucosa. They bring the MAGs and free fatty acids in close proximity to the enterocyte wall,

these molecules move out of micelles, diffuse through the mucosal lining of the small intestine and enter the enterocytes. After entering the enterocytes, MAGs and fatty acids go into the endoplasmic reticulum where they reassemble and regenerate TAG molecules (Silverthorn *et al.*, 2013; Tso *et al.*, 1986). TAG is then packaged into a lipoprotein-transport particle called chylomicron whose size ranges from 100 – 500 nm. TAG forms the core of a chylomicron and the outer shell is composed of cholesterol, phospholipids and the protein component, *i.e.* apolipoproteins (Schaefer *et al.*, 1978). Chylomicrons provide TAGs a water-soluble coat which aids their transport out of enterocytes through exocytosis. When chylomicrons leave the enterocyte, they enter the lacteals, *i.e.* lymphatic capillaries. The lymphatic system carries chylomicrons to the thoracic duct where they are introduced into the blood stream. With the help of the blood stream, chylomicrons travel throughout the body and distribute TAGs to various tissues (Silverthorn *et al.*, 2013) (Figure 1).

1.5.2. *In vitro* Lipolysis

Testing new drug delivery systems on humans in clinical trials is the ideal method since it would provide the most relevant results for the systems that are aimed to be used in humans. However, preclinical development is required to select the optimal system to bring to clinical trials since it is difficult and costly to test an array of formulations on human beings. *In vivo* tests on animal models are widely used in this context (Section 1.7). Nevertheless, *in vivo* experiments are also expensive and time consuming (Boisen *et al.*, 1991). These issues have led to the development of *in vitro* models which mimic human conditions and enable the testing of several formulations with cost and time flexibility (Hur *et al.*, 2011).

In vitro lipolysis is an experimental setup that simulates the small intestine conditions in the human body in which digestion of the lipid-based formulations or LBDD systems takes place (Larsen *et al.*, 2011). The GI tract is a complex environment that harbors several physiochemical and physiological events (Hur *et al.*, 2011). It should be noted that the actual *in vivo* conditions cannot be completely simulated in *in vitro* systems (Boisen *et al.*, 1991). However, the main purpose is to optimize the *in vitro* lipolysis system so that it would reflect the human small intestine as much as possible. Obtaining physiologically representative experimental conditions is crucial for the *in vitro* lipolysis experiments.

There are several experimental components in *in vitro* lipolysis. One of the components is the lipase source which enzymatically degrades the lipid-based systems in the lipolysis medium. Porcine pancreatin is commonly used as lipase source and it also contains a mixture of pancreatic enzymes such as pancreatic triacylglyceride lipase, phospholipase A_2, colipase and cholesterol esterase (Larsen *et al.*, 2011). The enzyme activity of the lipase source can be expressed in TBU (tributyrin) or USP (United States Pharmacopeia) units and different enzymatic activities were used in various previous studies (Sassene *et al.*, 2014).

The lipolysis media should also contain bile acids and phospholipids which naturally exist in the intestinal fluid. Calcium is another important component of the lipolysis medium since it activates pancreatic lipase (Kimura *et al.*, 1982). Furthermore, both calcium and bile acids facilitate the removal of free fatty acids from the lipolysis medium. This is important as free fatty acids may inhibit lipase activity by accumulating on the emulsion droplet and blocking the access of lipases to the interfacial region of the droplet (McClements *et al.*, 2010). The pH and the temperature of the *in vitro* lipolysis are conditions to be considered. In a review, the digestion temperature was reported as 37°C for all *in vitro* digestion studies (Hur *et al.*, 2011). The pH varies among different parts of the GI tract, as well as for fed or fasted state.

Therefore, the pH of the *in vitro* lipolysis medium was suggested to be between 6.5 to 8.5 (Larsen *et al.*, 2011).

The detection of the lipolysis activity can be obtained by monitoring the decrease in pH upon the release of free fatty acids from lipids. This technique was suggested as a standardized pH-stat method (Li *et al.*, 2011). The principle behind the pH-stat method lies in the titration of alkali, *i.e.* NaOH, into the lipolysis medium in order to keep the initial pH stable. 1 mol of titrated NaOH corresponds to 1 mol of fatty acids liberated from the triglycerides in the lipid based formulation. The titration pattern can then be analyzed to reveal the lipolysis rate for different lipid-based systems being tested (McClements *et al.*, 2010). Through a series of publications, standardized component concentrations in the lipolysis medium and physical conditions for the *in vitro* lipolysis experiment were proposed (Sassene *et al.*, 2014).

During lipolysis, the fatty acids which are hydrolyzed by lipase have to be ionized in order to be titrated with sodium hydroxide (NaOH) (Larsen *et al.*, 2011). In order to determine the total amount of generated unionized free fatty acids as a result of the lipolysis, a "Back-Titration" method was suggested (Beisson *et al.*, 2001). Back-Titration is performed at the end of an *in vitro* lipolysis experiment by increasing the pH (up to approximately 9) by the rapid addition of NaOH solution (Fernandez *et al.*, 2007). The theory behind the Back-Titration method resides in the probability of released fatty acids being only partially ionized at the lipolysis pH (approximately 7) due to their pKa (Logarithmic Acid Dissociation Constant) values. Additional NaOH added in Back-Titration facilitates the determination of the unionized fatty acid quantity. This amount must also be compared to the Back-Titration of a control solution without any fatty acids, as bile salts etc. may also have a buffer capacity in this pH area. Calculating the quantity of additional NaOH that is necessary to increase the pH in the Back-Titration protocol**,** provides the estimation of the total amount of hydrolyzed lipid-based formulation in the *in vitro* lipolysis experiment (Williams *et al.*, 2012). This estimation can be performed using following Eq. (1) (Hauss, 2007):

$$Extent\ of\ digestion\ (\%)$$
$$= \frac{ionized\ fatty\ acid + unionized\ fatty\ acid}{theoretical\ maximum\ fatty\ acid\ in\ the\ lipid\text{-}based\ formulation} \times 100 \tag{1}$$

Back-Titration method is important when comparing the lipolysis extent of different lipid-based formulations comprising oils, as different oils types contains different fatty acids with variable pKa values.

1.6. Emulsions

An emulsion is defined as a mixture of two immiscible liquids, usually oil and water, in which one of the liquids is dispersed in the other liquid in the form of spherical droplets. In an emulsion system, the dispersed phase makes up the droplets and the continuous phase consists of the liquid that surrounds the droplets (Figure 2). Emulsions are classified depending on which liquid is dispersed throughout the continuous phase. If a system contains oil droplets dispersed in an aqueous phase it is called an oil-in-water (O/W) emulsion. Similarly, if water droplets are dispersed in an oil phase it is called a water-in-oil (W/O) emulsion. In addition, it is possible to generate double emulsions such as water-in-oil-in-water (W/O/W) or oil-in-water-in-oil (O/W/O) emulsions. For instance in a W/O/W system, water droplets are dispersed in larger oil droplets which are dispersed throughout an aqueous phase (McClements, 2015).
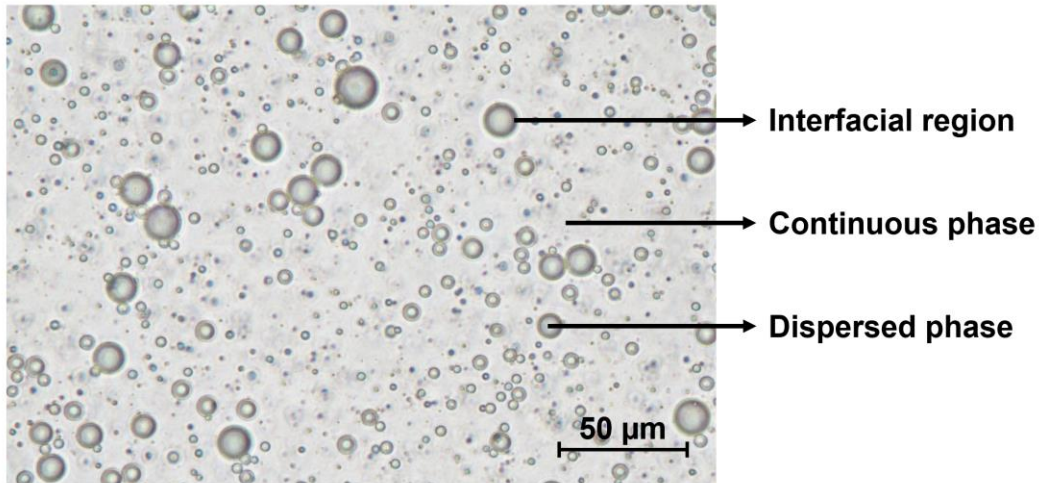
Figure 2: Coconut oil emulsion, stabilized by polysorbate 80. The photograph was taken with Nikon Eclipse TS100 at 40X magnification.

Emulsions are generated through a process called homogenization, in which two immiscible liquids are mixed and converted into an emulsion. Homogenization is achieved through instruments called homogenizers which apply intense mechanical agitation to the liquids (Loncin *et al.*, 1979). Homogenization can be divided into two categories: primary and secondary homogenization. Primary homogenization is the generation of an emulsion, directly from two immiscible liquids. Secondary homogenization is the reduction of the droplet size of an existing emulsion. There are several homogenization methods such as high-speed mixer, colloidal mill, high-pressure homogenizer, ultrasonic jet homogenizer, microfluidization and membrane processing (McClements, 2015). High-speed mixer and high-pressure homogenizer are going to be introduced further in Section 2.1, as they have been used in this research.

Interfacial tension (γ) is the constant of proportionality which is determined by the degree of imbalance of the molecular interactions between two immiscible liquids, due to cohesive forces between the molecules within the fluids (McClements, 2015). The interfacial tension seeks to minimize the interfacial area between an oil droplet and the aqueous continuous phase (Eq. (3)). This results in the spherical shape an oil droplet takes in order to achieve the minimum surface area.

The Laplace pressure (ΔP_L) is the interfacial force which is responsible for keeping a droplet in a spherical shape. ΔP_L generates a larger pressure inside an oil droplet compared to the continuous phase (McClements, 2015). The Δ in ΔP_L signifies the pressure difference that results from the interfacial tension of the interface between the dispersed and the continuous phases. ΔP_L is calculated with the following equation:

$$\Delta P_L = \frac{4\,\gamma}{d} \tag{2}$$

In Eq. (2), γ is the interfacial tension between oil and water phases and d is the diameter of the droplet (McClements, 2015). Therefore, as the droplet size decreases, ΔP_L increases. As an example, this formula can be applied to two emulsions with drastically different droplet size diameters; 1 mm and 1 μm.

The ΔP_L of an O/W emulsion with an interfacial tension (γ) of 10 mN/m and diameter of 1 mm is calculated from Eq. (2) as 160 Pa, *i.e.* 0.0016 atm. In this example, the ΔP_L is insignificant compared to standard atmospheric pressure, *i.e.* 1 atm. Whereas, the ΔP_L of an O/W emulsion with an interfacial tension (γ) of 10 mN/m and diameter of 1 μm is calculated as 160000 Pa, *i.e.* 1.578 atm. Therefore, when the droplet diameter reaches the micrometer scale, the ΔP_L starts becoming comparable to atmospheric pressure. In order to disrupt a droplet during homogenization process, the external stress applied by the homogenizer must be higher than the ΔP_L (Pieter Walstra, 1983). High ΔP_L causes difficulty to generate smaller droplet size emulsions, where the diameter is in the micrometer scale and below.

As can be seen in Eq. (2), ΔP_L is directly connected to interfacial tension. Thus, by reducing the interfacial tension, formation of small droplet sized emulsions becomes easier. The interfacial tension is reduced by the addition of surfactants, which is further described in Subsection 1.6.1.

Thermodynamic and kinetic stability of emulsions represent different things. The free energy change corresponding to the formation of an emulsion determines whether the emulsion is thermodynamically stable or unstable. The free energy change corresponding to the creation of an emulsion is given in the following equation (Rajagopalan *et al.*, 1997):

$$\Delta G_{formation} = \gamma \cdot \Delta A \tag{3}$$

In Eq. (3), γ is the interfacial tension, ΔA is the change in contact area between oil and water phases, and ΔG is the Gibbs free energy. During the formation of an emulsion ΔA increases and thus, homogenization increases ΔG. Therefore, creation of a new emulsion is thermodynamically unfavorable. This means that energy input is required to form an emulsion and kinetic stabilization is necessary to avoid destabilization or rapid coalescence (Subsection 1.6.2). There are systems where the entropy term dominates the interfacial free energy term where γ is very small. These systems are called microemulsions and they are thermodynamically stable (McClements, 2015). SMEDDS and SNEDDS are examples of these systems.

Emulsions can be classified according to their sizes: nanoemulsions, microemulsions and macroemulsions (Koroleva *et al.*, 2012). When the droplet size is between 20 – 200 nm, the emulsion is referred as a nanoemulsion. Microemulsions have a droplet size smaller than 100 nm. Macroemulsions are larger than 200 nm. However, it is important to note that microemulsions are fundamentally different from normal emulsions since microemulsions form spontaneously and are thermodynamically stable (McClements, 2015).

The kinetic stability of an emulsion informs about the rate at which the properties of an emulsion change throughout time. These properties include the dynamics and interactions between the droplets of an emulsion. Kinetically stable emulsions are able to prevent droplets from merging since their interfacial region resists rupture (McClements, 2015).

1.6.1. Stabilizers

Emulsions are thermodynamically unstable systems, *i.e.* $\Delta G > 0$ for emulsion formation. Mixing two immiscible liquids leads to phase separation since droplets tend to merge with neighboring droplets when they collide. As seen in Eq. (3), emulsions are thermodynamically unstable and the merging of droplets is

thermodynamically favorable. Including stabilizers in an emulsion system enables one to obtain kinetically stable emulsions since surfactants reduce γ (McClements, 2015). Reduced γ causes ΔG as well as ΔP_L to decrease, and these changes create advantageous conditions for emulsions to form. Stabilizers may increase kinetic stability through other means, such as electrostatic and steric stabilization and increased viscosity or gelling of the continuous phase. However, reduced γ does not protect against flocculation or creaming (Subsection 1.6.2).

Stabilizers contain the subgroup of emulsifiers which stabilize emulsions. There are many emulsifiers available for emulsion preparation such as small molecule surfactants, phospholipids, polysaccharides and proteins (Mun *et al.*, 2007). Surfactants are a subgroup of emulsifiers. They are small amphiphilic molecules which consist of a hydrophilic head and a lipophilic tail. Surfactants adsorb at interfacial regions and coat the oil droplets. They can form micelles above CMC (Holmberg *et al.*, 2003). Stabilizers are classified according to the electrostatic properties of the polar moiety; cationic, anionic, non-ionic or zwitterionic (Kim *et al.*, 2017). Steric and electrostatic stabilization of emulsion droplets can be achieved by using appropriate surfactants. This is important when orally delivered emulsions are being designed since they would go through the GI tract which exhibits different pH levels and salt concentrations in different compartments. Electrostatically stabilized droplets may destabilize in low pH and high salt concentrations. However, if an emulsion is sterically stabilized by a non-ionic surfactant, it would not be affected by pH changes and ionic strength in the GI tract (Hunter, 1986).

The solubility properties of an emulsifier determine the continuous phase. This principle is known as Bancroft's rule. If the emulsifier is water-soluble, homogenization yields an O/W emulsion, whereas if the emulsifier is lipid-soluble, homogenization yields a W/O emulsion (Holmberg *et al.*, 2003). To further embody this phenomenon, hydrophilic-lipophilic balance (HLB) was introduced (Griffin *et al.*, 1968). Surfactants with HLB values smaller than 6 are used in W/O emulsions and the others with an HLB value larger than 10 are used in O/W emulsions. This principle should be taken into account when the choice of surfactant is being made in an emulsion system.

1.6.2. Destabilizing Processes

Emulsions are thermodynamically unstable systems. Due to the immiscible nature of oil and water, kinetically stable emulsions destabilize over time. The destabilization process may take from days to years. There are several destabilization processes (Figure 3). Kinetically unstable emulsions also destabilize over time, although almost immediately.

One type is gravitational separation which occurs due to liquids with different density in an emulsion being subjected to gravitational force. In an O/W emulsion, oil droplets constitute the dispersed phase. Generally edible oils in liquid state have a lower density than water (McClements *et al.*, 1998). In such cases, oil droplets have the tendency to move upwards. This process is called creaming. Conversely, in a W/O emulsion the water droplets have the tendency to move downwards due to their higher density compared to the continuous oil phase. This process is called sedimentation. The creaming rate in an emulsion can be calculated with Stoke's law in the following equation (McClements, 2015):

$$v_{stokes} = \frac{2 \cdot g \cdot r^2 \left(\rho_{dispersed} - \rho_{continuous} \right)}{9 \cdot \eta_{continuous}} \tag{4}$$

In Eq. (4), v_{stokes} is the rate of creaming, g is the gravitational acceleration, ρ is the density, r is the droplet radius and η is the viscosity of the continuous phase.

In an emulsion, two droplets can aggregate without merging together. If weak forces are in charge, this aggregation is called flocculation. Flocculation is reversible when temporary shaking is applied. If strong forces are in charge, it is called coagulation which is irreversible. The size and structure of droplet aggregates have a large impact on the creaming rate of an emulsion (Bremer, 1992). When droplets flocculate, their interfacial membranes stay intact and the droplets conserve their individual integrities (Dickinson, 2009). However, the flocculated droplet aggregates act as larger droplets in regards to creaming or sedimentation, increasing the rate of gravitation based destabilization. In addition, larger droplets are observed in flocculated emulsions in the droplet size measurements. Coalescence is the process where two or more droplets merge to form a larger single droplet. Coalescence is irreversible. Through coalescence, an emulsion (unless it is a microemulsion) approximates its most thermodynamically stable state since its total surface area and its ΔG decreases ($\Delta G < 0$ for coalescence). Coalescence yields an increase in the average droplet size. Excessive coalescence may lead to phase separation of emulsions which yields two separate layers of immiscible liquids on top of each other (McClements, 2015).
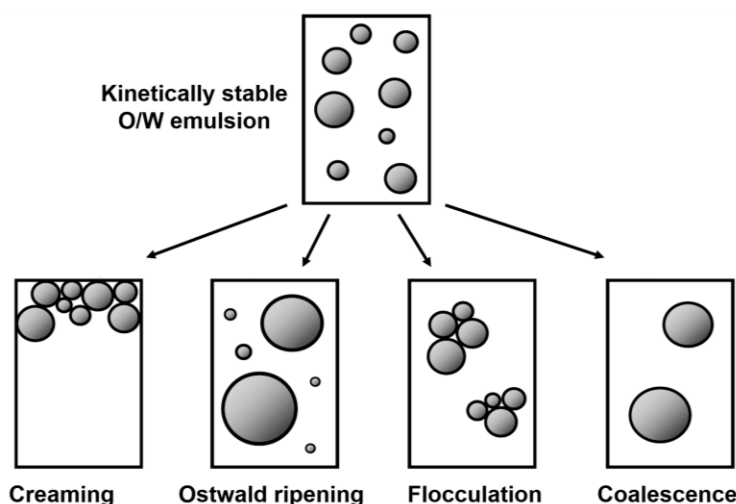
Figure 3: Possible destabilization fates of a kinetically stable O/W emulsion. Modified from McClements (2015).

Ostwald ripening is a type of destabilization which occurs due to increased solubility of the dispersed phase in the continuous phase. When the oil droplets get smaller, their solubility increases. In this process, a mass transport of dispersed phase takes place through the intervening continuous phase. Large droplets grow, whereas small droplets shrink. This causes an increase in the average droplet size over time (Taylor, 1998). Ostwald ripening is more often observed in emulsions whose oil phase is composed of medium chain triglycerides (MCTs), compared to long chain triglycerides (LCTs), since MCTs have higher water

solubility compared to LCTs (Subsection 1.6.4). Moreover, polydisperse emulsions are at higher risk for Ostwald ripening compared to monodisperse emulsions.

1.6.3. Droplet Size and Laser Diffraction Particle Size Analysis

Droplet size influences the stability and absorption of emulsions. Emulsions whose droplets have the same droplet size are called monodisperse, whereas emulsions whose droplet sizes show variability are called polydisperse (McClements, 2015). Since droplet size has an impact on stability and lipolysis rate, it is important to determine the droplet size distribution of an emulsion. There are several techniques to measure droplet size such as laser light scattering, electrozone counter, optical counter, time-of-flight counter, ultrasonic measurements, nuclear magnetic resonance (NMR), electron microscopy etc. (Coupland *et al.*, 2001; CPS Instruments, 2015).

Laser diffraction (LD, also known as low angle laser light scattering or LALLS) is one of the methods used for determining the droplet size of an emulsion. This technique can be used to measure the particle size ranging from 100 nm to 1 mm (Malvern Instruments, 2012). The theory behind this technique is measuring scattered light as a laser beam passes through a dispersed sample. A diffraction system measures the intensity of the scattered light as a function of scattering angle and generates a diffraction pattern. The diffraction pattern depends on the size of the particle that is exposed to the light source. In the LD method, the light source is a laser. Large particles intensely scatter light at smaller angles, whereas small particles intensely scatter light at wider angles (Figure 4).
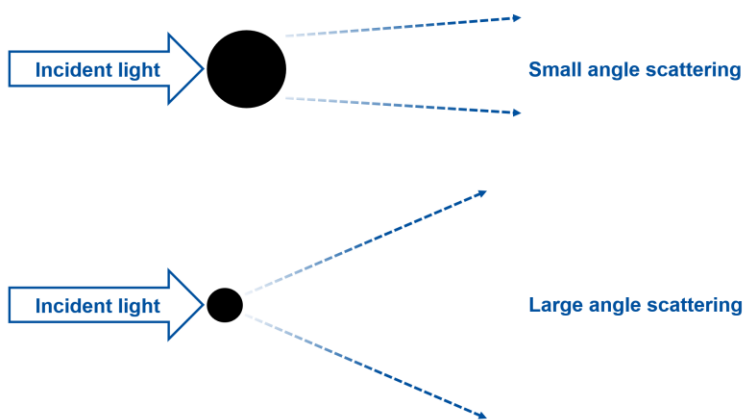
Figure 4: Light scattering angles for a large and small particle. Modified from Malvern Instruments (2012).

In a LD machine, the laser beams (470 nm blue light and 633 nm red light) hit the particles, *e.g.* emulsion droplets. Upon this hit, the laser light is scattered, and the laser light is detected on different detectors, *e.g.* focal plane, side scatter and back scatter detectors, at different angles. The minimum particle size that can be measured depends on the wavelength of the light being used. Using more than one wavelength of light allows for detection in a wider size range and provides more precise results (Malvern Instruments, 2012; Rawle, 2003).

Dynamic light scattering (DLS, also known as quasi-elastic light scattering or QELS) is another technique used for measuring particle size. It relies on the theory of measuring Brownian motion of particles as a

function of time. This method also uses a laser beam which is scattered by particles in a suspension. The scattering intensity is rapidly fluctuated by the diffusion of particles (CPS Instruments, 2015). With DLS, very small particle sizes can be measured, from 1 nm to 10 µm (Malvern Instruments, 2012).

There are several ways to define the average droplet size of an emulsion (or any particle). Commonly used parameters are mean values such as *D[4,3]* and *D[3,2]*, and median values such as Dv10, Dv50 and Dv90 (Horiba Instruments, 2017). The parameters measured and analyzed in this work are going to be introduced in further detail. Mean is the measure of the central tendency in a distribution. When this concept is applied to particle size distributions mean points out the mean particle diameter, shown as $\bar{x}$ (McClements, 2015). Volume mean, *i.e. D[4,3]*, volume moment mean, mass moment mean, *Xvm* or Brouckere mean diameter, reflects the size of the particles that make up the bulk of the sample volume. It is sensitive to the presence of large particles in the size distribution (Malvern Instruments, 2012). *D[4,3]* can be calculated from the following equation (Ng *et al.*, 2014):

$$D[4,3] = \frac{\sum D_i^4 \cdot n_i}{\sum D_i^3 \cdot n_i} \qquad (5)$$

In Eq. (5), D_i is the diameter of a particle and n_i is the number of particles. For *D[4,3]* parameter, the volume of a particle is the significant input.

Surface mean, also known as *D[3,2]*, surface area moment mean, *Xsv* or Sauter mean diameter, is related to the average surface area of droplets that are exposed to the continuous phase per unit volume of emulsion. In other words, it is the diameter of a droplet having the same volume/surface area ratio as the whole emulsion. *D[3,2]* is sensitive to the presence of finer particles in the size distribution (Malvern Instruments, 2012). *D[3,2]* can be calculated from the following equation (Horiba Instruments, 2017):

$$D[3,2] = \frac{\sum D_i^3 \cdot n_i}{\sum D_i^2 \cdot n_i} \qquad (6)$$

In Eq. (6), D_i is the diameter of a particle and n_i is the number of particles. For *D[3,2]* parameter, the surface area of a particle is the main concern. This becomes relevant where surface area of a particle of concern, *e.g.* the droplet surface area of an emulsion is critical for lipolysis.

If the droplet size measurement of an emulsion gives similar *D[4,3]* and *D[3,2]* values, the emulsion exhibits a rather monodisperse structure. On the contrary, if *D[4,3]* and *D[3,2]* values are dissimilar, then the emulsion is rather polydisperse. The reason for this principle is the fact that *D[4,3]* is sensitive to the presence of larger particles, whereas *D[3,2]* is sensitive to the presence of smaller particles (McClements, 2015).

Median values depict the value in which a percentage of the population lies below a certain diameter. Dv10, Dv50 and Dv90 are median values where 10%, 50% and 90% of the particles reside below, respectively (Malvern Instruments, 2012). Dv values refer to volume median. However, there are other

medians *e.g.* Dn50 which is used for number distributions and Ds50 which is used for surface distributions (Horiba Instruments, 2017).

1.6.4. Oil Types

Different types of oils can be used to compose the oil phase of an emulsion. When edible oils are used in this process, they yield non-toxic emulsions which are suitable for degradation in the GI tract. Edible oils are mostly in the form of TAGs. A TAG molecule consists of a glycerol backbone and three fatty acids bound to the backbone through ester linkages. Different fatty acids contain different amounts of carbon atoms. Fatty acids can be classified depending on the carbon atoms they contain in the chain; short chain fatty acids (SCFAs) have four to 10 carbons, medium chain fatty acids (MCFAs) have 12 to 14 carbons, long chain fatty acids (LCFAs) have 16 to 18 carbons and very long chain fatty acids contain 20 or more carbons (Valenzuela *et al.*, 2013). Fatty acids are named depending on the carbon atoms they contain in the chain, *e.g.* a fatty acid with 16 carbons is depicted as C_{16}. A fatty acid molecule is defined as saturated if it does not contain any double bonds between carbon atoms. An unsaturated fatty acid contains one or more double bonds. Monounsaturated fatty acids contain only one carbon-carbon double bond, whereas polyunsaturated fatty acids contain two or more double bonds. Double bonds are symbolized by Δ and their amount is depicted with a colon after the carbon number in the subscript *e.g.* $C_{16:2}$ has 16 carbons and two double bonds. Identification of the first carbon atom is achieved by naming the carbon on the methyl (CH_3) group as "ω1" or "n-1" (Salway, 2016). The consequent carbons are counted from left to right, as shown in Figure 5.
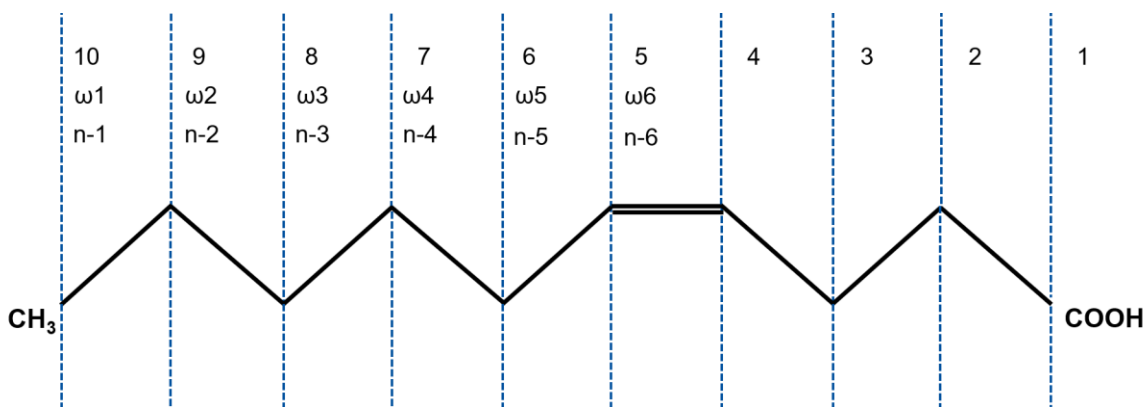
Figure 5: Nomenclature scheme for an example fatty acid: $C_{10:1}$ unsaturated fatty acid cis-Δ^4-decanoic acid. Modified from Salway (2016).

The location of the double bond is shown in the superscript of Δ, where the position is counted from the carboxyl group (-COOH). The isomeric form of the double bond is indicated as cis- or -trans. Therefore, the fatty acid in Figure 5 is called $C_{10:1}$ unsaturated fatty acid cis-Δ^4-decanoic acid and it is an n-6 (or ω6) unsaturated fatty acid.

Vegetable oils are composed of a spectrum of different fatty acids. Fatty acid compositions of corn oil, olive oil and coconut oil are presented in Table 1. Corn oil, also known as maize oil, is obtained from corn seeds (kernels) of corn (*Zea mays*) which contains 3 – 5% oil (Gunstone, 2011). Unsaturated fatty acids constitute 84% of corn oil whereas saturated fatty acids make 16% of total weight. Virgin olive oil is

extracted from the fruits of the olive tree (*Olea europaea*) by mechanical or physical methods. Olive oil contains 12% saturated fatty acids and 86% unsaturated fatty acids (Gunstone, 1996). It also comprises 2% of other compounds. These include vitamin E (tocopherol α, β and γ), hydrocarbons, pigments, sterols, tritepene dialcohols, fatty alcohols, waxes and diterpene alcohols, polyphenols, volatile and aroma compounds, phospholipids and metals (Gunstone, 2011). Coconut oil is a lauric oil meaning it has high levels of lauric acid. It is obtained from the fruit of coconut palm tree (*Cocos nucifera*). Coconut oil contains 90% saturated fatty acids and 9% unsaturated fatty acids. It also includes 1% of other compounds such as tocopherols, tocotrienols, sterols, hydrocarbons and lactones.

Melting temperature of an oil is important when they constitute the lipid phase of an emulsion. This is because the melting point affects the stability of an emulsion especially when the storage conditions are determined. Oils have characteristic melting points due to the fact that they have different fatty acid compositions which have individual melting points. SCFAs have lower melting points, whereas LCFAs have higher melting points. In addition, unsaturated fatty acids have lower melting points compared to saturated fatty acids when they have similar chain length (Chayanoot *et al.*, 2010). As shown in Table 1, corn oil has a melting point of -11°C to -8°C. Therefore, it is liquid at both room temperature and +4°C, *i.e.* in the fridge. Coconut oil melts at 23°C to 26°C and is therefore solid at room temperature as well as at +4° C. Olive oil has a melting temperature of -6°C and therefore it is liquid at room temperature and it is partially crystallized at +4°C.

Table 1: Fatty acid compositions (% wt) and melting points of corn oil, olive oil and coconut oil. Derived from Gunstone (1996).

Fatty acid	Corn oil		Olive oil		Coconut oil	
Caprylic (8:0)					8%	
Decanoic (10:0)					7%	
Lauric (12:0)					48%	
Myristic (14:0)					16%	90% saturated
Palmitic (16:0)	13%		10%		9%	
Stearic (18:0)	3%	16% saturated	2%	12% saturated	2%	
Oleic (18:1 n-9)	31%		78%		7%	
Linoleic (18:2 n-6)	52%	84% unsaturated	7%	86% unsaturated	2%	9% unsaturated
Linolenic (18:3 n-3)	1%		1%			
Other			2%		1%	
Melting point	-11°C – -8°C		-6°C		23°C – 26°C	

The pKa value represents the ionic environment of the solution where 50% of hydrogen atoms are removed from the carboxyl groups by the existing hydroxide ions in the solution (J. Kanicky *et al.*, 2000). The pKa of the fatty acids is important since it determines to which extent the free fatty acids would be ionized during lipolysis. Generally, shorter fatty acids have lower pKa values, whereas longer fatty acids have higher pKa values. Furthermore, a higher degree of unsaturation results in smaller pKa values. For

instance, for the same carbon number of 18, saturated fatty acids have a pKa of 10.15. Whereas, monounsaturated fatty acids have a pKa of approximately 9.90 and polyunsaturated fatty acids have a pKa of approximately 8.8 (J. R. Kanicky *et al.*, 2002).

TAGs can be classified as MCT and LCT. MCTs are TAGs which contain MCFAs with 12 to 14 carbon atoms. In MCTs, 2 to 3 of the attached fatty acids have medium chain length (St-Onge *et al.*, 2008). LCTs contain LCFAs with 16 to 18 carbon atoms (Jiang *et al.*, 1993).

Water solubility is another parameter which has an impact on emulsion stability. As a rule, shorter fatty acids are more water soluble when compared to longer chain fatty acids. MAGs have two free hydroxyl groups and thus, they are partially soluble in water. DAGs have one free hydroxyl group and they are less water soluble than MAGs. TAGs lack free hydroxyl groups since they contain three fatty acids and they are not water soluble. Also, TAGs are highly soluble in non-polar solvents (Valenzuela *et al.*, 2013). Water solubility is also studied in different triglycerides. MCTs have higher water solubility when compared to LCTs. LCTs are insoluble in water since they are bigger than MCTs (Jiang *et al.*, 1993). This dissimilarity in solubility results in different metabolization fates for MCTs and LCTs (Akoh, 2005).

In the small intestine, MCTs are rapidly hydrolyzed by pancreatic lipases and consequently they release MCFAs. Moreover, MCFAs may not need bile salts for emulsification since they may be water soluble. MCFAs passively diffuse from enterocytes into the portal system and therefore do not require energy for absorption. Consequently, MCFAs bypass the lymph system and enter the portal vein. Through the portal vein, they rapidly travel to the liver where they are oxidized for energy. Thus, MCFAs are quickly eliminated from the circulatory system (Akoh, 2005). Unlike MCFAs, LCFAs require bile salts for emulsification. Both MCFAs and LCFAs are surface active and can adsorb at interfaces, helping emulsification to some extent.

LCTs are subjected to 5 – 8 times slower hydrolysis by lingual lipase, compared to MCTs (Liao *et al.*, 1984). With gastric lipase, LCT emulsions are hydrolyzed 3.2 times slower than MCT emulsions (Borel *et al.*, 1994). Similarly, pancreatic lipase activity is slower with LCT, compared to MCT (Hamosh, 1987). Generally, MCTs are hydrolyzed more completely than LCTs. When in enterocytes, LCTs binds to phospholipids and proteins. Then, they are integrated into chylomicrons which are absorbed by the lymphatic system. Thus, LCTs followed the classical physiological pathway described in Subsection 1.5.1. Moreover, LCTs take twice as much time than MCTs to be cleared from the circulatory system (Akoh, 2005; You *et al.*, 2008). Theoretically, MCTs would generate smaller sized micelles, compared to LCTs. This would result in increased uptake and rapid transport of lipophilic components when being carried in lipid-based delivery systems that contains MCTs. However, smaller micelles would have smaller volumes which can carry a limited amount of transported components such as APIs and vitamins. In conclusion, triglyceride type, and therefore the oil type used in an emulsion, has an impact on the preferred distribution route of a molecule which is delivered to the body.

When a drug is being delivered in a lipid-based delivery system such as emulsions, it is important to consider bioavailability. When a drug reaches to the liver, hepatic first-pass metabolism reduces systemic bioavailability (Trevaskis *et al.*, 2008). Therefore, lymphatic transport was suggested to be more efficient when delivering APIs (Sun *et al.*, 2011).

1.7. Animal Studies

Invention of a new therapeutic and bringing it to the market is a complex and lengthy process. Drug development consists of several steps in order to reach patients. Development of a drug delivery system follows a similar path in which many requirements need to be met. General process of drug development can be summarized as the following four stages: (1) drug discovery; (2) preclinical development; (3) clinical development and (4) manufacturing (Lee *et al.*, 1999). Each stage has its own purpose and needs to be successful in order to continue with the subsequent stage (Figure 6).
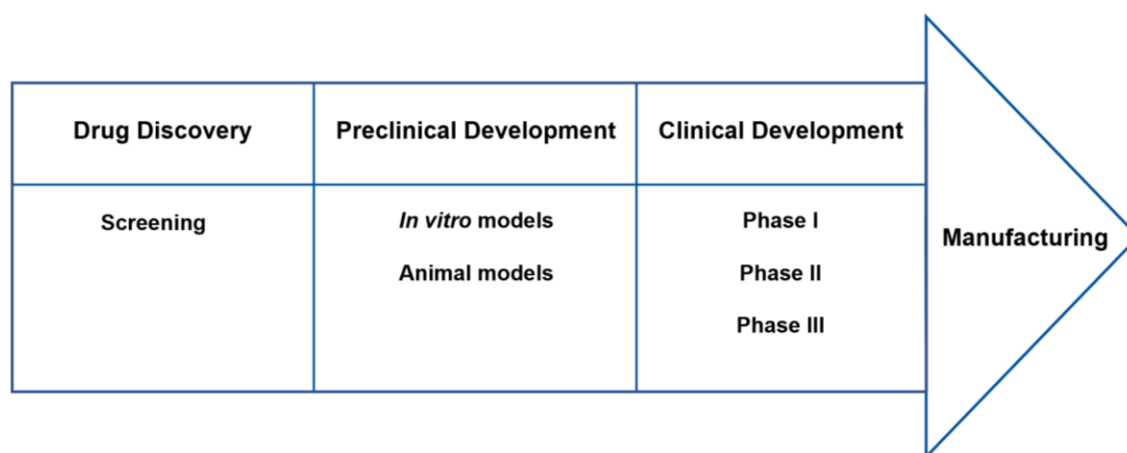
Figure 6: Drug development and its stages shown in a chronological manner.

The drug development process starts with drug discovery where several candidates are screened towards the goal of finding the lead candidate. During the screening process, pharmaceutical properties of molecules are assessed. Consequently, the lead candidate(s) goes through preclinical development. This stage includes several steps within; starting from *in vitro* experiments and leading to the animal models where the toxicity and the proof of mechanism of the developed system are evaluated. After satisfying certain regulatory approvals such as IND (Investigational New Drug) filing, the drug candidate goes into clinical development. Clinical trials consist of three main stages: (1) phase I, (2) phase II and (3) phase III. These phases assess distinct aspects of the new therapy, such as phase I focusing on safety and pharmacokinetic profile and phase II evaluating efficacy. Each phase requires a larger patient number. After passing new regulatory requirements, the drug proceeds with manufacturing. During the manufacturing stage, the process is observed and evaluated by regulatory authorities (Lee *et al.*, 1999).

Regarding this overview, animal models act as a bridge between *in vitro* experiments and clinical trials. Animal experiments are needed since *in vitro* models such as cell cultures do not represent all the complex mechanisms present in the human body. Hypotheses and potential therapies have to be tested in animals before proceeding with clinical trials because animal models reflect human biology more accurately than 2D or 3D cell culture models (Wall *et al.*, 2008). Furthermore, *in vivo* experiments are critical to understand the systemic effects of a drug or drug delivery system.

Preclinical development of delivery systems is efficiently established. However, animal models do not reflect human conditions accurately but only provide a predictive aspect for research. This is due to the fact that animals have different biology and physiology than humans (Mak *et al.*, 2014). Furthermore, obtained results from animal experiments may also depend on the animal type chosen for a particular

study of disease model (Croce, 1999). The results of animal experiments should be evaluated avoiding bias and random error to make decisions on whether the therapeutic or the delivery system should be taken forward to clinical trials (Perel *et al.*, 2007).

Generally, researchers who wish to perform animal experiments have to prepare an application and be assessed by an ethical committee. In Norway, FOTS (Forsøksdyrforvaltningens Tilsyns- og Søknadssystem) application is submitted to Mattilsynet (Norwegian Food Safety Authority) through an online application portal. FOTS applications are reviewed by an ethical committee which evaluates applications regarding the Principles of the 3Rs: replacement, reduction and refinement. Replacement is the principle in which animal experiments are avoided and substituted with *in vitro* studies, when *in vivo* experiments are not necessary. The reduction principle represents using as few animals as possible in an experimental setup. Since obtaining statistically significant results is the aim of any experiment, the decision of the sample size should be taken considering both reduction principle and the need of sufficient subjects. Refinement principle focuses on the well-being of the test animals (Flecknell, 2002). Welfare and the comfort of animals should be considered throughout the experiments in order to perform ethically acceptable research. Only the researchers who attend a training course, take a test and obtain an animal experimentation certificate can perform animal experiments. The course and the certificate have to be suitable to standards required by that particular country's regulatory rules. This is imposed in order to obtain a standard regards to the ethical treatment of experimental animals.

1.8. Liquid Chromatography/Mass Spectrometry

High performance liquid chromatography (HPLC) is a powerful and highly sensitive method that is used to convert complex mixtures to separated, individual components. The output of a HPLC analysis is a chromatogram which contains individual peaks for single components. Therefore, one can characterize and identify components of a complex mixture by analyzing the peaks in a chromatogram (Lee et al., 1999). Ultra-high performance liquid chromatography (UHPLC) systems provide higher resolution and increased sensitivity due to their high-performance pumps and faster analysis times (Editors, 2013).

Mass spectrometry (MS) is a technique that is used to sort the ions in a molecule based on their mass/charge ratio. A mass spectrometer consists of three basic components: (1) ionization source in which the molecules to be analyzed are ionized with several possible methods, (2) mass analyzer where ions are accelerated in an electric or magnetic field, and (3) detector which enables quantitative calculation of each ion (Glish *et al.*, 2003). In tandem mass spectrometry (MS/MS), multiple steps of mass spectrometry selection occur. In MS/MS technique mass analysis take place in a subsequent manner in different regions of the instrument and this causes MS/MS to be tandem-in-space. In triple quadrupole mass spectrometry (TQMS), which is a type of MS/MS, the mass analysis consists of the following steps; ionization of the sample molecules, mass selection of the primary ions, collision induced dissociation (CID) of the parent ions to produce daughter ions and the detection of the daughter ions (Johnson *et al.*, 1990).

HPLC and MS methods are combined in LC/MS technique. By utilizing powerful aspects of both techniques, separation through LC and specific identification through MS, highly sensitive results can be obtained. LC/MS interphase is the connection zone between two methods which transfers separated components from LC column to the MS ionization source (Lee *et al.*, 1999). Similarly, UHPLC – MS/MS is a combined method which is commonly used to analyze biological samples.

1.8.1. Vitamins

7-dehydrocholesterol, the provitamin of vitamin D, is found in animals. Exposure of 7-dehydrocholesterol to sunlight results in its conversion to vitamin D_3 (cholecalciferol). Vitamin D_3 is not biologically active and it is hydroxylated to 1,25-dihydroxy-cholecalciferol, also known as calcitriol which is the biologically active form of vitamin D_3 (Mazahery *et al.*, 2015). In rats, vitamin D may be digested upon oral consumption. The other source of this vitamin is its production from the provitamin in the skin upon exposure to sunlight. When digested, vitamin D_3 is absorbed through the lymphatic system and then transferred to the liver. In the liver, vitamin D_3 is hydroxylated to 25-hydroxyvitamin D_3 (25-OH-vitamin D_3). This compound is the main metabolite of vitamin D_3 in the blood circulation (Suckow *et al.*, 2005). Depending on the dose, vitamin D_3 may be toxic when swallowed or in contact with the skin, and fatal when inhaled (Aldrich, 2014). In rats, the oral LD50 is given as 42 mg/kg in its safety data sheet. Also, the digestive toxicity of vitamin D_3 was studied in rats. Cholecalciferol was orally given to rats for 14 days in several concentrations. At 650 nmol/day, all rats in the sample group of 10 survived with some health issues. When the concentration was risen to 6500 nmol/day 9 out of 10 rats died (Shepard *et al.*, 1980). Vitamin D_3 is light and air sensitive (Aldrich, 2014).

Vitamin E (tocopherol) is light sensitive (Aldrich, 2017). Its oral LD50 is >7000 mg/kg in rats (FAO, 1989). Even though menadione (Vitamin K_3) was not used in the *in vivo* experiments, its emulsions were prepared and subjected to stability studies. Vitamin K_3 has an oral LD50 of 500 mg/kg for rats and it is potentially harmful at doses smaller than the LD50 value. Vitamin K_3 is light sensitive, harmful to humans when swallowed and it causes skin and eye irritation (Aldrich, 2012b).

2. Materials and Methods

In Section 1.2, the objectives of the thesis were described. In order to reach these objectives, several scientific methods were used. Materials used in these methodologies, as well as complete protocols are stated in this chapter.

2.1. Preparation of the Emulsions

Initially, Milli-Q-water (MQ-water, Stakpure, Germany) with sodium azide (NaN$_3$, BDH, UK, lot# K24467106) was prepared by dissolving 0.4 gr of sodium azide in 2 l MQ-water (yields 0.02% w/w sodium azide solution). This step was only performed for the emulsions which were going to be used in the *in vitro* experiments. MQ-water (with or without sodium azide, depending on the emulsion type) was mixed with Polysorbate 80 (Tween 80 or T80, Sigma Aldrich, Fluka, UK, lot# BCBN2111V) in a 100 ml glass bottle, using magnetic stirring for approximately 10 minutes until fully dissolved. T80 is an emulsifier and a surfactant. Different T80 percentages (w/w) were used in different emulsions (Table 2).

Vegetable oils such as corn oil (Sigma Aldrich, USA, lot# MKCD1021), coconut oil (Sigma Aldrich, USA, batch#029K0193) and olive oil (Sigma Aldrich, Spain, lot#BCBT5204) form the lipid phase of the emulsions. In all emulsions, the oil amount was 20% (w/w). For the vitamin containing emulsions, vitamin D$_3$ (Cholecalciferol, in powder form, Sigma Aldrich, USA, lot#LRAB2929), vitamin E (Tocopherol, in liquid form, Sigma Aldrich, Germany, lot# MKCC3570) or vitamin K$_3$ (Menadione, in powder form, Sigma Aldrich, China, lot# WXBC4933V) were mixed with corn oil by magnetic stirring until a clear solution was obtained. The oil phase contained combinations of 0.125% (w/w) vitamin D$_3$ and 10% (w/w) vitamin E or 0.125% (w/w) vitamin D$_3$ and 0.011% (w/w) vitamin K$_3$. Vitamin D$_3$ was stored at -20°C, whereas vitamin E and vitamin K$_3$ were stored at +4°C.

For non-vitamin containing emulsions, corn oil, olive oil or coconut oil (depending on the emulsion type) was added to the MQ-water and T80 mixture and mixed further with magnetic stirring for 5 more minutes. The water and oil mixture was blended with the VDI 12 Homogeniser (VWR) machine at speed 5 for 30 minutes, if the emulsion would not go through any further homogenization. This type of emulsions are referred to as non-starbursted (No SB) in this study. If the emulsion would go through further homogenization, the blending time was 5 minutes. VDI 12 Homogeniser is a high-speed mixer which agitates the components to be homogenized at high speed. After this step, emulsions were degassed with the Diaphragm Vacuum Pump machine (Vacuubrand, MZ 2C) for at least 3 times or until no bubbles were observed in the bottle. The bottles containing the emulsions were weighted before and after the degassing procedure and weight losses were compensated with adding MQ-water to the emulsions. Depending on the emulsion type, emulsions were further processed in the Star Burst Mini machine (HJP-25001CE, Sugino, Japan) at 150 MPa for 5 times. This type of emulsions are referred to as starbursted. Star Burst is a wet milling and dispersing device which uses high pressures up to 245 MPa. The bottles were kept in cold water or on ice during the starbursting procedure to prevent the emulsions from being heated. The emulsions were kept at +4°C and/or room temperature to perform further stability analyses. Vitamin containing emulsions were kept in the dark since they are light sensitive (Subsection 1.8.1). Ingredient and preparation method information of all prepared emulsions can be found in Table 2.

Table 2: All prepared emulsions and their contents. Oil concentrations were kept constant at 20% (w/w).

Preparation date	Oil type	T80 [%] (w/w)	Starburst	Sodium azide	Vitamin
26.05.17	Corn oil	2	Yes	Yes	-
		1	Yes	Yes	-
		0.5	Yes	Yes	-
		0.25	Yes	Yes	-
		2	No	Yes	-
04.10.17	Olive oil	2	Yes	Yes	-
		1	Yes	Yes	-
		0.25	Yes	Yes	-
		2	No	Yes	-
11.10.17	Coconut oil	2	Yes	Yes	-
		1	Yes	Yes	-
		0.25	Yes	Yes	-
		2	No	Yes	-
25.10.17	Corn oil	1	Yes	Yes	D_3 and K_3
02.11.17	Corn oil	2	Yes	Yes	D_3 and K_3
14.01.18	Corn oil	2	Yes	No	D_3 and E
		0.25	Yes	No	D_3 and E
		2	No	No	D_3 and E
15.03.18	Corn oil	4	Yes	Yes	-
		8	Yes	Yes	-

While emulsions to be used in the *in vivo* experiments were prepared, the bottles containing the emulsions were continuously flushed with nitrogen (Nitrogen 5.0, Aga, Norway) in each step to remove oxygen from the bottles and prevent oxidation of the vitamin emulsions.

2.2. Droplet Size Measurements

Droplet sizes of the emulsions were measured with the Mastersizer 3000 Hydro MV (Malvern, UK). Mastersizer is a LD particle size analyzer and also provides a software which enables the visualization of the droplet size distribution in a sample. Each emulsion was dispersed by adding 1-10 droplets to 120 ml MQ-water under stirring until an obscuration rate of 5 – 18% was obtained. The dispersant refractive index (MQ-water) was set to 1.330, while the particle refractive indexes were set to 1.470 for corn oil and olive oil, and 1.449 for coconut oil (Ellis, 1999). Particle absorption index was 0.010 for all emulsions.

The Mastersizer 3000 machine utilizes two different wavelength light sources: red and blue light. The data collected from the detectors was analyzed by the Mastersizer software. The software provided average particle size parameters ($D[4,3]$, $D[3,2]$, $Dv50$ and $Dv90$) of five measurements, as well as the droplet size distribution of each emulsion. The data was plotted using MATLAB® R2017a (Appendix D E F and G, *p.* 78, 80, 83 and 88, respectively).

2.3. Microscopy

Four drops of emulsion were diluted in approximately 10 ml of MQ-water. The mixture was added onto the microscope slide (Thermo Scientific, Gerhard Menzel GmnH, Germany) and was covered with a cover slip (VWR, UK) (Chance Propper Ltd., UK). The sample was analyzed with inverted microscope (Nikon Eclipse TS100) and a photograph of the sample was taken with NIS Elements Imaging Software (Version 4.51).

2.4. *In vitro* Lipolysis

In vitro lipolysis of emulsions was performed to simulate the small intestinal conditions. 250 mg bile extract porcine (Sigma Aldrich, USA, lot# SLBT0867) was mixed with 14.5 ml 5 mM HEPES buffer (HEPES, 4-(2-hydroxyethyl)-1-piperazineethanesulfonic acid, Sigma Aldrich, USA, lot# 040M5432V) pH 7 in a 150 ml beaker by magnetic stirring until fully dissolved. A particulate respirator mask (8822, 3M, USA) was used while handling bile extract porcine since it may be harmful when inhaled (Aldrich, 2012a). Later on, 12.5 ml of $CaCl_2$ (Sigma Aldrich, Germany, lot# BCBV8659)/NaCl (VWR, Belgium, lot# 16K214132)/HEPES solution was added to the beaker.

In a separate 50 ml beaker, 19.5 ml 5 mM HEPES buffer (pH 7) was contained. The purpose of this beaker is to provide a temperature of 37°C for the emulsion to be heated before it is added to the bile salt mixture since the bile salts may interact with the emulsion. Both beakers were covered with parafilm (Parafilm M, Sigma Aldrich, USA) to prevent evaporation in the upcoming water bath step. Beakers were placed in the 37°C water bath (IKA-R RCT classic, Germany) and the 150 ml beaker which contains the bile extract and the salt mixture was kept in magnetic stirring for at least 10 minutes. The pH combination electrode (A 162 2M DI, SI Analytics, Germany) of the titrator machine (7000-M1/20, TitroLine, SI Analytics, Germany) was placed into the beaker which contained porcine bile extract and salt mixture, while the content of the beaker was under constant magnetic stirring. pH was approximately 6 at this point.

When the porcine bile extract and the salt mixture have been stirred for 10 minutes, 1.5 ml of the emulsion to be lipolyzed was added to the 50 ml beaker which contained 5mM HEPES buffer. After 3 minutes, the emulsion containing mixture was added to the 150 ml lipolysis beaker and the pH was approximately 6.3 at this point. The pH was adjusted to 7 by manually adding droplets of 1 mM and 0.1 mM NaOH. After approximately 2 minutes, 60 mg pancreatin from porcine pancreas (Sigma Aldrich, USA, lot# SLBP9482V) and 60 mg lipase from porcine pancreas (Sigma Aldrich, USA, lot# SLBL2143V) were dissolved in 5mM HEPES buffer (pH 7) in separate eppendorf tubes through vortex mixing (Reax 2000, Heidolph, Germany) for approximately 3 minutes. The titrator was set to maintain the pH at 7 by adding droplets of 0.1 mM NaOH. The titrator was started and 1 ml of each enzyme mixture was simultaneously added to the beaker to start the lipolysis reaction. The final concentration of each enzyme in the intestinal medium was 1.2 mg/ml. Final concentration of each ingredient in the intestinal medium can be found in Table 3.

Table 3: Ingredients and their final concentrations in intestinal medium.

Ingredients	Final concentration in intestinal medium
Bile extract (fasted)	5 mg/ml
Pancreatin	1.2 mg/ml
Lipase	1.2 mg/ml
$CaCl_2$	10 mM
NaCl	150 mM
HEPES	~5 mM

2.5. Animal Experiments

For the *in vivo* experiments, Sprague Dawley rats were ordered from Envigo, the Netherlands. Upon their arrival to the Comparative Medicine Core Facility (CoMed) in St. Olav's Hospital in NTNU, the rats were acclimatized for ten days. They were played with and pet for several days in this time interval so that they could be more comfortable with the researchers. The rats were born on 13.11.2017, and they were approximately 2 months old when they arrived the CoMed facility. The rats were male and had a body weight of 200-250 grams when they first arrived the facility. See Appendix A (*p.* 63) for the complete FOTS application.

2.5.1. Maintenance of Rats

Four rats were kept in one cage (1500U, Blue Line Next, Techniplast, Italy). Each cage had bedding material, a wooden chewing stick and a plastic house. The room in which the cages were kept had a light cycle of 12:12 light:dark with one hour gradient in between. The temperature of the room was 20-22°C. The rats had access to filtered (through 10 micron, 1 micron and 0,2 micron filters) tap water and rat food (RM1, Special Diets Services, UK). The nutritional values of the rat food can be found in Appendix B (*p.* 72).

2.5.2. Administration of the Emulsions

Rats were fasted starting from 12 hours before the experimental feeds were fed. The rats only had access to sugar water (20 g sucrose/l). They were put in a grid cage without bedding to prevent coprophagy and the ingestion of bedding material. At 0h, the rats were fed with different emulsions (1 ml) or liquid non-emulsified oil (0.2 ml) using oral gavage technique (feeding needle, size 16). The feed was given in a randomized fashion by randomly assigning rats in each cage to one of the feeds. This was achieved by using an online pseudo-random number generator (Urbaniak *et al.*, 2013). The assigned numbers from one to four were marked on the root of the tail with a permanent marker (Figure 7). The animals were monitored for any negative reaction to the feed, *e.g.* possible throw up or difficulty breathing.

2.5.3. Blood Sampling

Blood sampling was performed at 7 time points (0h, 1h, 2h, 4h, 6h, 8h and 24h) for each rat. The exact times of sampling can be found in Appendix C (*p.* 75). Before the 0h sample, the rats were weighed with Adventurer® (Ohaus, USA) to note their weight distribution. The rat was put in a gas chamber (Mssn, UK) and was given approximately 1.5 – 2 l/min Isoflurane (Baxter, Norway) and approximately 0.7 l/min O_2 to provide mild anesthesia. The chamber was also connected to a suction machine (Aga, Finland) to provide air circulation. When the rat was unconscious (approximately 4 minutes later), the rat was taken onto the bench and connected to the face mask which provided constant isoflurane and O_2. The rat was placed onto the heating pad (Physitemp Instruments Inc., USA) which was set to 37.5°C to conserve animals body temperature (Figure 7). The eyes of the rat were covered with Viscotears® (Thea, Norway) to prevent them from drying. The tail of the rat was supported with a glove (Klinion, UK) filled with warm water to promote dilation of the tail veins.
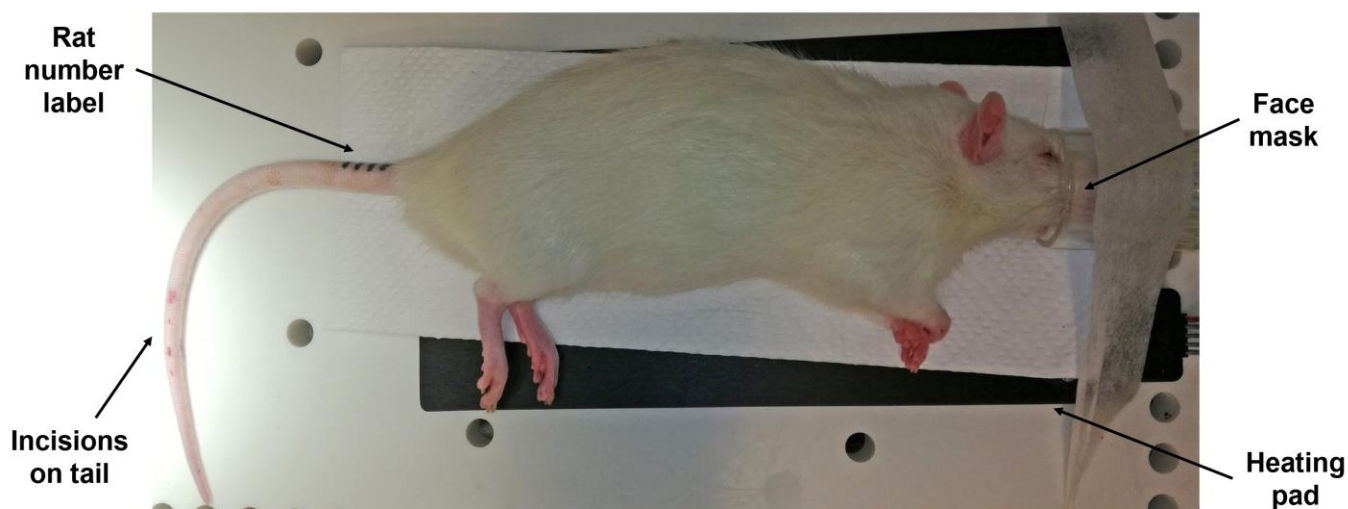
Figure 7: Blood sampling set up of the rat experiments.

A small incision was made at the tail vein with a scalpel (Aesculap AG, Germany). Blood flow was enhanced by gently massaging the tail if necessary. The blood was collected into Mikro-Hämatokrit-Kapillaren Na-heparinized capillary tubes (Brand GMBH & Co Kg, Germany) (Vitrex, Denmark) and then transferred into a Microvette® coagulant tube (Sarstedt, Germany). At each sampling approximately 200 µl blood was collected from each rat. After each collection, the incision was cleaned with a swab (Onemed, Finland) dipped into 0.9% NaCl solution (Braun Melsungen AG, Germany). If the bleeding did not stop, the cut was patched with the Histoacryl® (Braun, Spain) tissue glue (Figure 8). The coagulant tube was centrifuged (Fresco 21, Thermo Scientific, USA) for 5 minutes at 10000 g force and the plasma was separated from blood cells. Plasma was taken into a 1.5 ml eppendorf tube with a micropipette (Thermo Scientific, USA) and was stored at -20°C. At the 24h time point, the rat was heavily anesthesized with either Isoflurane or Sevofluran (Baxter, Norway) as well as 0.6 l/min N_2O and 0.3 l/min O_2 in the gas chamber for approximately 5 minutes. When the rat was unconscious, the rat was connected to the mask and provided with the same anesthetic gases. The technician removed the hair from the abdominal area of the rat with Isis machine (Aesculap Inc., USA) and performed an incision to reach the vena cava. From

the vein approximately 5 ml blood was collected and saved for plasma analysis as described above. Then the heart was removed to euthanize the rat.

Figure 8: Rat tail with 4 incisions performed at different blood collection time points. The top incision was patched with tissue glue to prevent further bleeding.

2.5.4. Analysis of the Plasma Samples with UHPLC – MS/MS

To represent lipophilic compounds in emulsions, fat soluble vitamins were chosen as marker molecules in this study. Emulsions with Vitamin D_3, vitamin E and vitamin K_3 were prepared. However, only cholecalciferol and tocopherol containing emulsions were tested *in vivo* (Section 3.1). The synthesis, toxicity and stability of these vitamins are important since they were used as marker molecules to be delivered with the emulsions. After being orally delivered to animals embedded in emulsions, the vitamins were analyzed with UHPLC – MS/MS method.

The sample preparation protocol was modified from MassTrak Vitamin D kit (Waters, USA). First, 30 µl of internal standard (IS) mix was added into the 700 µl 96-well, round collection plate (Part# 186005837, Waters, USA). ISs of Vitamin D_3-[d6], 25-OH-vitamin D_3-[23,24,25,26,27-13C5] and tocopherol-[d6] were purchased from Cambridge Isotope Laboratories, USA. A series of standard solutions were prepared with known concentrations (50 nM, 125 nM, 250 nM, 500 nM, 1000 nM and 5000 nM) of vitamins in 58:39:3 methanol/water/isopropanol (IPA, VWR, batch# UP647476) diluent. A blank solution which only contained the diluent was prepared. 30 µl of standard solutions, blank or plasma was added onto the IS mix, pipetted up/down and shaken gently with microplate shaker (Grant-bio, Thermo-Shaker PHMP-4) at 700 rpm for 5 minutes. The plasma samples were loaded to the plate as undiluted and 25 times diluted forms. Vitamin E was analyzed from the diluted samples, whereas, vitamin D_3 and 25-OH-vitamin D_3 were analyzed from the undiluted samples. 150 µl 0.1 M zinc sulphate heptahydrate (Sigma Aldrich, Germany, lot# STBH3080) was added onto the mix and shaken gently for 3 minutes. 300 µl of LC/MS-grade methanol (Hypergrade for LC-MS, Merck, Germany, CAS# 67561) was added and shaken gently for 3 minutes. Following the precipitation step, the 700 µl ml 96-well, round collection plate was centrifuged (Centrifuge 5804 R, Eppendorf, Germany) at 1800 rpm for 5 minutes. Oasis HLB µElution Plate 30 µm (Waters, USA) was conditioned using 200 µl of LC/MS-grade methanol followed by 200 µl of 60:40 methanol/water (VWR, France, lot# 17I124015). 300 µl of the supernatant was transferred onto the Oasis HLB µElution Plate 30 µm. The sample was washed using 200 µl of 5:95 methanol/water followed by 200 µl of 60:40 methanol/water. The Oasis HLB µElution Plate was transferred above the 700 µl 96-well, round collection

plate and the sample was eluted in 80 μl of 100% IPA followed by 50 μl of LCMS (liquid chromatography mass spectrometry) – grade water. After each step of liquid addition to the Oasis HLB μElution Plate, the plate was processed with the Positive pressure-96 nitrogen pump (Waters, USA) running at approximately 13 psi for 2 minutes. 700 μl 96-well round collection plate was sealed with a pre-slit cap mat and placed on the shaker to be mixed for 3 minutes prior to analysis.

Analyses were performed with an ACQUITY UPLC® BEH C18 (Waters, USA) system coupled to a Xevo TQ-S Triple Quadrupole Mass Spectrometer (Waters, USA) equipped with an electrospray (ESI) source operating in positive mode. Ultra-high performance liquid chromatography – tandem mass spectrometry (UHPLC – MS/MS) data were acquired and processed using MassLynx software (v4.1) and TargetLynx application manager. The chromatographic columns pore size was 100 Å, particle size was 1.7 μm, ID was 2.1 mm and length was 50 mm. The column manager was set to 45 °C.

Mobile phase A consisted of water with 2 mM ammonium formate (Prepared by mixing ammonium hydroxide solution (Fluka, Germany, lot# PCBS2194V) with formic acid (Fluka Analytical, Germany, lot# BCBQ7913V)) and 0.1% (v/v) formic acid. Mobile phase B consisted of methanol with 2 mM ammonium formate and 0.1% (v/v) formic acid. Flow rate was set at 0.5 ml/min. Conditions were kept constant at 25% A for half a minute, then a linear gradient was programmed from 25% A to 1% A in 1.5 minute, followed by 1% A kept for a 1.5 minutes period, before the gradient was brought back to 25% A in 0.1 min. Finally, the column was equilibrated for 0.9 minute before starting a new injection. Ethanol was used as wash solvent. The injection volume was 2 μl.

MS and MS/MS analyses were performed under constant ESI conditions. The capillary voltage and source offset voltages were set at 2 kV and 30 V, respectively. The source temperature was maintained at 150°C, desolvation gas temperature at 500 °C and gas flow rate at 1000 l/h. The cone gas flow rate was fixed at 150 l/h and the nebulizer gas flow was maintained at 6 bar. The collision gas flow was set to 0.2 ml/min of argon. All standards were dissolved in 100% (v/v) IPA to stock solutions of 1 mM, and diluted with a solvent mixture consisting of 58% (v/v) methanol, 40% (v/v) water and 2% (v/v) IPA. Cone voltages (CV), collision energies (CE) and MS/MS transitions (precursor and product ions) of vitamin D_3, 25-OH-vitamin D_3 and α-tocopherol was optimized using Intellistart (Waters, USA) by infusing 500 nM standard solutions at 10-20 μl/min, combined with a 0.05 ml/min 50% A flow from the LC-system. The same mobile phases described above were used.

Vitamin D_3 was quantified by means of one selected precursor ion-product ion transition (m/z 385.40-259.17, CV = 26 V, CE = 12 eV), and its identity was confirmed by one transition (m/z 385.40-107.04, CV = 26 V and CE = 22 eV). 25-OH-vitamin D_3 was quantified in the same way with one selected precursor ion-product ion transition (m/z 401.35-383.26, CV=22, CE=8 V), and its identity was confirmed by one transition (m/z 401.35-105.01, CV=22, CE=44 V). For α-tocopherol, a single reaction monitoring (SRM) ion (m/z 431.40-165.05, CV=46, CE=18 V), and a confirmation SRM (m/z 431.40-137.04, CV=46, CE=44 V) were selected. As ISs, Vitamin D_3-[d6], 25-OH-vitamin D_3-[23,24,25,26,27-13C5] and tocopherol-[d6] were used with the following SRM transitions m/z 391.67-265.17, m/z 406.59-388.26, m/z 437.20-171.00, respectively. The same collision voltages and energies as the unlabeled compounds were utilized. A 10-20 ms dwell time was calculated for each transition as recommended by the auto dwell function in MassLynx to ensure 20 data points across the peaks.

3. Results and Discussion

In this chapter, the results obtained from the experiments and their discussion takes place. In Section 3.1, the preparation of emulsions and the droplet size measurements are discussed. In Section 3.2, stability analyses of different emulsions are given. In Section 3.3, *in vitro* lipolysis experiment results with subsections which focus on Back-Titration, enzyme optimization and oil type comparison are discussed. Lastly, in Section 3.4, the results of animal experiments, with an emphasis on the UHPLC – MS/MS analyses of the rat plasma samples and sample preparation protocol optimization, were discussed.

3.1. Preparation of the Emulsions and Droplet Size Analysis

Every experiment started with the preparation of emulsions. In this protocol, a standardized method was used for all emulsions in order to obtain emulsions which differ only at intended parameters: oil type and emulsifier concentration (w/w). Optimization and establishment of the emulsion preparation protocol enabled the production of standardized emulsions that can be compared in the upcoming analyses.

The emulsions which were to be used in the *in vivo* studies did not contain sodium azide. Sodium azide is a preservative with an oral LD50 value of 27 mg/kg for rats (VWR, 2014). Even though 0.02% (w/w) sodium azide would result in a concentration far below the LD50 value, it was avoided to prevent any possible toxic effects. Whereas, the utilization of sodium azide in the emulsions that are to be used in the *in vitro* lipolysis is critical since this chemical prevents the growth of microorganisms in emulsions that are to be stored for an extended period.

The choice of emulsifier was made considering several criteria such as water-solubility, nature of its head and tail groups, CMC, HLB, etc. Polysorbate 80, *i.e.* polyoxyethylene (20) sorbitan monooleate, is derived from ethoxylated sorbitan, esterified with fatty acids. It is non-ionic and water soluble, with a HLB value of 15. These properties enable T80 to generate stable O/W emulsions that are mostly unaffected by pH. This property becomes important in orally delivered systems where the GI tract exhibits variable pH values, *e.g.* in the stomach. The concentration of polysorbate in the emulsion mixture plays an important role in the generation of different droplet sized emulsions. Higher concentrations of T80 (up to 8%) provides smaller sized oil droplets, whereas, low concentrations of T80 generate larger sized oil droplets. T80 reduces the interfacial tension which has a direct impact on the Laplace pressure (ΔP_L). Whenever a T80 concentration is mentioned in this work, it should be regarded as % (w/w).

The amount of times that an emulsion should be run through the Star Burst machine was calibrated by trial and error. Runs of one, two, three, four and five times on a particular emulsion were performed and the droplet size of the emulsion was measured after each run. The $D[4,3]$ and $D[3,2]$ means were decreased approximately 17 times and approximately 10 times after the first run, respectively. However, the decrease in the droplet size plateaus after four times of starbursting (Data not shown, M. J. Dille, personal communication, 19.05.2017). Therefore, running each emulsion five times was decided to be standardized. This plateau observation of droplet size upon starbursting might be due to ΔP_L (Section 1.6). When the droplet size of an oil droplet decreases, its internal pressure increases which makes it even more difficult to break down smaller droplets. This phenomenon becomes significant when droplet sizes are below μm scale (Section 1.6). The plateau observation might also be due to insufficient T80 to stabilize

smaller droplets, since the total surface area of the emulsion considerably increases as the droplets get smaller.

Microscopy images of a corn oil emulsion were taken before and after starbursting (Figure 9A and Figure 9B respectively). From the images, it is observed that the droplet size of the emulsion noticeably decreased upon starbursting. In Figure 9A, large as well as small droplets are seen which indicates a polydisperse droplet size distribution. However, in Figure 9B, oil droplets are closer to a monodisperse distribution.
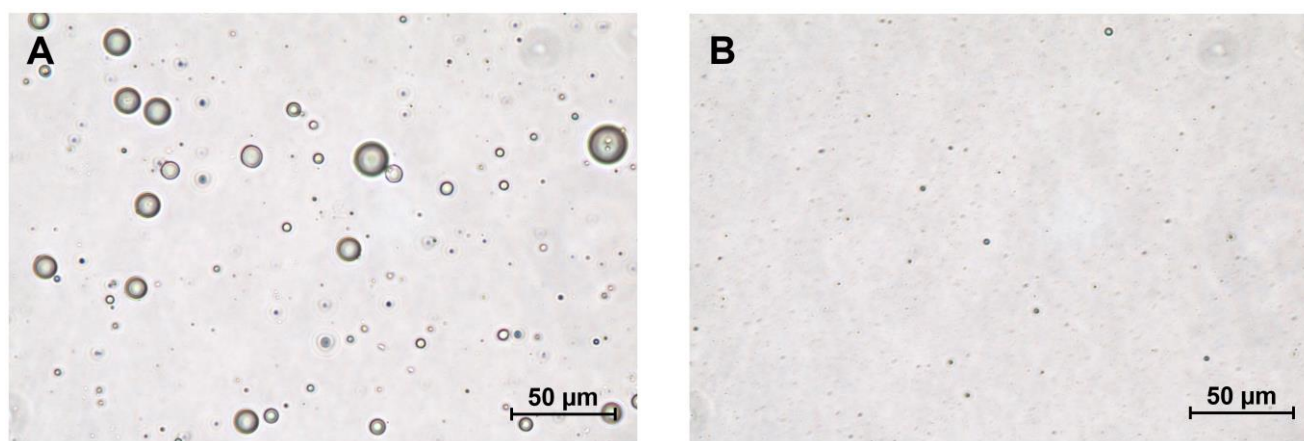
Figure 9: A) Non-starbursted and **B)** starbursted coconut oil emulsion with 2% (w/w) T80. The photograph was taken with Nikon Eclipse TS100 at 40X magnification.

The droplet size measurements were performed using the Mastersizer 3000 machine. In Figure 10, droplet size measurements of the corn oil emulsions can be found. The emulsions differ in the percentage (w/w) of T80 emulsifier they contain. The bar plot presents $D[4,3]$ and $D[3,2]$ mean parameters. It is observed that the droplet size decreases as T80 percentage increases. The non-starbursted emulsion results in the largest droplet size means. In addition, the $D[4,3]$ and $D[3,2]$ means of the non-starbursted emulsion are significantly different, indicating the polydisperse nature of this emulsion. Whereas, the starbursted emulsions give rather similar $D[4,3]$ and $D[3,2]$ means, indicating a rather monodisperse distribution. Droplet size means of all emulsions can be found in Table 4. The droplet size plots of other emulsions can be found in Appendix D (*p.* 78).

As pointed out in Subsection 1.6.3, the mean parameters only provide representative values for droplet size of an emulsion. Droplet size distribution chromatogram of the same emulsions in Figure 10 are given in Figure 11. Droplet size distribution chromatograms of other emulsions can be found in Appendix E (*p.* 80).
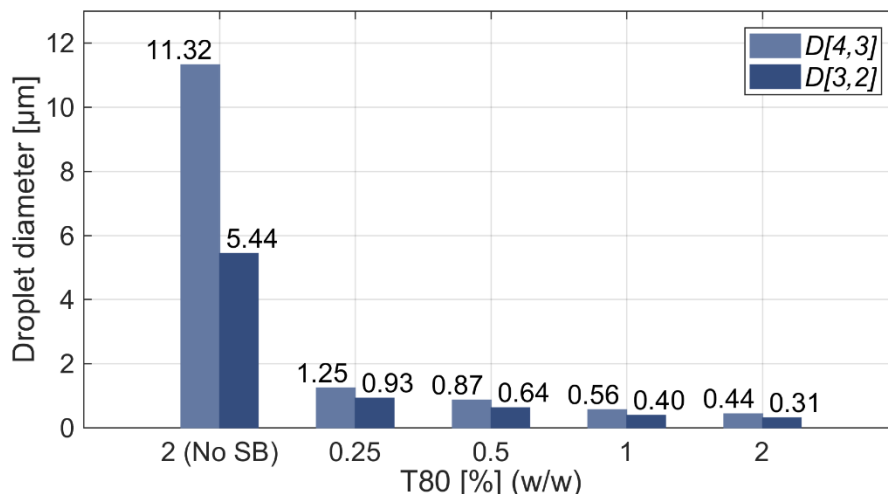
Figure 10: Droplet size plot of 20% (w/w) corn oil emulsions with T80 percentage ranging from 2 to 0.25. The non-starbursted emulsion is generated by the VDI 12 Homogeniser and the other emulsions are generated with a combination of the VDI 12 Homogeniser and the Star Burst Mini. The $D[4,3]$ volume mean and $D[3,2]$ surface mean of each emulsion are shown in separate bars.

In Figure 11, the x-axis shows droplet diameters in logarithmic scale and the y-axis indicates the percentage of particles that have the corresponding droplet diameter. The projection of the top point of a peak onto the x-axis is the mode of that distribution. The mode denotes the particle size which is most commonly found in a distribution. It should be noted that mode is not the same as mean. In Figure 11, the black curve representing the droplet size distribution of the non-starbursted emulsion is polydisperse. The curve has a large top peak at approximately 10 μm and smaller peaks formed around 1 μm, indicating the presence of smaller droplets. This can also be observed in Figure 9A.
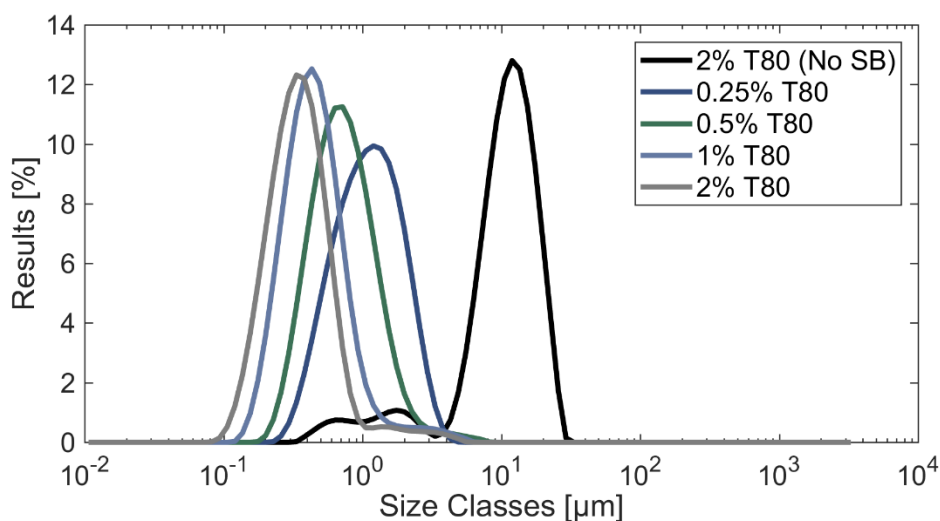
Figure 11: Size distribution chromatogram of 20% (w/w) corn oil emulsions with T80 percentage (w/w) ranging from 2 to 0.5. The non-starbursted emulsion is generated by the VDI 12 Homogeniser and the other emulsions are generated with a combination of the VDI 12 Homogeniser and the Star Burst Mini.

Table 4: Droplet sizes of all prepared emulsions, expressed as different particle size measurement parameters.

Emulsion			Particle size parameters [µm]			
Oil type	T80 [%] (w/w)	Vitamin	*D[4,3]*	*D[3,2]*	*Dv50*	*Dv90*
Corn	8	-	0.208	0.162	0.185	0.355
	4	-	0.283	0.225	0.257	0.473
	2	-	0.436	0.309	0.342	0.647
		D_3 and K	0.434	0.317	0.351	0.663
		D_3 and E	0.349	0.281	0.314	0.551
	1	-	0.562	0.402	0.438	0.861
		D_3 and K	0.620	0.449	0.489	0.992
	0.5	-	0.869	0.637	0.708	1.446
	0.25	-	1.250	0.933	1.100	2.200
		D_3 and E	1.390	1.020	1.262	2.430
	2 (No SB)	-	11.320	5.442	11.060	18.900
		D_3 and E	8.890	2.888	8.404	17.500
Olive	2	-	0.435	0.315	0.347	0.651
	1	-	0.575	0.421	0.458	0.903
	0.25	-	1.420	0.994	1.270	2.580
	2 (No SB)	-	11.300	4.290	11.200	20.28
Coconut	2	-	0.467	0.336	0.368	0.682
	1	-	0.564	0.414	0.447	0.857
	0.25	-	1.230	0.967	1.080	2.100
	2 (No SB)	-	15.800	3.904	9.724	18.200

Measuring the droplet size of very small oil droplets with the Mastersizer 3000 machine was difficult. This might be due to the T80 emulsifier layer around the droplets, which has a different refractory index than the oils composing the oil phase of the emulsions. This was observed for the corn oil emulsion prepared with 8% T80. While analyzing the droplet size of this emulsion with the Mastersizer software, refractory index curve did not provide an ideal fit as the other emulsions. Changing the refractory index provided a better fit. However, the mean droplet size values also changed. Therefore, it was concluded that the size of smaller droplets was hard to estimate with the Mastersizer 3000 machine whose range is specified as 10 nm – 3.5 mm (Malvern Instruments, 2018). Using the Zetasizer machine which utilizes DLS technology may be a better alternative for measuring the droplet sizes of the 4% and 8% T80 emulsions which have droplet sizes in nanometer range (Subsection 1.6.3).

Droplet size measurements of emulsions with different oil types is given in Table 4. Since each presented mean value is the average of five measurements, performed by the Mastersizer 3000 machine (Section 2.2), the analysis of variance (ANOVA) test was performed to see if the droplet size means of emulsions

prepared with three different oil types (corn oil, olive oil, coconut oil) were significantly different from each other when the T80 concentration was kept constant. The one-way ANOVA test was separately applied to $D[4,3]$ volume mean and $D[3,2]$ surface mean. The $D[4,3]$ volume mean measurement results of the 0.25% T80 emulsions did not have any variance, therefore, in order to be able to perform the test 0.00001 variance was added to one of replicas of each oil type emulsion.

When significant difference was detected among groups, the Student's T-tests was performed between pairs of emulsions which were prepared with different oil types (and contained the same amount of T80). This test was conducted since the ANOVA results only provide information about if at least one oil type results in a significantly different droplet size means, however does not point out which oil type is different than the others. In the two-sample unequal variance T-test, the number of distribution tails was set to 2 and α was set to 0.05. The p values obtained from the one-way ANOVA and the Student's T-tests are presented in Table 5.

Table 5: p value results of one-way ANOVA and Student's T-tests performed for $D[4,3]$ volume mean and $D[3,2]$ surface mean, between the droplet sizes of emulsions prepared with different oil types.

T80 [%] (w/w)	$D[4,3]$ volume mean			$D[3,2]$ surface mean		
	ANOVA p value	Compared oil type	T-test p value	ANOVA p value	Compared oil type	T-test p value
2	$7.096 \cdot 10^{-15}$	Corn – olive	0.157	$4.286 \cdot 10^{-15}$	Corn – olive	0.00041
		Olive – coconut	$4.163 \cdot 10^{-14}$		Olive – coconut	$4.750 \cdot 10^{-8}$
		Corn – coconut	$9.076 \cdot 10^{-7}$		Corn – coconut	$1.548 \cdot 10^{-6}$
1	$4.502 \cdot 10^{-7}$	Corn – olive	$5.667 \cdot 10^{-5}$	$3.979 \cdot 10^{-16}$	Corn – olive	$3.181 \cdot 10^{-12}$
		Olive – coconut	0.00036		Olive – coconut	$7.595 \cdot 10^{-9}$
		Corn – coconut	0.445		Corn – coconut	$1.376 \cdot 10^{-10}$
0.25	$1.140 \cdot 10^{-52}$	Corn – olive	$6.576 \cdot 10^{-36}$	$6.315 \cdot 10^{-18}$	Corn – olive	$4.941 \cdot 10^{-8}$
		Olive – coconut	$2.701 \cdot 10^{-36}$		Olive – coconut	$6.522 \cdot 10^{-10}$
		Corn – coconut	$1.792 \cdot 10^{-28}$		Corn – coconut	$4.034 \cdot 10^{-7}$
2 (No SB)	$4.22 \cdot 10^{-18}$	Corn – olive	0.374	$5.94 \cdot 10^{-26}$	Corn – olive	$2.865 \cdot 10^{-15}$
		Olive – coconut	$1.654 \cdot 10^{-10}$		Olive – coconut	$6.404 \cdot 10^{-13}$
		Corn – coconut	$1.400 \cdot 10^{-7}$		Corn – coconut	$1.527 \cdot 10^{-18}$

In all applied ANOVA tests, p value was smaller than α (0.05). Moreover, for all ANOVA tests, F-critical was smaller than F value (Data not shown). This indicated that at least one of the oil types resulted in significantly different droplet size means, i.e. *D[4,3]* volume mean and *D[3,2]* surface mean. The Student's T-test results provided α values smaller than 0.05 for all *D[3,2]* surface mean tests. However, for the *D[4,3]* volume mean, this was not the case for three out of 12 comparisons. When T80 percentage is kept constant at 2%, corn oil and olive oil did not result in significantly different means for starbursted and non-starbursted emulsions (α = 0.157 and α = 0.374, respectively). Similarly, at 1% T80, corn oil and coconut oil did not result in significantly different means (α = 0.445). The rest of the T80 percentage and oil type combinations resulted in significantly different means (Table 5). This observation is relevant when the *in vitro* lipolysis rates of different oil types are compared, since it should not be assumed that different oil types would result in the same droplet sizes when the T80 concentration in the emulsions is kept constant. More importantly, when the second part of the *in vivo* experiments is performed in the future, where the delivery rate of different oil type emulsions is compared (Appendix A (*p.* 63) and Section 4.2), these results become of utmost importance.

3.2. Stability of the Emulsions

Stability of the emulsions was tested through comparing the droplet size of emulsions at different time points and visual inspection of the emulsion. The comparison was made on the *D[4,3]* volume and *D[3,2]* surface means (Table 6). Size distribution chromatograms plotted at different time points were also used in order to obtain a visual reference for the comparison. Appendix F (*p.* 83) presents a range of comparative size distribution chromatograms of different emulsions. Table 18 (*p.* 83) in Appendix F presents the time points when different emulsions were analyzed for stability. This study provided insight on possible destabilizing processes which might have occurred in different emulsions.

Upon a droplet size measurement, the Malvern software provides five values for each means and medians (*D[4,3]*, *D[3,2]*, *Dv10*, *Dv50* and *Dv90*). For most of the emulsions, the results of a parameter, *e.g.* mean, give similar values. In such cases, the standard deviation of the results is less than 0.05 µm. However, for some emulsions, the results may have a standard deviation up to 4 µm. The general reason for this observation might be because of a gas bubble intervening with the detector while the droplet size measurement is being performed at the liquid phase. This results in one or two extreme values among the five measurement values. In such cases, the measurement is repeated and if the problem persisted, the outlier values are removed during the calculation of the average and the new mean values are presented in Table 6. Such cases are discussed in the text.

Corn oil emulsions with 2% T80, 0.25% T80 and non-starbursted 2% T80 were tested for stability upon storage at +4°C and room temperature, for 3.5 and 9.5 months from preparation. The 2% T80 emulsion exhibited similar droplet size after 3.5 months and 9.5 months storage at both +4°C and room temperature. This was confirmed with the droplet size distribution chromatogram (Appendix F, Figure 30A and B (*p.* 83)). Similarly, the 0.25% T80 emulsion showed stability after 3.5 and 9.5 months storage at +4°C and room temperature (Appendix F, Figure 31A and B (*p.* 84)). However, the non-starbursted 2% T80 emulsion resulted in smaller means after 3.5 and 9.5 months of storage at +4°C and room temperature (Table 6 and Appendix F, Figure 32A and B, (*p.* 84)). The reason for this observation might be due to the large oil droplets sticking to the wall of the glass bottle, while smaller droplets remaining at the middle part of the bottle. Therefore, the large droplets might not be collected when the droplet size analysis was being

performed. At the 3rd droplet size measurement of corn oil emulsions, small oil droplets were observed at the surface of the emulsion for the bottles being stored at +4°C. This observation points out possible coalescence that took place. However, no oil droplets were observed at the surface for the corn oil emulsions that have been stored at room temperature.

Corn oil emulsions containing vitamin D_3 and vitamin K_3 were only prepared to test their stability. The 1% and 2% T80 containing vitamin D_3 and K_3 emulsions were prepared and their stability was studied as a primary attempt to generate a convenient vitamin containing emulsions for the upcoming *in vivo* studies. The 1% T80 vitamin emulsion was stored at +4°C for a week and preserved its droplet size (Table 6). Another droplet size measurement of this emulsion was performed 4.5 months after its preparation and it still exhibited similar mean values upon storage at +4°C and room temperature. The stability of the 1% T80 emulsion was confirmed with droplet size chromatogram (Appendix F, Figure 33A (*p.* 85)). However, for the emulsion which was kept +4°C, small oil droplets, which indicate coalescence, were observed at the surface.

The 2% T80 emulsion with vitamin D_3 and K_3 was also stable after 4.5 months storage at +4°C and room temperature (Table 6 and Appendix F, Figure 33B (*p.* 85)). However, small oil droplets were observed at the surface of the emulsion upon storage at +4°C, pointing out to possible destabilization in the form of coalescence.

The vitamin D_3 and K_3 containing emulsions were not tested on animals. Vitamin K_3 was substituted with vitamin E for the *in vivo* experiments. The main reason for that was the possibility of vitamin K_3 being oxidized. The preparation and stability of a trial corn oil emulsion containing vitamin D_3 and vitamin E were tested by Morten J. Dille. After this step, the actual corn oil emulsions for the *in vivo* experiments were prepared. The emulsions were only stored at +4°C. The 1st and 2nd droplet size measurements were taken two months apart. The size distribution chromatogram comparison for these emulsions can be found in Figure 12. A significant increase of the *D[4,3]* volume means is observed for 2% T80 and non-starbursted 2% T80 emulsions. Whereas, the 0.25% T80 emulsion was stable after two months regarding both *D[4,3]* and *D[3,2]* means. The non-starbursted emulsions droplet size measurements resulted in a standard deviation of 11.358 μm and 0.228 μm, for *D[4,3]* and *D[3,2]* means, respectively. *D[4,3]* mean of the 2% T80 emulsion exhibited two outlier results among five measurements (0.357, 0.357, 0.357, 3.06 and 4.37 μm) and the standard deviation was 1.696 μm. When these two outliers are excluded, the new volume mean was 0.357 μm (rather than 1.7 μm) and the standard deviation was 0 μm. The outliers might be due to an air bubble blocking the detectors. This possibility is supported by the size distribution chromatogram of the emulsions (Figure 12), where the 2% T80 emulsion exhibits a stable curve after two months. Therefore, it is concluded that only the non-starbursted 2% T80 corn oil emulsion with vitamin D_3 and E is unstable when stored at +4°C for two months, as both *D[4,3]* and *D[3,2]* means increased significantly (Table 6). All three emulsions contained oil droplets on their surfaces, implying possible coalescence.

Table 6: Droplet size measurements of corn oil, olive oil and coconut oil emulsions with and without indicated vitamins, taken at different time points shown as the 1st, 2nd and 3rd measurements upon storage at +4°C or room temperature (RT). The unit of all presented mean values is µm.

Oil type	T80 [%] (w/w)	Vitamin	1st Measurement D[4,3]	1st Measurement D[3,2]	2nd +4°C D[4,3]	2nd +4°C D[3,2]	2nd RT D[4,3]	2nd RT D[3,2]	3rd +4°C D[4,3]	3rd +4°C D[3,2]	3rd RT D[4,3]	3rd RT D[3,2]
Corn	2	-	0.436	0.309	0.430	0.309	0.418	0.305	0.417	0.299	0.422	0.303
Corn	2	D₃ and K₃	0.434	0.317	0.440	0.314	0.440	0.311			-	
Corn	2	D₃ and E	0.349	0.281	0.357	0.284		-		-		
Corn	1	D₃ and K₃	0.620	0.449	0.615	0.445		-	0.630	0.447	0.630	0.446
Corn	0.25	-	1.250	0.933	1.210	0.882	1.230	0.918	1.268	0.942	1.240	0.934
Corn	0.25	D₃ and E	1.390	1.020	1.400	1.020		-		-		
Corn	2 (No SB)	-	11.320	5.442	9.268	3.370	9.254	3.394	9.452	3.682	9.344	3.604
Corn	2 (No SB)	D₃ and E	8.890	2.888	37.520	3.442		-		-		
Olive	2	-	0.435	0.315	0.439	0.308	0.441	0.309		-		
Olive	0.25	-	1.420	0.994	1.456	1.036	12.310	1.204		-		
Olive	2 (No SB)	-	11.300	4.290	8.272	3.144	11.560	4.540		-		
Coconut	2	-	0.467	0.336	0.411	0.326	0.483	0.335		-		
Coconut	0.25	-	1.230	0.967	2.204	0.932	1.242	0.990		-		
Coconut	2 (No SB)	-	15.800	3.904	42.84	5.822	9.888	4.014		-		
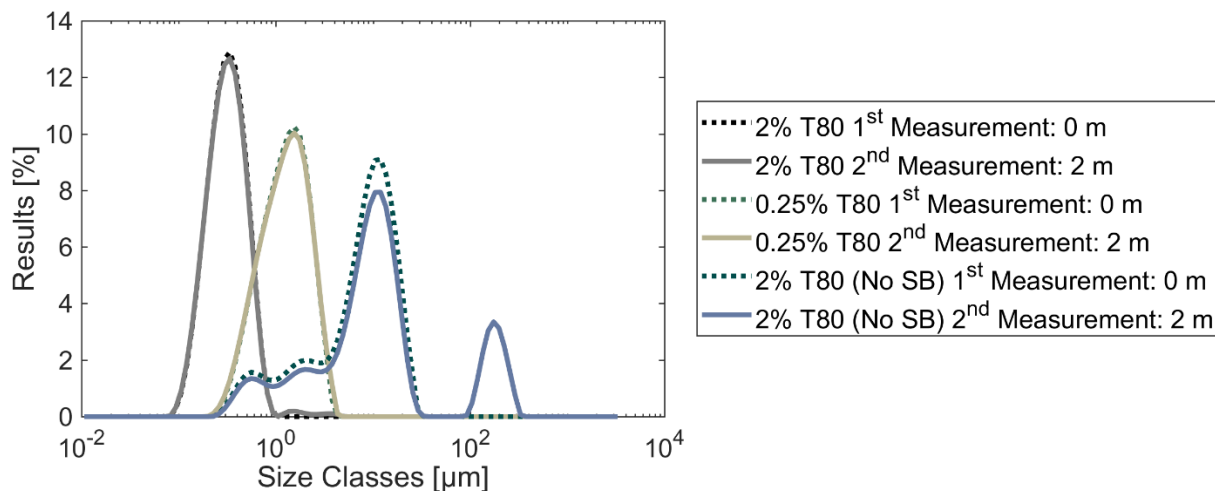
Figure 12: Stability chromatogram of the 20% (w/w) corn oil emulsion with 2% T80, 0.25% T80 and 2% T80 (non-starbursted). Emulsions were used in *in vivo* experiments and they contain 0.125% (w/w) vitamin D_3 and 10% (w/w) vitamin E. The second measurement was performed on the emulsions that were stored at +4°C.

2% T80, 0.25% T80 and non-starbursted 2% T80 olive oil emulsions were tested for stability. When the emulsions were stored at +4°C for five months, the 2% T80 containing emulsion remained stable (Table 6). After five months at +4°C, 0.25% T80 emulsion was also stable, however with a slightly larger *D[4,3]* volume and *D[3,2]* surface mean. The non-starbursted 2% T80 emulsion exhibited smaller droplet size means after five months. This phenomenon is similar to the one observed for the non-starbursted 2% T80 corn oil emulsion, where large oil droplets might be sticking to the walls of the glass bottle and leaving out the smaller oil droplets in the middle of the mixture. These findings were confirmed with the droplet size chromatograms (Appendix F, Figure 34 (*p.* 85)). The non-starbursted emulsion showed solid creaming on its surface, whereas the 0.25% T80 emulsion contained one very large oil droplet on the surface. In addition, both the non-starbursted and the 0.25% T80 emulsions exhibited a pink-orange color in the water phase. This might be due to the presence of non-fatty acid compounds in olive oil, such as pigments and metals (Subsection 1.6.4). These compounds might have reacted with other compounds or oxidized to yield the described color.

When the olive oil emulsions were stored at room temperature for five months, 2% T80 and non-starbursted 2% T80 emulsions were stable with slightly larger *D[4,3]* and *D[3,2]* means (Appendix F, Figure 35 (*p.* 86)). However, the 0.25% T80 olive oil emulsion had significantly larger droplet size means, compared to its first measurement. Especially, for the *D[4,3]* volume mean, the droplet size was approximately 9 times larger. Five values obtained from this measurement (7.07, 9.38, 12.4, 14.6 and 18.1 μm) had a large standard deviation (3.868 μm). Although this measurement was performed several times, the results always exhibited high standard deviation. The reason for this observation might be due to the destabilization of the emulsion in the given storage conditions (at room temperature). All three olive oil emulsions stored at room temperature contained small oil droplets on their surfaces, indicating possible coalescence.

In general, for both corn oil and olive oil, the emulsions which were stored at +4°C exhibited lower visual stability, *i.e.* the presence of larger droplets on the surface, solid creaming or color change, compared to

the emulsions which were stored at room temperature. This observation is intriguing since one would consider colder temperatures to provide better storage conditions for the conservation of emulsions. The reason for this observation should be further investigated. Possible reasons include density, viscosity and flexibility changes of the oils, and changes in the strength of hydrogen bonds between the T80 molecules at different storage temperatures.

In general, corn oil emulsions exhibited higher stability compared to olive oil emulsions. This might be due to the presence of compounds in olive oil, other than fatty acids (Subsection 1.6.4). These compounds might have led to the destabilization of olive oil. This stands as a disadvantage for olive oil to be considered being tested in the *in vivo* experiments, since corn oil shows higher stability as a LCT.

2% T80, 0.25% T80 and non-starbursted 2% T80 coconut oil emulsions were tested for stability. When the emulsions were stored at +4°C for five months, 2% T80 emulsion was stable. Although, the 0.25% T80 emulsion showed a larger *D[4,3]* volume mean, it had a similar *D[3,2]* surface mean when compared to the first measurement. The non-starbursted 2% T80 emulsion exhibited significantly larger droplet size for both *D[4,3]* volume mean and *D[3,2]* surface mean (Table 6). These results were confirmed with the droplet size chromatogram (Appendix F, Figure 36 (*p.* 86)). The increase in the droplet size for the non-starbursted 2% T80 emulsion can clearly be observed through a phase shift-like curve after five months storage at +4°C. Five values obtained for the *D[4,3]* mean measurements of the 2% T80 emulsion had a standard deviation of 2.785 µm. This extreme increase (from 15.800 µm to 42.840 µm) in droplet size can be explained by the melting temperature (approximately 24.5°C) of coconut oil. Upon storage at +4°C, coconut oil is expected to be crystallized. The crystallization of the emulsion was also observed with naked eye, in the form of several solid-like particles. Partial fat crystallization of O/W emulsions causes the droplets to penetrate into each other and stick together (P Walstra, 1987). This phenomenon is called partial coalescence and has an important impact on the stability of an emulsion (McClements, 2015). Furthermore, when the oil phase of an O/W emulsion is crystallized, an embedded molecule in the oil phase cannot diffuse out of the oil droplets and the release rate of the molecule decreases (Akoh, 2005).

When the coconut oil emulsions were stored at room temperature for five months, 2% T80 and 0.25% T80 emulsions showed stability (Table 6). Even though all coconut oil emulsions exhibited an almost perfect fit in the droplet size chromatogram (Appendix F, Figure 37 (*p.* 87)), the non-starbursted 2% T80 emulsion resulted in a smaller *D[4,3]* volume mean and a slightly larger *D[3,2]* surface mean upon storage at room temperature. The observation of smaller *D[4,3]* mean may be due to larger droplets that stick to the walls of the glass bottle and the smaller droplets which remain in the middle of the bottle, as discussed earlier for other emulsions.

The melting point of the different oils plays a significant role regarding their long term stability. Coconut oil emulsions were concluded to show poor stability at +4°C, and therefore presented a disadvantage to be used in an optimized emulsion based oral delivery system since logistic conditions may cause instability for a potential emulsion. On the other hand, starbursted corn oil emulsions were concluded to be stable at +4°C and room temperature, and this property points out to its feasibility to be chosen as the optimized emulsion.

Water solubility of different fatty acids in different oil types may play a significant role in the destabilization of emulsions. Shorter fatty acids are more water soluble than longer fatty acids (Valenzuela *et al.*, 2013). This becomes relevant for Ostwald ripening, since the rate of Ostwald ripening is proportional to the

solubility of the dispersed phase, *i.e.* oil droplets in an O/W emulsion (Weers, 1998). Ostwald ripening leads to an overall increase in the mean droplet size (McClements, 2015).

It should be noted that the stability studies discussed in this section are not highly relevant for the *in vivo* experiments since before each *in vivo* experiment, the emulsions were freshly prepared. However, the results obtained from the stability studies are influential for the conclusions of this thesis. Considering the main purpose of this work, long term stability characteristics of an emulsion plays an important role when the optimized emulsion system is to be chosen.

3.3. *In vitro* Lipolysis

Initially, *in vitro* lipolysis was performed with Method 1. This method takes 3600 seconds, records pH (and accordingly the titrated NaOH volume) less frequently (every 30 seconds) to the measurement file. Later, Method 2 was developed to be able to lipolyze more emulsions in a shorter time interval. It was observed that reaching the plateau took place well before 1500 seconds and this change in method would not affect the data obtained from the experiments. Method 2 takes 2000 seconds and records pH (and accordingly the titrated NaOH volume) more frequently (every 2 seconds) to the measurement file. It should be noted that Method 1 and Method 2 do not differ in reading the pH or titration frequency, but only in the frequency of recording the pH and the titrated NaOH amount. These two methods also differed in the emulsion percentage (v/v) they contained in the lipolysis medium. Moreover, Method 2 follows established time points for the addition of each ingredient to the lipolysis medium. This provides a standardized protocol to obtain comparable results from different *in vitro* lipolysis experiments. The comparison between these *in vitro* lipolysis methods regarding the final concentrations of lipolysis medium ingredients and duration is given in Table 7. In Section 2.4 of Materials and Methods, the *in vitro* lipolysis protocol with later developed Method 2 is explained in detail.

As introduced in Subsection 1.5.2, it is important to perform the *in vitro* lipolysis experiment in a way that the lipolysis medium reflects the actual human small intestine conditions. The components of the lipolysis medium and the optimization of their concentrations is crucial in order to achieve this. In the jejunum, *i.e.* the middle segment of the small intestine, of a fasted human, the concentration of the following compounds was determined as; bile salts 2 ± 0.2 mM, sodium 142 ± 13 mM, chloride 126±19 mM, calcium 0.5±0.3 mM (Mudie *et al.*, 2010). In an attempt to standardize these concentrations in an *in vitro* lipolysis protocol, the values were determined to be as in Table 7 (Li *et al.*, 2011). The salt mixture containing $CaCl_2$ and NaCl in the lipolysis medium, precipitates with bile salts and removes lipolysis products from the solution.

Throughout the lipolysis experiment, the titrator instrument records the amount of NaOH added to the lipolysis mixture at different time points and saves these time points in a measurement file. Complete *in vitro* lipolysis of an emulsion yields in a typical curve as shown in Figure 13, where a corn oil emulsion containing 2% T80 was lipolyzed using 1.2 mg/ml pancreatin and 1.2 mg/ml lipase. The typical curve can be analyzed in two separate areas. The first area contains an increasing steep slope until around 500 seconds. The second area contains a shallow slope that reaches a plateau. However, there were emulsions which did not exhibit this typical curve. Complete *in vitro* lipolysis plots of these emulsions can be found in Appendix G (*p.* 88). MQ-H_2O and pure T80 were also subjected to *in vitro* lipolysis in order to observe any possible lipolysis or buffer capacity of the bile salts. The complete *in vitro* lipolysis plots of H_2O and T80 can be found in Appendix G, Figure 38 and Figure 39, respectively (*p.* 88). These plots also did not exhibit the typical curve.

Table 7: Final concentrations of lipolysis ingredients, duration and pH recording frequency of Method 1 and Method 2.

Ingredients	Final concentration in intestinal medium	
	Method 1	Method 2
Bile extract (fasted)	5 mg/ml	5 mg/ml
Pancreatin (fasted)	0.4 mg/ml	1.2 mg/ml
Lipase (fasted)	-	1.2 mg/ml
$CaCl_2$	10 mM	10 mM
NaCl	150 mM	150 mM
HEPES	~5 mM	~5 mM
Emulsion	4% (v/v)	3% (v/v)
Lipolysis duration	3600 or 7200 s	2000 s
pH recording	Every 30 seconds	Every 2 seconds
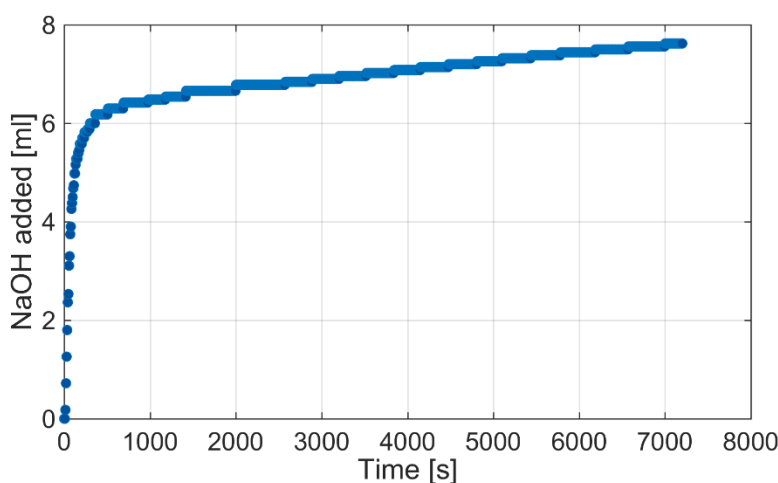
Figure 13: *In vitro* lipolysis of 20% (w/w) corn oil emulsion with 2% T80. 1.2 mg/ml pancreatin and 1.2 mg/ml lipase were used in the reaction. *In vitro* lipolysis was performed with Method 1.

Lipolysis of H_2O was performed with 0.4 mg/ml pancreatin. There was an initial addition of 0.12 ml NaOH and no further NaOH was added throughout the *in vitro* lipolysis. This resulted in a linear straight line at 0.12 ml NaOH which indicated negligible lipolysis activity of the bile salt mixture and other lipolysis medium components (Appendix G, Figure 38 (*p.* 88)).

Lipolysis of T80 with 0.4 mg/ml pancreatin resulted in an increasing curve with a final NaOH volume of 0.27 ml (Appendix G, Figure 39 (*p.* 88)). T80 contains oleic acid which is a monounsaturated fatty acid with 18 carbons. Oleic acid forms ester bonds with the sorbitan head of T80 that are cleavable by lipase. This experiment indicated that pure T80 contributes to the total lipolysis taking place in the *in vitro* lipolysis of other emulsions. This also points out the possibility of T80 being lipolyzed by gastric lipase *in vivo*, potentially leading to loss of emulsification ability and destabilization of the emulsion.

Figure 40 in Appendix G (*p.* 89) shows the complete *in vitro* lipolysis curve of 20% (w/w) corn oil emulsion with 2% T80. The difference between Figure 40 and Figure 13 is the utilization of different *in vitro* lipolysis methods. Figure 40, performed with Method 2, shows an unusual pattern when compared to Figure 13 which represents the typical curve. With Method 2, the two areas of the curve are separated from each other with an instant bending. However, with Method 1, the transition between the two areas is smoother and more continuous. Figure 41 and Figure 42 in Appendix G (*p.* 89 and 90, respectively) are further examples of the *in vitro* lipolysis experiments, performed with Method 2, which deviates from the typical curve.

The complete *in vitro* lipolysis curve contains information about the initial lipolysis rate of an emulsion (Subsection 3.3.2 and 3.3.3). Furthermore, different emulsions require different NaOH amounts to reach the plateau, which can be used as a source of information about the lipolysis capacity (Table 19 (*p.* 93)).

3.3.1. Back-Titration Experiments

As introduced in Subsection 1.5.2, Back-Titration experiments were performed to estimate the total extent of lipolysis of different emulsions. To find the quantity of unionized fatty acids, NaOH was added manually after the lipolysis was completed at pH 7, and the pH was increased to 10 gradually. The results of all performed Back-Titration experiments can be found in Table 8.

The additional NaOH added in the Back-Titration of emulsions are compared to the Back-Titration of a control solution, *i.e.* the emulsion is substituted with MQ-H_2O, since without fatty acids bile salts might also have a buffer capacity. Emulsions of different oil types are of interest when performing Back-Titration experiments since different oils contain different fatty acids with different pKa values. It is also known that different triglycerides may not be completely lipolyzed to the same extent (Benito-Gallo et al., 2015). In this context, the Back-Titration results of corn oil, olive oil and coconut oil emulsions containing 2% T80 were compared in Figure 14. The results were normalized to complete to 100%.

In Subsection 1.6.4, fatty acid compositions of different oils were introduced (Table 1). Each of these fatty acids have a pKa value. As a rule, fatty acids with shorter chain length have lower pKa values, whereas longer chain length results in higher pKa. From this principle, it is expected that coconut oil would have a lower pKa average, compared to corn oil and olive oil. Another rule for the pKa of fatty acids is the unsaturation level. The more unsaturated a fatty acid is, the lower its pKa value is. Olive oil is mostly composed of oleic acid (78%), while corn oil is mostly composed of linoleic acid (52%). From the aforementioned rule, olive oil is expected to have a higher average pKa value, compared to corn oil. Therefore, coconut oil, corn oil and olive oil can be sorted from the lowest pKa value to the highest (from calculated values at 20°C: coconut oil approximately 5.6, corn oil 8.9 and olive oil 9.3). Figure 14 indicates that at pH 7, coconut oil requires the largest volume of NaOH to be titrated, compared to corn oil and olive oil. At pH 7, 74% of the fatty acids of coconut oil were ionized, whereas this number was 55% and 64% for corn oil and olive oil, respectively. This outcome fits with the fact that MCFAs, like in coconut oil have lower pKa values. However, observing that olive oil requires more NaOH at pH 7, compared to corn oil, does not fit with the pKa estimations which were made earlier.

Table 8: All Back-Titration experiments were performed after in vitro lipolysis with Method 1. "P" stands for pancreatin and "L" stands for lipase.

	T80 [%] (w/w)	Enzyme concentration	Cumulative NaOH [ml] added			
			Direct Titration	Back Titration		
			pH 7	pH 8	pH 9	pH 10
H_2O	-	0.4 mg/ml P	0.120	1.236	1.900	2.546
H_2O	-	1.2 mg/ml P and 1.2 mg/ml L	0.450	2.149	3.599	5.507
T80	100	0.4 mg/ml P	0.270	1.372	1.990	2.584
Emulsion oil type						
	2	0.4 mg/ml P	5.880	8.434	9.682	10.148
	2	1.2 mg/ml P and 1.2 mg/ml L	7.840	11.538	13.416	15.850
	2	1.2 mg/ml P and 1.2 mg/ml L	7.620	11.278	13.430	15.587
	2	1.2 mg/ml P and 1.2 mg/ml L	8.550	11.592	13.996	16.603
Corn oil	1	0.4 mg/ml P	6.133	8.787	9.655	10.557
	0.5	0.4 mg/ml P	6.768	9.702	10.732	11.590
	0.25	0.4 mg/ml P	6.840	9.434	10.570	11.412
	2 (No SB)	0.4 mg/ml P	5.161	7.545	8.561	9.451
	2 (No SB)	0.8 mg/ml P and 0.8 mg/ml L	6.241	8.359	9.098	10.327
Olive oil	2	1.2 mg/ml P and 1.2 mg/ml L	9.525	12.278	14.338	17.068
Coconut oil	2	1.2 mg/ml P and 1.2 mg/ml L	13.679	16.377	18.332	20.864

The number of moles of fatty acids that can potentially be lipolyzed in different oils can be estimated. In order to do that, the average molecular weight of the TAGs in corn oil, olive oil and coconut oil were calculated. The fatty acid composition and their percentages are considered (Table 1). The individual molecular weight of each fatty acid was multiplied with the percentage they compose in an oil type. When this number was divided by the percentage, the average fatty acid molecular weight was found. Since a TAG molecule contains three fatty acids and a glycerol backbone, the average fatty acid molecular weight was multiplied by three and summed with the molecular weight of glycerol (92.1 g/mol).
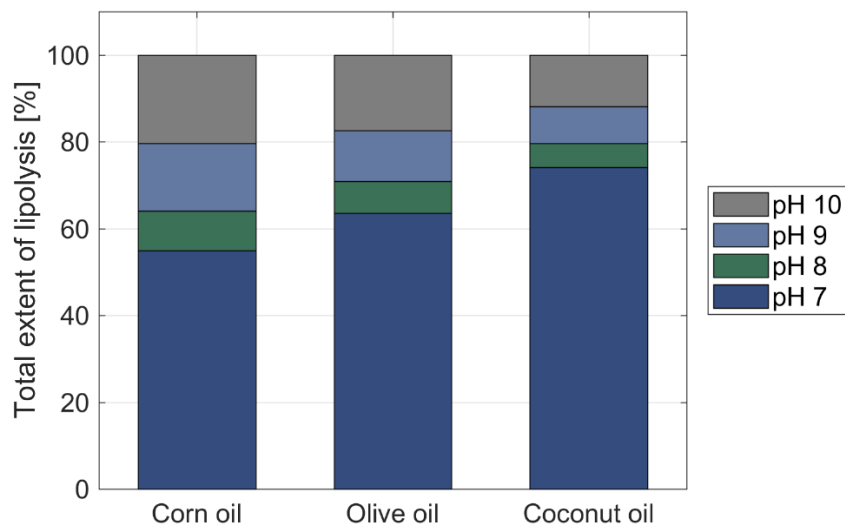
Figure 14: Back titration of the corn oil, olive oil and coconut oil emulsions containing 2% (w/w) T80. Titrated NaOH to maintain pH at 7, 8, 9 and 10 were subtracted from the control lipolysis medium which contained MQ-H_2O.

The calculations resulted in the following numbers for the average molecular weight of TAGs in each oil type: corn oil 834.1 g/mol, olive oil 839 g/mol and coconut oil 637.7 g/mol. Therefore, in each gram of corn oil there are 1 / 834.1 = 0.001199 moles of TAGs. With a similar calculation, olive oil has 0.001192 and coconut oil has 0.001568 moles of TAGs. When these values are compared, corn oil was found to have 0.58% more fatty acids in the same amount of oil, when compared to olive oil. Coconut oil was found to have 30.8% more fatty acids in the same amount of oil when compared to corn oil, and 30.6% more fatty acids in the same amount of oil when compared to olive oil. Therefore, coconut oil was expected to require 30% more volume of NaOH to be completely titrated, compared to both corn oil and olive oil. Whereas, the difference between corn oil and olive oil was expected to be insignificant.

These theoretical calculations are to some extent confirmed by the results of the Back-Titration experiments (Figure 14). Coconut oil, as expected, required more NaOH to be completely titrated when compared to corn oil and olive oil, although the difference was 21% for corn oil and 25% for olive oil rather than the theoretical 30%. The *in vitro* lipolysis is a closed system where released free fatty acids may accumulate at the droplet surfaces and inhibit further lipase activity. It is possible that this inhibition effect stopped the lipolysis reaction before full breakdown of the coconut oil was achieved. Furthermore, the titrated NaOH difference between olive oil and corn oil was 3.2%, rather than an insignificant percentage. This observed difference in the lipolysis extent for corn oil and olive oil can be caused by random errors or the other compounds in olive oil which may have unknown effects on lipolysis (Subsection 1.6.4). A possible reason for the incomplete ionizations of the fatty acids may be the miscalculation of the fatty acid pKas since the apparent pKa of fatty acids within an aqueous micellar solution is usually higher than the values calculated in standard conditions (Williams *et al.*, 2012).

3.3.2. Enzyme Optimization

Throughout this study, the *in vitro* lipolysis protocol was optimized regarding enzyme type and concentration in order to understand if the reactions were enzyme limited or substrate limited. It is possible

to simulate the enzyme composition of the small intestine by mixing appropriate amounts of enzymes in the lipolysis medium (Boisen *et al.*, 1991). As introduced in Subsection 1.5.1, gastric lipase and pancreatic lipase are two important enzymes that play role in the digestion of lipids in humans. Gastric lipases were not available for purchase; therefore, they could not be included in this study. Initially only pancreatin from porcine pancreas (0.4 mg/ml or 0.8 mg/ml) was used in the *in vitro* lipolysis experiments. Later in the optimization process, even though pancreatin from porcine pancreas contains lipase (>2 USP units/mg), a combination of pancreatin (1.2 mg/ml) and lipase from porcine pancreas (1.2 mg/ml) were used as the enzyme source (Table 7). The reason for including lipase in the enzyme mixture was the inadequacy of only pancreatin (0.4 mg/ml) to lipolyze the smallest droplet sized emulsions at maximum initial rate. Therefore, to avoid having to use a large amount of pancreatin to be able to reach several hundred units/mg that would provide the maximum initial lipolysis rate for the starbursted emulsions, lipase from porcine pancreas was included in the enzyme mixture. The enzymes were prepared fresh during each *in vitro* lipolysis experiment since the activity of an enzyme may be reduced over time (Hur *et al.*, 2011).

Several combinations and concentrations of enzymes were tested to investigate the lipolysis capacity of different emulsions (Table 9). In this enzyme optimization study, although all tested emulsions were corn oil emulsions, they differed in the T80 concentration (w/w) they contained. Initial *in vitro* lipolysis plots of all lipolysis experiments can be found in Appendix H (*p.* 91).

Table 9: Different combinations and concentrations of the digestive enzymes tested in this study. "+" indicates the presence of the enzyme, whereas "-" indicates the absence of the enzyme.

Concentration (mg/ml)	Enzyme	
	Pancreatin from porcine pancreas	Lipase from porcine pancreas
0.4	+	-
	+	+
0.8	+	+
1.2	+	+
2.4	+	+
3.6	+	+

The activity of pancreatin from porcine pancreas and lipase from porcine pancreas were noted in USP units as 16 USP units/mg, *i.e.* 8x USP, and 100 – 500 USP units/mg, respectively. One USP unit of lipase activity is contained in the amount of pancreatin which liberates 1 µmol fatty acid per minute from the olive oil/acacia emulsion substrate under standard USP assay conditions, *i.e.* at pH 9 and 37°C ("The United States Pharmacopoeia-National Formulary (USP 30 NF 25)," 2007). Although pH is set to 7 for the *in vitro* lipolysis experiments in this study, the USP activity unit was accepted.

Estimation of the initial rate of an *in vitro* lipolysis experiment is possible through generating a scatter plot of titrated NaOH versus time, inserting a linear trendline and calculating the slope of the trendline. When doing this, it is important to select a time interval that lays at the initial seconds and fits the regression line *i.e.* R^2. Selecting a time interval for a particular *in vitro* lipolysis experiment plot can be challenging since different intervals may yield different initial rates. Therefore, in this study, time points whose trend line had

an R^2 value larger than 0.95 were selected. Furthermore, the time points were selected after pH was stabilized at 7 through rapid NaOH titration.

The complete *in vitro* lipolysis curves, whether or not they fit the typical curve, have the characteristics of starting with an increasing steep slope, bending and reaching a plateau (Section 3.3). This is due to the digestive enzymes catalyzing the lipolysis of emulsions, liberating fatty acids until the substrate in the reaction is depleted. Focusing only on the initial curve is sufficient to observe the lipolysis rate since the lipolysis reaction speed decreases and the titration curve reaches a plateau. The lipolysis rate is expressed as millimole FA/min (mmol FA/min) throughout this study. This unit expresses millimoles of titrated fatty acids per minute. The lipolysis rate corresponds to the initial slope obtained from the *in vitro* lipolysis curve.

Earlier, Method 1 and Method 2 were compared in Section 3.3. *In vitro* lipolysis of these two methods yield different styles of curves. In Figure 15, the non-starbursted corn oil emulsion with 2% T80 was lipolyzed with different enzyme concentrations, combinations and methods. It is observed that Method 2 results in a ladder-like scatter plot with several seconds at a stable titrated NaOH amount. Whereas, In Method 1, the scatter plot is increasing without step-like lines. The main reason for this observation is the difference in recording intervals of each method, *i.e.* Method 1 records every 30 seconds and Method 2 records every 2 seconds. For this particular plot, the time intervals for the trendline were selected between approximately 25 to 250 seconds.

Legend:
- 0.4 mg/ml pancreatin (Method 1)
  y = 0.0046 x + 0.580
- 0.4 mg/ml pancreatin (Method 2)
  y = 0.0032 x + 0.554
- 0.8 mg/ml pancreatin + 0.8mg/ml lipase (Method 1)
  y = 0.0055 x + 0.993
- 1.2 mg/ml pancreatin + 1.2 mg/ml lipase (Method 2)
  y = 0.0037 x + 0.936
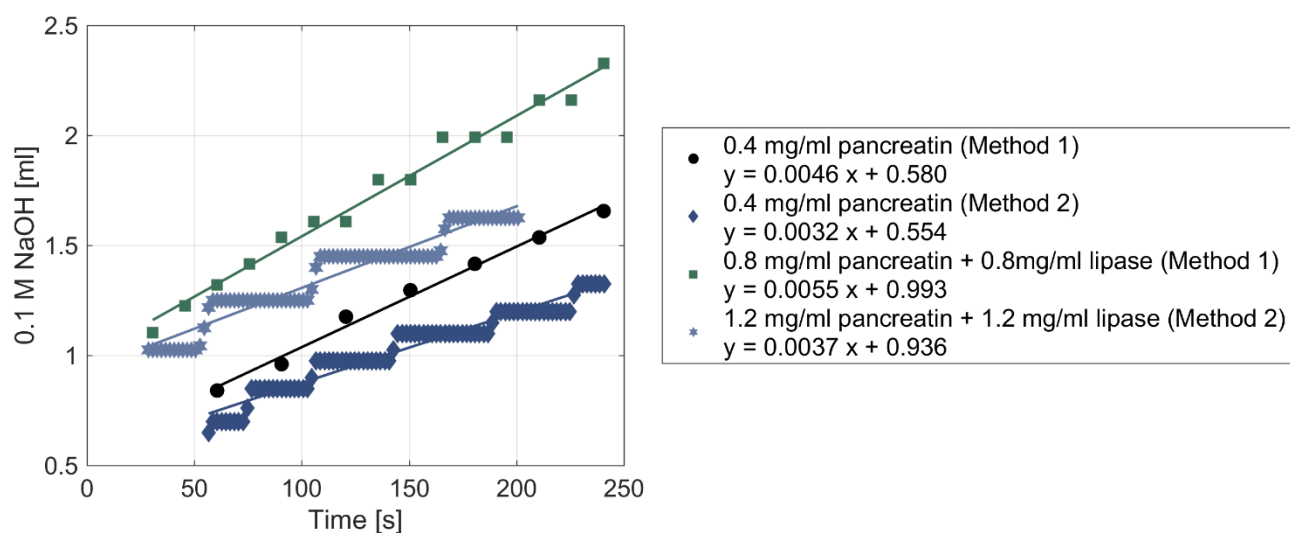
Figure 15: *In vitro* lipolysis of the non-starbursted 20% (w/w) corn oil emulsion with 2% T80. Different enzyme concentrations and compositions were used in the reaction. The *in vitro* lipolysis method used in each experiment was denoted in the figure legend.

Figure 15 compares several factors. First, Method 1 and 2 were compared through keeping the enzyme concentration constant at 0.4 mg/ml pancreatin. These two experiments resulted in different initial rates, 0.0046 mmol FA/min and 0.0032 mmol FA/min respectively. Method 1 contains 0.5 ml more emulsion than Method 2 (Table 7). Therefore, the difference in the initial rates can be explained by possible substrate limitation due to the non-starbursted emulsion. It should be noted that Method 1 and Method 2 are comparable since they do not differ in NaOH titration speed. Secondly, addition of lipase to the enzyme mixture results in faster lipolysis. Since an *in vitro* lipolysis was not performed with only 0.8 mg/ml

pancreatin, comparing 0.8 mg/ml pancreatin and lipase to 0.4 mg/ml pancreatin is not ideal. Nevertheless, it is observed that the non-starbursted corn oil emulsion yields faster lipolysis with additional lipase (0.0055 mmol FA/min) compared to pancreatin only (0.0046 mmol FA/min). The increased enzyme concentration of 1.2 mg/ml pancreatin and 1.2 mg/ml lipase did not result in faster lipolysis (0.0037 mmol FA/min) compared to 0.8 mg/ml pancreatin and lipase. Considering the enzyme activity of pancreatin (16 USP units/mg) and lipase (100 – 500 USP units/mg), the addition of lipase to pancreatin would result in at least 10 times higher enzyme activity. Despite this theoretical combined enzyme activity, it is observed that the initial rates do not differ as much. This points out a substrate limited lipolysis reaction for the non-starbursted emulsion. Since the non-starbursted emulsion exhibits large droplet size ($D[4,3]$ volume mean is 11.320 and $D[3,2]$ surface mean is 5.442), the enzymes might not be able to find sufficient surface area to catalyze the lipolysis reaction when their concentration is increased to 1.2 mg/ml.

A similar experiment was performed for the 2% starbursted corn oil emulsion (Figure 16). As the enzyme concentration increased and the lipase was added to the enzyme mixture, the lipolysis rate increased. When lipolysis was performed with 0.4 mg/ml pancreatin the lipolysis rate was 0.0134 mmol FA/min and the rate increased approximately 3 times when the enzyme concentration was increased 3 times and lipase was added to the mixture. However, after 1.2 mg/ml pancreatin and lipase, the lipolysis rate (0.0708 mmol FA/min) did not proportionally increase compared to 2.4 mg/ml pancreatin and lipase (0.0818 mmol FA/min) and 3.6 mg/ml pancreatin and lipase (0.0888 mmol FA/min). This plateau behavior can also be explained with substrate limited lipolysis reaction.

Legend:
- 0.4 mg/ml pancreatin
  y = 0.0134 x + 0.365
- 1.2 mg/ml pancreatin + 1.2 mg/ml lipase
  y = 0.0708 x - 0.066
- 2.4 mg/ml pancreatin + 2.4 mg/ml lipase
  y = 0.0818 x + 0.098
- 3.6 mg/ml pancreatin + 3.6 mg/ml lipase
  y = 0.0888 x + 0.227
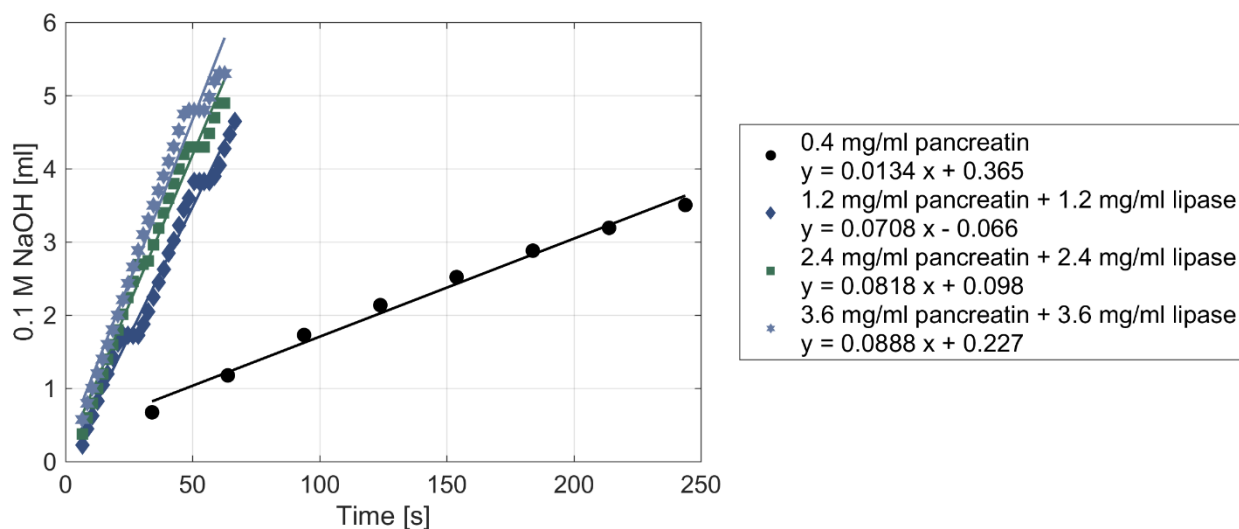
Figure 16: *In vitro* lipolysis of the 20% (w/w) corn oil emulsion with 2% T80. Different enzyme concentrations were used in the reaction. The *in vitro* lipolysis with 0.4 mg/ml was performed with Method 1, whereas the other experiments were performed with Method 2.

Figure 17 provides an overview of the initial rates of different corn oil emulsions lipolyzed with different enzyme combinations and concentrations. The insufficiency of 0.4 mg/ml pancreatin to lipolyze the starbursted emulsions is noted as higher concentrations of pancreatin and lipase provided faster lipolysis. The initial rates, *i.e.* slope values, for each *in vitro* lipolysis experiment can be found in Appendix H, Table 19 (*p.* 93).
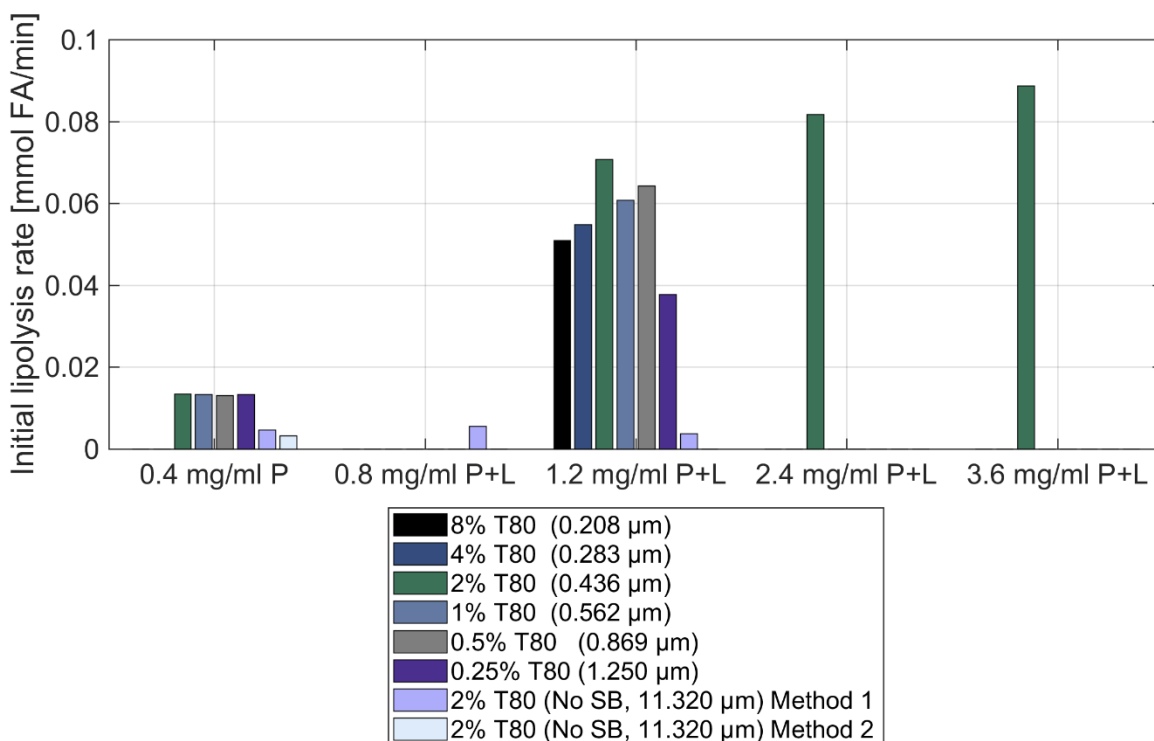
Figure 17: Initial rates of corn oil emulsions obtained from the *in vitro* lipolysis plots. The emulsions contained 8 – 0.25% T80. "P" stands for pancreatin and "L" stands for lipase. The non-starbursted emulsion was lipolyzed with Method 1 and Method 2 with 0.4 mg/ml pancreatin. The other corn oil emulsions were lipolyzed with Method 1 with 0.4 mg/ml pancreatin. The experiments with the remaining enzyme concentrations were performed with Method 2. The *D[4,3]* volume mean of each emulsion is presented next to the T80 percentage in the figure legend.

Corn oil emulsions with different T80 concentrations and therefore with different droplet sizes were subjected to *in vitro* lipolysis with 1.2 mg/ml pancreatin and 1.2 mg/ml lipase (Appendix H, Figure 44 (*p.* 91)). The lipolysis rate was expected to increase as the T80 concentration increases since the droplet size decreases. This trend was observed until 2% T80 (highest lipolysis rate of 0.0708 mmol FA/min). With higher T80 concentrations (at 4% and 8%), the lipolysis rate decreased (0.0549 mmol FA/min and 0.0510 mmol FA/min, respectively). This points out an enzyme limited reaction at 1.2 mg/ml pancreatin and lipase. It was concluded that higher enzyme concentrations were needed to lipolyze 4% and 8% T80 emulsions at maximum rate. The decrease in the lipolysis rate can be explained by the excess T80 in the reaction. The effect of excess T80 on the lipolysis rate was tested by M. J. Dille. The T80% of the tested emulsion was kept constant at 0.25%, and 1.2 mg/ml pancreatin and 1.2 mg/ml lipase were used in the reaction. Introducing twice as much T80 to the *in vitro* lipolysis reaction resulted in 21.6% slower lipolysis. When four times more T80 was added to the reaction, the lipolysis rate decreased by 41% (Data not shown, M. J. Dille, personal communication, 05.08.2018).

Another similar comparison was studied on the corn oil emulsions with different T80 concentrations where they were lipolyzed at a constant enzyme concentration of 0.4 mg/ml pancreatin (Appendix H, Figure 43 (*p.* 91)). The results indicated an enzyme limited lipolysis reaction since the starbursted emulsions exhibited similar initial rates amongst themselves.

3.3.3. Oil Type Comparison

The effect of oil type on the initial lipolysis rate was investigated at three different droplet sizes. Non-starbursted 2% T80, 0.25% T80 and starbursted 2% T80. Corn oil, olive oil and coconut oil emulsions were subjected to *in vitro* lipolysis at constant 1.2 mg/ml pancreatin and 1.2 mg/ml lipase.

In Figure 18, oil type comparison of the 2% T80 emulsions is given. The initial lipolysis rate of coconut oil was the highest with 0.0981 mmol FA/min. Following coconut oil, corn oil had an initial lipolysis rate of 0.0708 mmol FA/min and the slowest lipolysis rate belonged to olive oil with 0.0651 mmol FA/min.
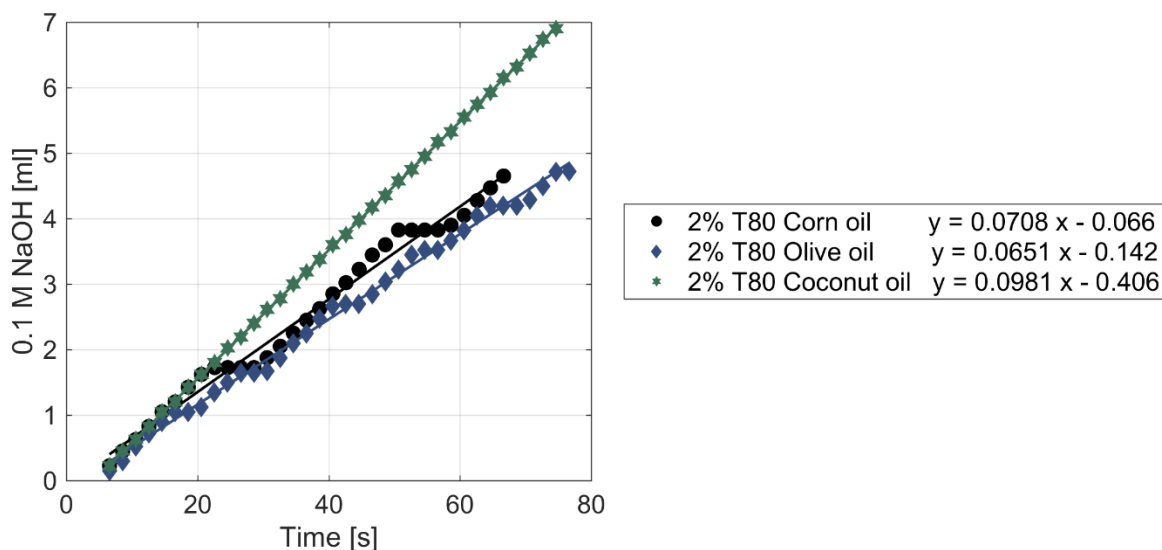
Figure 18: *In vitro* lipolysis of 20% (w/w) oil emulsions with different oil types (corn oil, olive oil and coconut oil). All emulsions contained 2% T80. 1.2 mg/ml pancreatin and 1.2 mg/ml lipase were used in the reaction. The *in vitro* lipolysis experiments were performed with Method 2.

The oil type comparison of 0.25% T80 emulsions with 1.2 mg/ml pancreatin and lipase can be found in Appendix H, Figure 45 (*p.* 92). As in 2% T80 emulsions, coconut oil had the highest initial lipolysis rate with 0.0707 mmol FA/min. However, corn oil and olive oil had similar rates with 0.0445 mmol FA/min and 0.0475 mmol FA/min, respectively. It should be noted that the initial lipolysis rate of the 0.25% T80 corn oil emulsion (0.0445 mmol FA/min) is different than the initial rate which was presented in the comparison for different droplet sized corn oils with 1.2 mg/ml pancreatin and 1.2 mg/ml lipase (0.0311 mmol FA/min) (Appendix H, Figure 44 (*p.* 91)). The reason for this difference was because two identical experiments were performed in order to investigate the reproducibility of the *in vitro* lipolysis protocol. The average value of these two experiments was presented in Table 19 (*p.* 93) with the uncertainty as the standard deviation (0.0378 ± 0.0067 mmol FA/min). The two replicas, and the standard deviation, indicate that the reproducibility of the *in vitro* lipolysis experiments may not be very high. Although, considering the method has shown very good reproducibility in other earlier tests, this difference in the lipolysis rate may be due to random errors.

Figure 46 in Appendix H (*p.* 92), shows the oil type comparison of the non-starbursted emulsions with 1.2 mg/ml pancreatin and 1.2 mg/ml lipase. As observed in the 2% T80 and 0.25% T80 emulsions of oil type comparison studies, the coconut oil emulsion had the highest initial lipolysis rate with 0.0080 mmol FA/min.

Corn oil followed with 0.0037 mmol FA/min and olive oil was last with 0.0031 mmol FA/min. The visual summary of the oil type comparisons for different droplet sized emulsions can be found in Figure 19.
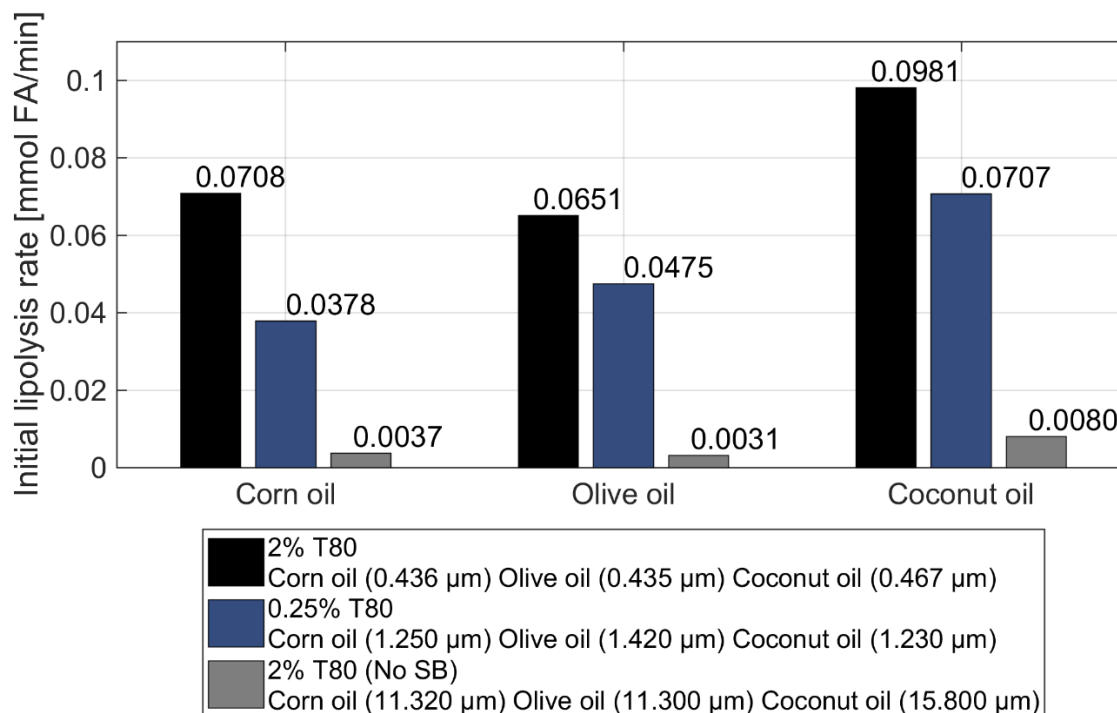
Figure 19: Oil type comparison of the initial rates obtained from the *in vitro* lipolysis experiments of different droplet sized emulsions prepared with 2% T80 (starbursted), 0.25% T80 and 2% T80 (non-starbursted). 1.2 mg/ml pancreatin and 1.2 mg/ml lipase were used in the reaction. The *in vitro* lipolysis experiments were performed with Method 2. The $D[4,3]$ volume mean of each emulsion is presented under the T80 percentage in the figure legend.

Considering all oil comparison experiments performed, it can be concluded that coconut oil is lipolyzed faster than corn oil and olive oil since it contains a high percentage of MCTs. MCTs have lower molecular weight and therefore, smaller size compared to LCTs. This provides more available triglycerides to be lipolyzed and results in faster lipolysis when the reaction is not enzyme limited. It should be noted that the oil type comparisons were performed when the T80 percentage was kept constant. However, this does not indicate that the droplet sizes of emulsions prepared with different oil types are the same (Figure 19). See Table 5 and the corresponding discussion in Section 3.1.

The initial rate difference between corn oil and olive oil is hard to determine since it changes for different T80 percentage comparisons. Moreover, olive oil is 2% (wt) composed of other compounds different than fatty acids. As described in Subsection 1.6.4, these other compounds are versatile, and the list includes phospholipids. The additional phospholipids in olive oil might affect the lipolysis by contributing to micelle formation. Phospholipids may inhibit pancreatic lipase – colipase complex activity by forming mixed micelles with bile salts and displacing pancreatic lipase form the oil-water interface (Larsen *et al.*, 2011; Patton *et al.*, 1981). On the other hand, considering *in vivo* conditions, the formation of mixed micelles facilitates the transport of emulsion contents, i.e. APIs. Therefore, finding an optimal phospholipid concentration for the *in vitro* lipolysis medium would reflect *in vivo* conditions more accurately and enable

the assessment of lipolysis rate evaluations for olive oil emulsions correctly since the phospholipid content in olive oil might be negligible compared to *in vivo* conditions.

3.4. Animal Experiments

The feeding scheme of rats was structured in a randomized fashion. Each five cages contained four rats with randomly assigned different feeds. This prevented an experimental error to influence all replicates in one feeding group, and provided the possibility of only random errors to occur in the experimental design.

The animal experiments were performed in accordance with the principles of 3Rs: replacement, reduction and refinement. Initially, blood sampling was attempted without any anesthetics by rolling the rat into a towel and stabilizing its movement by gently holding. However, this technique was not comfortable for the rat as it caused stress. Therefore, after the first attempt with this technique, the blood sampling was performed under anesthesia.

Before starting the animal experiments, a method testing was run to test the efficiency of the blood sampling from rats. This was performed on additional rats provided by CoMed, St. Olav's Hospital, NTNU. In the trial sampling, the blood was collected directly into the pro-coagulant tubes. This resulted in rapid coagulation and the clogging of the tube which prevented obtaining adequate volumes to be tested. Therefore, in the actual animal experiments, blood from the tail vein was first collected in heparinized tubes. Heparin is an anti-coagulant factor and when the blood contacts the tube walls, heparin dissolves in blood and prevents its coagulation. Later, the blood was transferred from the anti-coagulant tubes to the pro-coagulant eppendorfs before centrifugation. This step prevented the blood to be coagulated before centrifugation and enabled the separation of plasma from red and white blood cells. Plasma contains fibrinogen and coagulation factors. Utilization of anti-coagulants is necessary to separate plasma (Maton, 1993).

It was important to collect the blood samples from rats in an organized, time-dependent manner in order to obtain accurate results when the samples were analyzed with the UHPLC – MS/MS method. The exact times of each blood sampling can be found in Appendix C (*p.* 75). Blood sampling at 0h, *i.e.* before feeding, allowed each rat to be its own control, so that the natural vitamin levels from the rat feed could be removed if necessary. Immediately after the eppendorf tubes were centrifuged, the tubes were stored at -20°C. The plasma in the tubes were not thawed until the samples were to be pipetted to the sample analysis plate during sample preparation.

In rats, when dietary fats are consumed, lipolysis starts in the mouth with lingual lipases which are secreted along with saliva by serous lingual glands. Lingual lipases break down TAGs into DAGs and free fatty acids (Hamosh *et al.*, 1973). A difference between humans and rats is that in humans, lingual lipases do not contribute to lipolysis in a significant level (Feher, 2017). Whereas, in rats up to 30% of the ingested lipids are lipolyzed with lingual lipases (Hamosh *et al.*, 1979). In this experimental setup, contribution of lingual lipases to total lipolysis should not be overlooked. Even though, gavage feeding bypasses the rat mouth, lingual lipases also act in the rat stomach (Hamosh *et al.*, 1979).

3.4.1. Optimization of Sample Preparation for LC-MS Analyses

Plasma samples preparation for the UHPLC – MS/MS method was optimized. The sample preparation protocol was modified from MassTrak Vitamin D kit (Waters, 2017). However, this protocol was designed and developed for 25-hydroxyvitamin-D_3 (25-OH-vitamin D_3 and 25-OH-vitamin D_2) and its application to the other analyzed vitamins, *i.e.* vitamin D_3 (cholecalciferol) and vitamin E (tocopherol), required time-consuming optimization of the protocol. The optimized solid phase extraction (SPE) protocol can be found in Subsection 2.5.4.

For each sample preparation a standard curve was generated using standard solutions, which are known concentrations of the vitamins, and a blank solution. Mixing the standard solutions (or samples) together with the IS mixture, containing vitamin D_3-[d6], 25-Hydroxyvitamin-D_3-[23,24,25,26,27-13C5] and tocopherol-[d6], thoroughly was a crucial step. This enables the calibration of the response from samples with unknown concentrations of vitamins, using the ratio of the response of known concentration of the IS mixture. Thus, the IS corrects for the errors that may occur in the upcoming steps of the sample preparation protocol. All generated standard curves can be found in Appendix I (*p.* 94).

Initially, a pilot test using the additionally collected 24h rat plasma samples was performed. The results indicated that the response of tocopherol was too high to be detected with the current method. Therefore, a separate set of 25x diluted samples were prepared for the upcoming analyses of tocopherol. In general, the standard curve solutions of tocopherol presented high standard deviations, compared to vitamin D_3 and 25-OH-vitamin D_3.

Liquid/liquid extraction (LLE), as an alternative to SPE, was performed in a trial experiment. LLE is an extraction method which manipulates aqueous pH to extract molecules into an organic solvent (Juhascik *et al.*, 2009). The prepared standards and samples were analyzed with both Acquity UPC^2 System and UHPLC. The UPC^2 System resulted in considerably lower sensitivity compared to UHPLC. Therefore, the UPC^2 System was crossed out. The results with UHPLC exhibited variation among replicates of standard solutions and the samples. This variation was thought to be due to the utilization of an old column that is used by many research groups in the laboratory. Thus, a new column was purchased solely for this project. Since the results of the LLE method did not exceed the SPE method, the LLE was concluded not to be used in this work.

With the purchase of the new column, the SPE method was applied on the Cage 1 samples. The IS response of tocopherol was completely lost during SPE. Moreover, the sensitivity of all vitamins decreased, yielding smaller peaks of ISs. Whereas, when the ISs that were not subjected to SPE were analyzed with UHPLC – MS/MS method, they resulted in high peaks with good sensitivity. Therefore, the problem was determined to be with the SPE method. The cause of this problem was investigated by comparing the slight changes in the method, to the earlier tests, and resolving a single issue at a time.

First, the light sensitivity of the vitamins was considered. When the SPE was performed on all cage 1 samples as well as their 25x diluted samples, it required several hours to complete the protocol. Throughout the pipetting, the plate was subjected to light. Vitamin D_3 and vitamin E are known to be light sensitive (Aldrich, 2014, 2017). In order to test if the light exposure had an impact on the obtained response, one blank, *i.e.* only containing the diluent solution and IS mixture, was kept under light for an hour and then compared to another blank which was kept under light for a shorter period of time. The results showed no significant difference and the light sensitivity was crossed out as the potential problem.

Later, a freshly prepared wash solution, 60:40 methanol/water, was investigated. The solution was prepared again and was tested together with 40:60 methanol/water wash solution. The hypothesis was that some of the analyte might be lost in the washing step. However, there was no significant difference between the results of the two wash solutions. For the next trial, UHPLC – MS/MS method was finely tuned. The upcoming step was to try elution solutions with different polarity. In the established MassTrak Vitamin D kit, the elution was performed with 95:5 methanol/IPA. To increase the apolarity of the elution solution, 85:15 methanol/IPA and 100% IPA solutions were prepared and tested on blank samples and additionally collected 24h plasma samples. Compared to the previously tried 95:5 methanol/IPA solution, 85:15 methanol/IPA and 100% IPA showed greater elution capacity and resulted in higher response of ISs, blank solutions and samples (approximately 10 times increase with 100% IPA elution solution). Increasing the apolarity of the elution solution might result in the elution of unwanted compounds such as phospholipids, and cause ion suppression. From the results of the UHPLC – MS/MS analysis, it was observed that 85:15 methanol/IPA resulted in tocopherol IS response at $2.78 \cdot 10^5$, whereas 100% IPA provided $8.24 \cdot 10^5$ response. Since the height of the peak increased in the sample when 100% IPA was used, this provided some evidence that ion suppression is not severe. Therefore, it was decided to continue the analyses with 100% IPA as elution solution.

3.4.2. Plasma Sample Analyses with UHPLC – MS/MS

After thorough optimization of the SPE protocol and fine tuning the UHPLC – MS/MS method, the data was collected from the MassLynx software (v4.1) and TargetLynx application manager. Firstly, the retention time (RT) of the analytes were compared to the standard solutions. Incompatible RT values may indicate the observation of other analytes, rather than the one that is intended to detect. All RT values of analytes fitted the RT values of corresponding standards. Furthermore, the concentration of the analytes is supposed to be within the limits of the standard concentrations. The analytes whose concentrations exceeded the standard concentrations were eliminated from the analysis. In addition, the peak integration of each result was checked. The integrator is supposed to integrate the whole peak correctly to baseline, for both IS and the analyte transition. When the correct integration was not observed, the peak was integrated manually. The qualifier transition was also observed for each analyte. For vitamin D_3 and 25-OH-vitamin D_3, the signal to noise ratio was assumed to be 10:1 or higher. The complete processed results from the TargetLynx application manager can be found in Appendix I (*p.* 94).

The UHPLC – MS/MS results of tocopherol were only presented as raw data in Appendix I (*p.* 94), Table 22, Table 25, Table 28, Table 31 and Table 34. From the tables it is observed that several analyte concentrations could not be detected and shown as "N/A". In addition, the IS of tocopherol was lost in some Cage 1 and Cage 2 results and was low for most of the samples in the other cages. In general, the quality controls (QCs) of tocopherol showed high standard deviation. Moreover, the standard solutions of tocopherol showed standard deviation up to 539.8%. Because of all these reasons, it was concluded that vitamin E is not possible to be accurately analyzed with the current SPE method. Since the sample preparation protocol was modified from MassTrak Vitamin D kit, and the protocol was designed to analyze 25-hydroxyvitamin-D_3 compound, its application to vitamin E was unsuccessful. One possible explanation for this may be when tocopherol is eluted from the SPE column with 100% IPA, some phospholipids and compounds with similar polarity might also be eluted which consequently causes ion suppression in the UHPLC – MS/MS assay. Tocopherol may also be co-precipitated with the proteins in the samples during

the precipitation step. Either of these reasons or possibly a combination of them, might have resulted in the low ISTD response of tocopherol.

The standard curves exhibited different concentrations at different responses for the same analyte (From Figure 47 (*p.* 94) to Figure 57 (*p.* 121)), *e.g.* in the standard curve plots of vitamin D_3, the 5000 nM standard corresponded to 5 and $2 \cdot 10^4$ responses in Figure 47 (*p.* 94) and Figure 52 (*p.* 106), respectively. The reason behind this difference should be further investigated. For vitamin D_3 and 25-OH-vitamin D_3, the standard solutions showed standard deviation up to 157.2%.

The results of vitamin D_3 and 25-OH-vitamin D_3 can be found in Figure 20 and Figure 21, respectively. Figure 20A and Figure 21A shows raw concentration data obtained from the tables presented in Appendix I (*p.* 94), whereas Figure 20B and Figure 21B shows modified data where the analyte concentrations that exceeds the limits of standard concentrations were eliminated. In addition, in Figure 20B, cage 4 results were omitted when the average concentrations of vitamin D_3 were calculated. The reason for this was an unexpectedly and systemically observed high vitamin D_3 concentrations obtained from cage 4. This may be due to a systematic error and its possible reasons should be investigated further. It should be noted that cage 4 contained four rats with four different feed types. Therefore, its removal only affects the average vitamin D_3 concentrations at different time points and the standard deviations of the averages.

In Figure 20A, very high standard deviations, presented as error bars, are observed. Figure 20A only provides information about the pharmacokinetic trends of vitamin D_3 for different feed types, since the average values were not representative of the five rat replicas, *i.e.* high standard deviation was observed among the five replicas. With the modified results, Figure 20B exhibits lower standard deviations. From Figure 20B, the impact of different feed types on vitamin D_3 pharmacokinetics is analyzed through C_{max}, T_{max} and area under the concentration-time curve (AUC) values (Table 10). C_{max} is the maximum concentration of analyte, in this case vitamin D_3, in rat plasma. T_{max} shows the time point when C_{max} was reached in rat plasma. AUC provides information about the total vitamin D_3 compound in the rat plasma. AUC_{24h} is the cumulative vitamin D_3 concentration calculated at 24 hours.

B
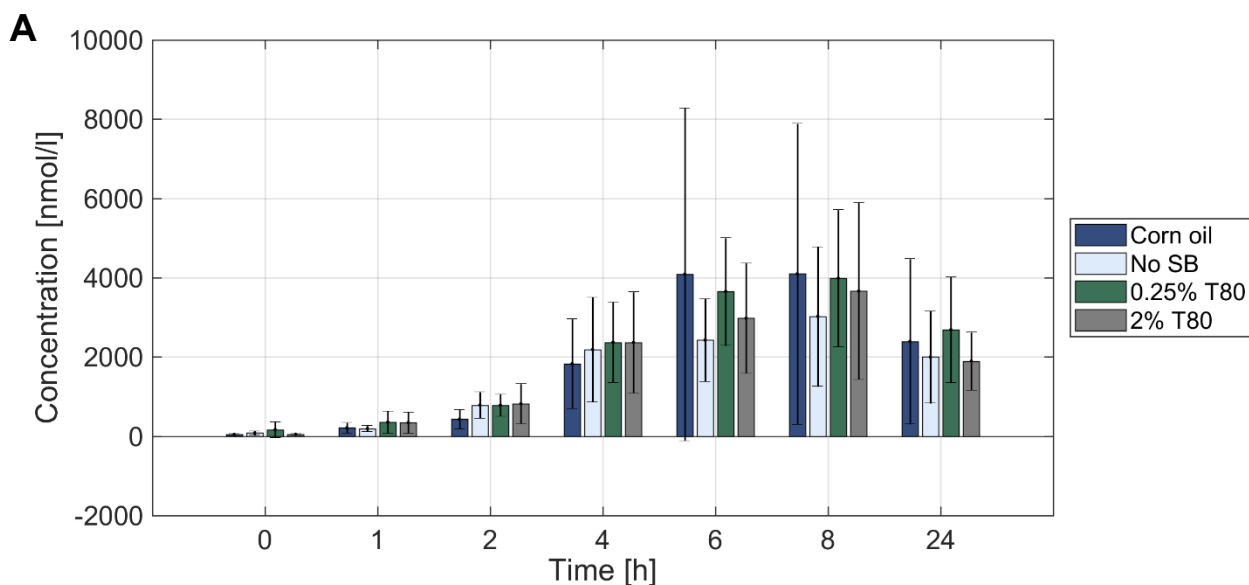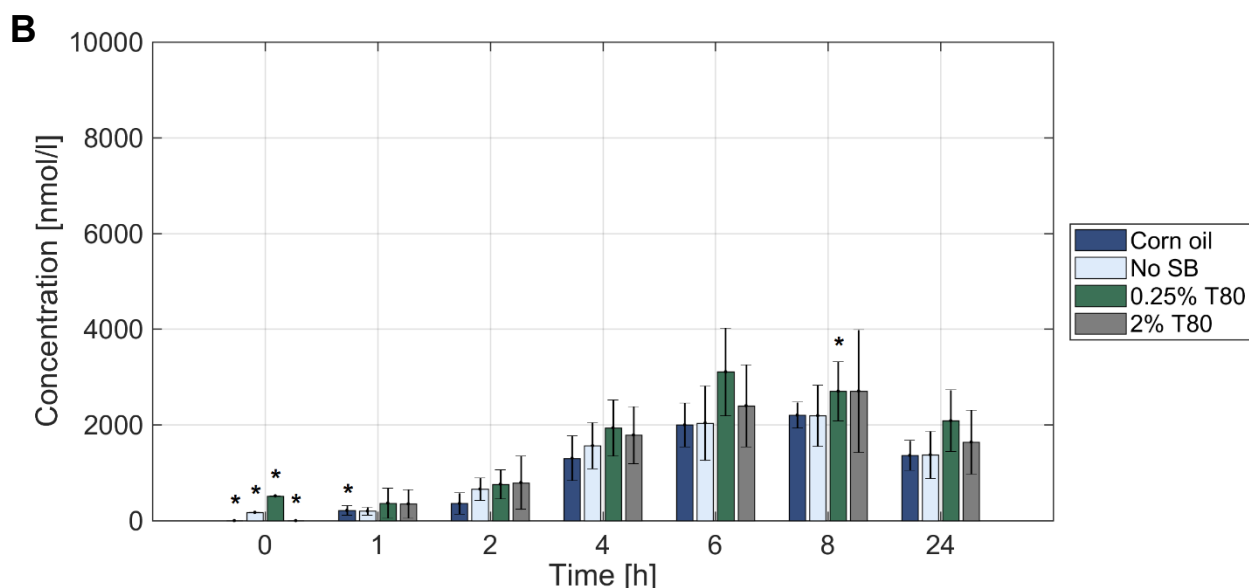
Figure 20: Time (h) vs. concentration (nmol/l) of vitamin D_3 in rat plasma upon feeding with pure corn oil and three corn oil emulsions with T80 concentrations. The non-starbursted emulsion (No SB) contained 2% T80. The error bars express the standard deviation of the average values. **A)** Concentration data including all samples. **B)** The concentrations exceeding the standard solution limits and cage 4 results were removed. "*" indicates the averages with removed outlier concentration values.

Table 10: Pharmacokinetics of vitamin D_3 in rat plasma upon being delivered with different feed types. The C_{max} values were presented as mean ± standard deviation.

Feed Type	C_{max} (nmol/l)	T_{max} (hours)	AUC_{24h} (nmol/l · hours)
Corn oil	2204 ± 271	8	38092
Non-starbursted 2% T80 corn oil emulsion	2191 ± 641	8	41919
0.25% T80 corn oil emulsion	3108 ± 915	6	55511
2% T80 corn oil emulsion	2706 ± 1279	8	50451

When cage 4 results and the concentrations exceeding the standard concentration limits were removed from Figure 20A, and Figure 20B was generated, the standard deviations of the average concentrations reduced. Nevertheless, this reduction still did not result in very small standard deviations. Although from Figure 20B, it is possible to comment on the pharmacokinetics of vitamin D_3 in rat plasma, its discussion is based on preliminary calculations and visual inspections. In order to investigate the UHPLC – MS/MS results in depth, further analysis should be performed (preferably by a medical analyst).

ANOVA test was performed on the C_{max} means in order to investigate if at least one feed type resulted in a significantly different C_{max} mean. In the test α was set to 0.05. The ANOVA test provided a p value of 0.523 and the F value (0.789) was smaller than F-critical value (3.490). These results indicated that there was no significant difference among the C_{max} means obtained from different feed types. Despite statistical insignificance, the 0.25% T80 emulsion resulted in the highest mean C_{max}, T_{max} and AUC_{24h} values at 3108

± 915 nmol/l, 6 hours and 55511 nmol/l, respectively. These results point out that the 0.25% T80 emulsion might have resulted in higher uptake when compared to the other feed types. In the *in vitro* lipolysis tests, 2% T80 emulsion exhibited 2.3 times faster lipolysis compared to 0.25% T80 emulsion when the lipolysis was catalyzed with 1.2 mg/ml pancreatin and 1.2 mg/ml lipase (Appendix H, Figure 44 (*p.* 91)). However, when these emulsions were compared at 0.4 mg/ml pancreatin, they resulted in almost the same initial lipolysis rate (Appendix H, Figure 43 (*p.* 91)). *In vivo*, observing possibly higher lipolysis rate with 0.25% T80, rather than 2% T80 emulsion, points out to a possible enzyme limited lipolysis reaction. In addition, the extra amount of T80 in the 2% T80 system might have slightly inhibited lipolysis. Other conclusions include the indication of the emulsion systems being superior to pure oil systems as corn oil resulted in the lowest AUC_{24h} value. It should be noted that a statistical test was not performed on the AUC_{24h} values.

25-OH-vitamin D_3 is the main metabolite of vitamin D_3 in the blood circulation (Subsection 1.8.1). Vitamin D_3 is hydroxylated to 25-OH-vitamin D_3 in the liver by cholecalciferol 25-hydroxylase, also known as vitamin D3-25-hydroxylase. The average of four rats plasma 25-OH-vitamin D_3 concentrations upon being fed three emulsions and one pure oil were plotted at seven time points (Figure 21).

In Figure 21B, cage 1 results were omitted when the average concentrations of 25-OH-vitamin D_3 were calculated. Cage 1 results exhibited very high concentrations when compared to the other cages. It should be noted that, throughout the SPE optimization protocol, cage 1 samples were eluted with 95:5 methanol/IPA. Nevertheless, the rest of the cages were eluted with 100% IPA solution, as the elution solution was optimized later. This might have resulted in drastically higher concentrations of 25-OH-vitamin D_3 in the cage 1 results. However, in theory, the ISs are supposed to correct for any changes in the SPE protocol and there should not be any difference between cage 1 and the results of other cages even though the SPE method was optimized. This issue remains unsolved and should be investigated further.

Similar to vitamin D_3 plots, in Figure 21A, very high standard deviations, presented as error bars, are observed. With the modified results, Figure 21B exhibited lower standard deviations. The removal of cage 1 from the average concentrations resulted in slightly steeper curves for all feed types. Initially obtained 0 hours concentrations of 25-OH-vitamin D_3 are in accordance with previously reported baseline levels of 25-OH-vitamin D_3 in the blood of rats (30 – 80 nmol/l) which were fed a normal diet (Stavenuiter *et al.*, 2015). The impact of different feed types on 25-OH-vitamin D_3 kinetics is preliminarily analyzed through C_{max}, T_{max} and AUC_{24h} values (Table 11).
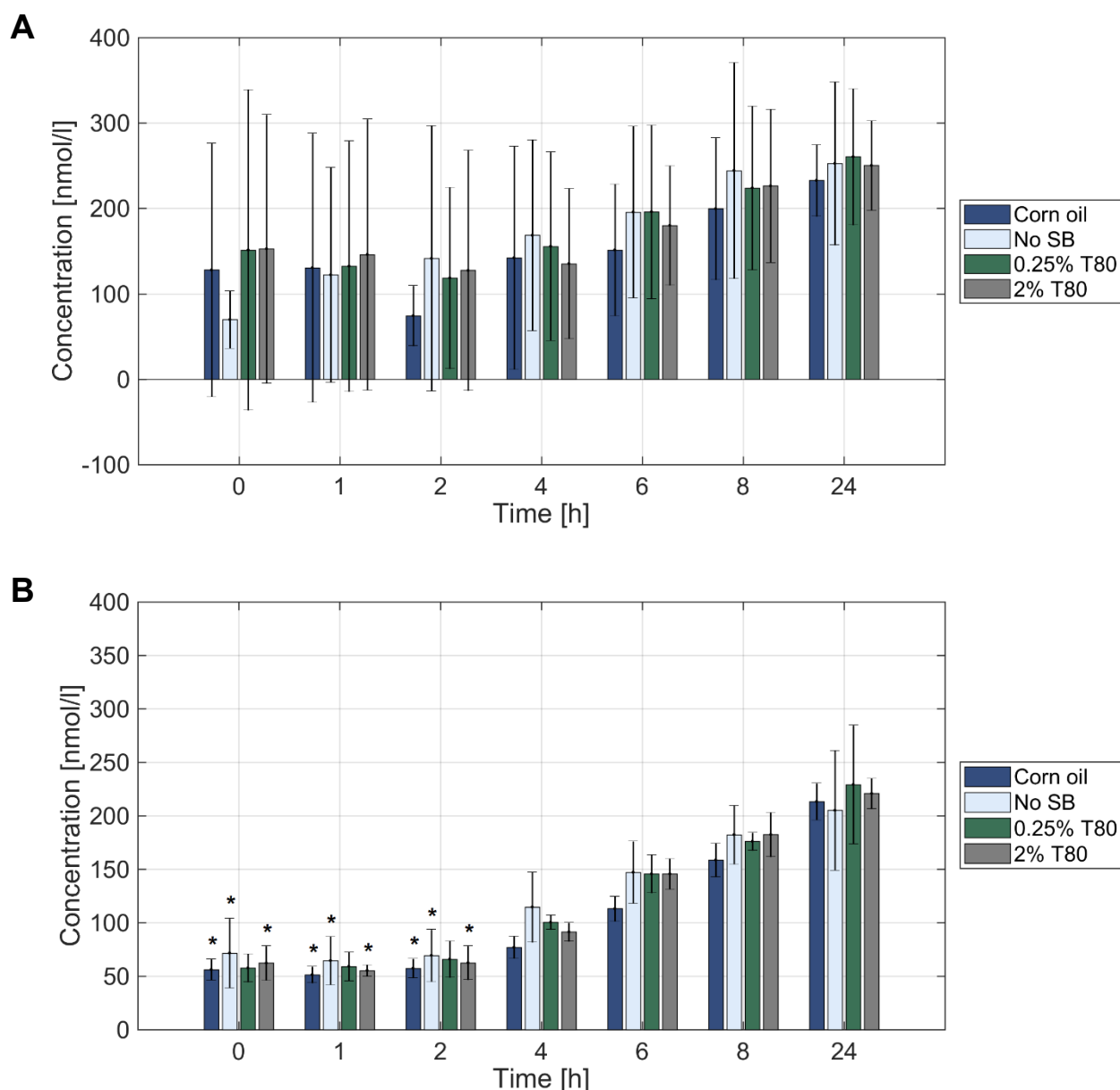
Figure 21: Time (h) vs. concentration (nmol/l) of 25-OH-vitamin D_3 in rat plasma upon feeding with pure corn oil and three corn oil emulsions with T80 concentrations. The non-starbursted emulsion (No SB) contained 2% T80. The error bars express the standard deviation of the average values. **A)** Concentration data including all samples. **B)** The concentrations exceeding the standard solution limits and Cage 1 results were removed. "*" indicates the averages with removed outlier concentration values.

As seen in Table 11, all feed types exhibited the highest concentration at 24 hours (T_{max}) which was the end point of this experiment. In a previous study, a human subject was orally given a single dose of 25 mg vitamin D_3 and the serum 25-OH-vitamin D_3 concentrations peaked at approximately day 10 (Haddad *et al.*, 1974). A similar trend would be expected for rats. Therefore, for the current study, the T_{max} is anticipated to be observed at a time point later than 24 hours. From visual inspection of Table 11, it was observed that 0.25% T80 corn oil emulsion showed the highest mean C_{max} and AUC_{24h} values at 229 ± 56 nmol/l and 4097 nmol/l · hours, respectively. However, no statistical significance test was applied on the results. This was because the peak point of 25-OH-vitamin D_3 in plasma could not be obtained (Figure

21B), *i.e.* T_{max} and C_{max} were not reached within this experiment. In general, similar pharmacokinetics were observed for the different feed types. This points out to the possibility that D3-25-hydroxylase enzyme might be saturated and catalyzing the hydroxylation reaction at maximum speed for all feed systems since the rats were fed with a large dose of vitamin D_3. Considering that the C_{max} means of vitamin D_3 was approximately 10 times higher than the C_{max} means of 25-OH-vitamin D_3, obtained data suggests an enzyme limited conversion of vitamin D_3 to 25-OH-vitamin D_3.

Table 11: Pharmacokinetics of 25-OH-vitamin D_3 in rat plasma upon being delivered with different feed types. The C_{max} values were presented as mean ± standard deviation.

Feed Type	C_{max} (nmol/l)	T_{max} (hours)	AUC_{24h} (nmol/l · hours)
Corn oil	213 ± 17	24	3679
Non-starbursted 2% T80 corn oil emulsion	205 ± 56	24	4008
0.25% T80 corn oil emulsion	229 ± 56	24	4097
2% T80 corn oil emulsion	221 ± 14	24	4061

The *in vitro* lipolysis experiments provided an understanding of the enzyme/substrate limitations for different emulsions and enzyme concentrations. However, the *in vitro* model is a static and closed system which cannot account for the complete series of reactions that take place *in vivo* (Kollipara *et al.*, 2014). On the other hand, the *in vivo* experiments provided a superior overview of the performance of different oil based formulations, *i.e.* pure corn oil and emulsions with different droplet sizes, in an open system. The *in vitro* experiments aided with the interpretation of the *in vivo* results regarding the determination of reaction limitations.

4. Conclusions and Future Perspectives

4.1. Conclusions

In this study, a series of *in vitro* and *in vivo* experiments were performed to optimize emulsions in order to designate the system which results in the fastest lipolysis/uptake of lipophilic compounds.

Although some exceptions were observed, the droplet size means of emulsions prepared with different oil types were found to be different when the T80 concentrations were kept constant. In the long term stability studies, starbursted corn oil emulsions were found to be visually more stable, upon long term storage at room temperature, compared to storage at +4°C, since they did not exhibit coalescing oil droplets on the surface. Vitamin D_3 and vitamin K_3 containing corn oil emulsions (1% T80 and 2% T80) were found to exhibit more visual destabilization in the form of coalescing oil droplets on the surface when stored at +4°C, compared to storage at room temperature. Vitamin D_3 and vitamin E containing starbursted corn oil emulsions were found to be stable upon long term storage at +4°C. In general, olive oil emulsions showed more visual destabilization in the form of creaming and color change when stored at +4°C, compared to storage at room temperature. Coconut oil emulsions, exhibited less stability when stored at +4°C, compared to storage at room temperature.

According to the Back-titration experiment results, the fatty acids in coconut oil were found to be ionized to a larger degree at pH 7, compared to corn oil and olive oil. In addition, coconut oil required 21% and 25% more NaOH to be completely titrated rather than the theoretical 30%, compared to corn oil and olive oil, respectively. Possible reasons for this observation include the inhibition of lipase activity by the free fatty acids of coconut in the closed *in vitro* system. *In vitro* lipolysis of corn oil emulsions with 0.4 mg/ml pancreatin was found to be enzyme limited for the starbursted emulsions. Whereas, with 1.2 mg/ml pancreatin and 1.2 mg/ml lipase 2% T80 corn oil emulsion exhibited the highest lipolysis rate. When the non-starbursted, 0.25% T80 and 2% T80 emulsions with different oil types were compared, coconut oil showed the highest lipolysis rate compared to olive oil and corn oil.

Considering the UHPLC – MS/MS results, the current SPE method was concluded to be unsuccessful to analyze tocopherol in rat plasma. Upon visual inspection of the pharmacokinetics data, Vitamin D_3 exhibited the highest T_{max}, C_{max} and AUC_{24} values when delivered with the 0.25% T80 corn oil emulsion. However, ANOVA test revealed no significant difference for the C_{max} means of different feed systems. The pharmacokinetics data only provided a trend-wise suggestion for the 25-OH vitamin D_3 concentrations in rat plasma. The T_{max} and C_{max} of 25-OH vitamin D_3 could not be reached within the current time points of the *in vivo* experiment. 25-OH vitamin D_3 showed the highest C_{max} and AUC_{24} values when delivered with the 0.25% T80 corn oil emulsion. However, all feed types resulted in similar trends. This observation pointed out to an enzyme limited conversion of vitamin D_3 to its circulating form 25-OH-vitamin D_3. Due to suggesting a possible increase in the uptake of vitamin D_3 based on the evaluation of different feed type trends, 0.25% T80 corn oil emulsion may be considered to be used in the upcoming steps of the *in vivo* tests.

In short, regarding all the results obtained in this study it can be concluded that there are differences in the rate of uptake of fat soluble compounds, *e.g.* vitamin D_3, when emulsified and the rate of uptake may depend on emulsion characteristics. However, vitamin D_3 is not biologically active until it is converted to

calcitriol and the *in vivo* results suggest the conversion of vitamin D_3 to 25-OH-vitamin D_3 is the rate limiting step. The detection of 25-OH vitamin D_3 in the rat plasma was concluded to be independent from the emulsion characteristics that delivered vitamin D_3 as there does not seem to be a substrate limitation in the conversion of vitamin D_3 to its circulating form 25-OH-vitamin D_3. Nevertheless, the studied vitamins were only model compounds and these differences in the emulsion characteristics might be important for pharmaceutical ingredients that are going to be tested in the upcoming *in vivo* experiments.

4.2. Future Perspectives

In most of the *in vitro* lipolysis rate results uncertainties could not be tested since only one experiment was carried out. In order to present statistically valid results, the replicas of the *in vitro* experiments should be performed and the lipolysis rate difference between the independent replicas should be presented as uncertainties. The Back-Titration experiments should be reperformed with equimolar amounts of triglycerides in order to obtain more easily comparable results. Since the droplet size means of emulsions prepared with different oil types were found to be different when the T80 concentration was kept constant, T80 percentages should be optimized to obtain different oil type emulsions with the same droplet size means. Subsequently, the oil type comparison for the *in vitro* lipolysis experiments should be repeated with the emulsions which have the same droplet size means.

For the detection of vitamin E with the UHPLC – MS/MS method, the current SPE protocol was concluded to be unsuccessful. Further optimization of the SPE protocol might solve this problem. Alternatively, a new protocol, different than the MassTrak Vitamin D kit, can be used to analyze tocopherol.

As pointed out in the FOTS application (Appendix A, *p.* 63), the animal experiments consist of three parts. In this thesis, only the first part, the emulsion droplet size comparison test, could be completed due to time and technical constraints. Therefore, in the future, the second part, *i.e.* oil type comparison test, and third part, *i.e.* the API delivery test, of the *in vivo* experiments should be completed as planned. An additional experiment for the *in vivo* studies may be the investigation of which route, lymphatic system or liver, MCTs and LCTs follow upon digestion in small intestine. This can be studied by feeding the rats with MCT or LCT, *i.e.* corn oil and coconut oil, emulsions containing lipophilic marker molecules and then collecting liver and lymph nodes. Collected organs may be used to extract lipophilic marker molecules to perform UHPLC – MS/MS analyses to detect the markers. An alternative would be tagging the feeding emulsions with a marker and imaging the animals real-time throughout the digestion and distribution of lipophilic marker molecules.

Upon completion of the *in vivo* experiments the optimized emulsion system would be established. The optimized emulsion can then be compared to SMEDDS/SNEDDS. After completing all the aforementioned future experiments, clinical trials should be carried out to test the efficacy of the optimized emulsion system in humans.

References

Akoh, C. C. (2005). *Handbook of functional lipids*: CRC press.

Aldrich, S. (2012a, 31.10.2012). Safety Data Sheet, Bile Extract, Porcine. Retrieved from
https://www.sigmaaldrich.com/MSDS/MSDS/DisplayMSDSPage.do?country=NO&language=EN-generic&productNumber=B8631&brand=SIGMA&PageToGoToURL=https%3A%2F%2Fwww.sigmaaldrich.com%2Fcatalog%2Fproduct%2Fsigma%2Fb8631%3Flang%3Den

Aldrich, S. (2012b). Safety Data Sheet, Menadione. Retrieved from
https://www.sigmaaldrich.com/MSDS/MSDS/DisplayMSDSPage.do?country=NO&language=EN-generic&productNumber=M5625&brand=SIGMA&PageToGoToURL=https%3A%2F%2Fwww.sigmaaldrich.com%2Fcatalog%2Fproduct%2Fsigma%2Fm5625%3Flang%3Den

Aldrich, S. (2014). Safety Data Sheet, Cholecalciferol. Retrieved from
https://www.sigmaaldrich.com/MSDS/MSDS/DisplayMSDSPage.do?country=NO&language=EN-generic&productNumber=PHR1237&brand=SIAL&PageToGoToURL=https%3A%2F%2Fwww.sigmaaldrich.com%2Fcatalog%2Fproduct%2Fsial%2Fphr1237%3Flang%3Den

Aldrich, S. (2017). Safety Data Sheet, (±)-α-Tocopherol. Retrieved from
https://www.sigmaaldrich.com/MSDS/MSDS/DisplayMSDSPage.do?country=NO&language=EN-generic&productNumber=T3251&brand=SIGMA&PageToGoToURL=https%3A%2F%2Fwww.sigmaaldrich.com%2Fcatalog%2Fproduct%2Fsigma%2Ft3251%3Flang%3Den

Beisson, F., Ferté, N., Bruley, S., Voultoury, R., Verger, R., & Arondel, V. (2001). Oil-bodies as substrates for lipolytic enzymes. *Biochimica et Biophysica Acta (BBA)-Molecular and Cell Biology of Lipids, 1531*(1), 47-58.

Benito-Gallo, P., Franceschetto, A., Wong, J. C., Marlow, M., Zann, V., Scholes, P., & Gershkovich, P. (2015). Chain length affects pancreatic lipase activity and the extent and pH–time profile of triglyceride lipolysis. *European Journal of Pharmaceutics and Biopharmaceutics, 93*, 353-362.

Berg, J. M., Tymoczko, J. L., & Stryer, L. (2012). *Biochemistry*. Basingstoke: W.H. Freeman.

Boisen, S., & Eggum, B. (1991). Critical evaluation of in vitro methods for estimating digestibility in simple-stomach animals. *Nutrition research reviews, 4*(1), 141-162.

Borel, P., Armand, M., Ythier, P., Dutot, G., Melin, C., Senft, M., . . . Lairon, D. (1994). Hydrolysis of emulsions with different triglycerides and droplet sizes by gastric lipase in vitro. Effect on pancreatic lipase activity. *The Journal of Nutritional Biochemistry, 5*(3), 124-133.

Bremer, L. G. (1992). *Fractal aggregation in relation to formation and properties of particle gels.* Bremer,

Carey, M. C., Small, D. M., & Bliss, C. M. (1983). Lipid digestion and absorption. *Annual Review of Physiology, 45*(1), 651-677.

Caspary, W. F. (1992). Physiology and pathophysiology of intestinal absorption. In: Oxford University Press.

Chayanoot, S., & Ausa, C. (2010). Separation of Olein-Stearin from Crude Palm Oil at Different Temperatures and Solvents by Centrifugation. *Asian Journal of Chemistry, 22*(2), 1453-1461.

Coupland, J. N., & McClements, D. J. (2001). Droplet size determination in food emulsions: comparison of ultrasonic and light scattering methods. *Journal of Food Engineering, 50*(2), 117-120.

CPS Instruments, E. (2015). Comparison of particle sizing methods. In.

Croce, P. (1999). Vivisection or science? An investigation into testing drugs and safeguarding health.

Dickinson, E. (2009). Hydrocolloids and emulsion stability. In *Handbook of Hydrocolloids (Second Edition)* (pp. 23-49): Elsevier.

Editors, L. (2013). Market Profile: UHPLC Versus Standard HPLC. *LCGC North America, 31*(5), 360.

Ellis, W. B. (1999). Books: Ullmann's Encyclopedia of Industrial Chemistry. *Journal of Industrial Ecology, 3*(2-3), 192-195.

FAO, W. (1989). *Toxicological evaluation of certain food additives and contaminants.* Paper presented at the The 33rd Meeting of the Joint FAO/WHO Expert Commitee on Food Additives. Cambridge: Cambridge University Press, Cambridge.

Feher, J. J. (2017). *Quantitative human physiology: an introduction*: Academic press.

Fernandez, S., Jannin, V., Rodier, J.-D., Ritter, N., Mahler, B., & Carrière, F. (2007). Comparative study on digestive lipase activities on the self emulsifying excipient Labrasol®, medium chain glycerides and PEG esters. *Biochimica et Biophysica Acta (BBA)-Molecular and Cell Biology of Lipids, 1771*(5), 633-640.

Flecknell, P. (2002). Replacement, reduction and refinement. *Altex, 19*(2), 73-78.

Fluttert, M., Dalm, S., & Oitzl, M. S. (2000). A refined method for sequential blood sampling by tail incision in rats. *Laboratory Animals, 34*(4), 372-378.

Gargouri, Y., Pieroni, G., Rivière, C., Lowe, P. A., Saunière, J.-F., Sarda, L., & Verger, R. (1986). Importance of human gastric lipase for intestinal lipolysis: an in vitro study. *Biochimica et Biophysica Acta (BBA)-Lipids and Lipid Metabolism, 879*(3), 419-423.

Glish, G. L., & Vachet, R. W. (2003). The basics of mass spectrometry in the twenty-first century. *Nature Reviews Drug Discovery, 2*(2), 140.

Griffin, W. C., & Lynch, M. J. (1968). Surface active agents. *Handbook of food additives, 2nd edn.(Ed.: Furia, TE)*, 397.

Gunstone, F. D. (1996). *Fatty acid and lipid chemistry*. London: Blackie Academic & Professional.

Gunstone, F. D. (2011). *Production and trade of vegetable oils*: Wiley Online Library.

Haddad, J. G., & Stamp, T. (1974). Circulating 25-hydroxyvitamin D in man. *The American journal of medicine, 57*(1), 57-62.

Hamosh, M. (1987). Development of Lipase Activity *Nestlé Nutrition Workshop Series, 2*.

Hamosh, M., Ganot, D., & Hamosh, P. (1979). Rat lingual lipase. *J Biol Chem, 254*, 12121-12125.

Hamosh, M., & Scow, R. O. (1973). Lingual lipase and its role in the digestion of dietary lipid. *The Journal of clinical investigation, 52*(1), 88-95.

Haug, I. J., Sagmo, L. B., Zeiss, D., Olsen, I. C., Draget, K. I., & Seternes, T. (2011). Bioavailability of EPA and DHA delivered by gelled emulsions and soft gel capsules. *European journal of lipid science and technology, 113*(2), 137-145.

Hauss, D. J. (2007). *Oral lipid-based formulations: enhancing the bioavailability of poorly water-soluble drugs* (Vol. 170): CRC Press.

Hofmann, A. (1963). The function of bile salts in fat absorption. The solvent properties of dilute micellar solutions of conjugated bile salts. *Biochemical Journal, 89*(1), 57.

Holmberg, K., Jönsson, B., Kronberg, B., & Lindman, B. (2003). *Surfactants and polymers in aqueous solution* (Vol. 2): Wiley Online Library.

Horiba Instruments, I. (2017). A Guidebook to Particle Size Analysis. In.

Hunter, R. J. (1986). *Foundations of Colloid Science* (Vol. 1). Oxford, UK: Oxford University Press.

Hur, S. J., Lim, B. O., Decker, E. A., & McClements, D. J. (2011). In vitro human digestion models for food applications. *Food Chemistry, 125*(1), 1-12.

Jiang, Z., Zhang, S., Wang, X., Yang, N., Zhu, Y., & Wilmore, D. (1993). A comparison of medium-chain and long-chain triglycerides in surgical patients. *Annals of surgery, 217*(2), 175.

Johnson, J. V., Yost, R. A., Kelley, P. E., & Bradford, D. C. (1990). Tandem-in-space and tandem-in-time mass spectrometry: triple quadrupoles and quadrupole ion traps. *Analytical Chemistry, 62*(20), 2162-2172.

Juhascik, M. P., & Jenkins, A. J. (2009). Comparison of liquid/liquid and solid-phase extraction for alkaline drugs. *Journal of chromatographic science, 47*(7), 553-557.

Kalepu, S., Manthina, M., & Padavala, V. (2013). Oral lipid-based drug delivery systems–an overview. *Acta Pharmaceutica Sinica B, 3*(6), 361-372.

Kanicky, J., Poniatowski, A., Mehta, N., & Shah, D. (2000). Cooperativity among molecules at interfaces in relation to various technological processes: effect of chain length on the p K a of fatty acid salt solutions. *Langmuir, 16*(1), 172-177.

Kanicky, J. R., & Shah, D. O. (2002). Effect of degree, type, and position of unsaturation on the pKa of long-chain fatty acids. *Journal of colloid and interface science, 256*(1), 201-207.

Kim, I., Worthen, A. J., Lotfollahi, M., Johnston, K. P., DiCarlo, D. A., & Huh, C. (2017). *Nanoparticle-stabilized emulsions for improved mobility control for adverse-mobility waterflooding.* Paper presented at the IOR 2017-19th European Symposium on Improved Oil Recovery.

Kimura, H., Futami, Y., Tarui, S.-i., & Shinomiya, T. (1982). Activation of human pancreatic lipase activity by calcium and bile salts. *The Journal of Biochemistry, 92*(1), 243-251.

Kollipara, S., & Gandhi, R. K. (2014). Pharmacokinetic aspects and in vitro–in vivo correlation potential for lipid-based formulations. *Acta Pharmaceutica Sinica B, 4*(5), 333-349.

Koroleva, M. Y., & Yurtov, E. V. e. (2012). Nanoemulsions: the properties, methods of preparation and promising applications. *Russian Chemical Reviews, 81*(1), 21-43.

Larsen, A. T., Sassene, P., & Müllertz, A. (2011). In vitro lipolysis models as a tool for the characterization of oral lipid and surfactant based drug delivery systems. *International journal of pharmaceutics, 417*(1-2), 245-255.

Lee, M. S., & Kerns, E. H. (1999). LC/MS applications in drug development. *Mass Spectrometry Reviews, 18*(3-4), 187-279.

Li, Y., Hu, M., & McClements, D. J. (2011). Factors affecting lipase digestibility of emulsified lipids using an in vitro digestion model: proposal for a standardised pH-stat method. *Food Chemistry, 126*(2), 498-505.

Liao, T. H., Hamosh, P., & Hamosh, M. (1984). Fat digestion by lingual lipase: mechanism of lipolysis in the stomach and upper small intestine. *Pediatric research, 18*(5), 402.

Loncin, M., & Merson, R. L. (1979). *Food Engineering: Principals And Selected Applications*. New York: Academic Press.

Mak, I. W., Evaniew, N., & Ghert, M. (2014). Lost in translation: animal models and clinical trials in cancer treatment. *American journal of translational research, 6*(2), 114.

Malvern Instruments, I. (2012). A basic guide to particle characterization. In *MRK1806-01*.

Malvern Instruments, I. (2018). Mastersizer 3000. Retrieved from https://www.malvernpanalytical.com/en/products/product-range/mastersizer-range/mastersizer-3000

Maton, A. (1993). *Human biology and health: Laboratory manual*: Prentice Hall.

Mazahery, H., & von Hurst, P. R. (2015). Factors affecting 25-hydroxyvitamin D concentration in response to vitamin D supplementation. *Nutrients, 7*(7), 5111-5142.

McClements, D. J. (2015). *Food emulsions: principles, practices, and techniques*: CRC press.

McClements, D. J. (2018). Enhanced delivery of lipophilic bioactives using emulsions: a review of major factors affecting vitamin, nutraceutical, and lipid bioaccessibility. *Food & function, 9*(1), 22-41.

McClements, D. J., & Demetriades, K. (1998). An integrated approach to the development of reduced-fat food emulsions. *Critical Reviews in Food Science and Nutrition, 38*(6), 511-536.

McClements, D. J., & Li, Y. (2010). Review of in vitro digestion models for rapid screening of emulsion-based systems. *Food & function, 1*(1), 32-59.

Mudie, D. M., Amidon, G. L., & Amidon, G. E. (2010). Physiological parameters for oral delivery and in vitro testing. *Molecular pharmaceutics, 7*(5), 1388-1405.

Mun, S., Decker, E. A., & McClements, D. J. (2007). Influence of emulsifier type on in vitro digestibility of lipid droplets by pancreatic lipase. *Food research international, 40*(6), 770-781.

References

N'Goma, J.-C. B., Amara, S., Dridi, K., Jannin, V., & Carrière, F. (2012). Understanding the lipid-digestion processes in the GI tract before designing lipid-based drug-delivery systems. *Therapeutic Delivery, 3*(1), 105-124.

Ng, S. P., Lai, O. M., Abas, F., Lim, H. K., & Tan, C. P. (2014). Stability of a concentrated oil-in-water emulsion model prepared using palm olein-based diacylglycerol/virgin coconut oil blends: Effects of the rheological properties, droplet size distribution and microstructure. *Food research international, 64*, 919-930.

Öztürk, B. (2017). Nanoemulsions for food fortification with lipophilic vitamins: Production challenges, stability, and bioavailability. *European journal of lipid science and technology, 119*(7), 1500539.

Patton, J. S., & Carey, M. C. (1981). Inhibition of human pancreatic lipase-colipase activity by mixed bile salt-phospholipid micelles. *American Journal of Physiology-Gastrointestinal and Liver Physiology, 241*(4), G328-G336.

Perel, P., Roberts, I., Sena, E., Wheble, P., Briscoe, C., Sandercock, P., . . . Khan, K. S. (2007). Comparison of treatment effects between animal experiments and clinical trials: systematic review. *Bmj, 334*(7586), 197.

Phan, C. T., & Tso, P. (2001). Intestinal lipid absorption and transport. *Frontiers in bioscience : a journal and virtual library, 6*, D299-319.

Porter, C. J., & Charman, W. N. (2001). In vitro assessment of oral lipid based formulations. *Advanced drug delivery reviews, 50*, S127-S147.

Pouton, C. W. (2006). Formulation of poorly water-soluble drugs for oral administration: physicochemical and physiological issues and the lipid formulation classification system. *European Journal of Pharmaceutical Sciences, 29*(3-4), 278-287.

Prabhu, S., Ortega, M., & Ma, C. (2005). Novel lipid-based formulations enhancing the in vitro dissolution and permeability characteristics of a poorly water-soluble model drug, piroxicam. *International journal of pharmaceutics, 301*(1-2), 209-216.

Rajagopalan, R., & Hiemenz, P. C. (1997). *Principles of colloid and surface chemistry* (Vol. 8247).

Rawle, A. (2003). Basic of principles of particle-size analysis. *Surface coatings international. Part A, Coatings journal, 86*(2), 58-65.

Roger, E., Lagarce, F., & Benoit, J.-P. (2011). Development and characterization of a novel lipid nanocapsule formulation of Sn38 for oral administration. *European Journal of Pharmaceutics and Biopharmaceutics, 79*(1), 181-188.

Salvia-Trujillo, L., Martín-Belloso, O., & McClements, D. J. (2016). Excipient nanoemulsions for improving oral bioavailability of bioactives. *Nanomaterials, 6*(1), 17.

Salway, J. G. (2016). *Metabolism at a Glance*: John Wiley & Sons.

Sassene, P., Kleberg, K., Williams, H. D., Bakala-N'Goma, J.-C., Carrière, F., Calderone, M., . . . Marchaud, D. (2014). Toward the establishment of standardized in vitro tests for lipid-based formulations, part 6: effects of varying pancreatin and calcium levels. *The AAPS journal, 16*(6), 1344-1357.

Schaefer, E. J., Jenkins, L. L., & Brewer Jr, H. B. (1978). Human chylomicron apolipoprotein metabolism. *Biochemical and biophysical research communications, 80*(2), 405-412.

Senior, J. R. (1964). Intestinal absorption of fats. *Journal of Lipid Research, 5*(4), 495-521.

Shepard, R. M., & Deluca, H. F. (1980). Plasma concentrations of vitamin D3 and its metabolites in the rat as influenced by vitamin D3 or 25-hydroxyvitamin D3 intakes. *Archives of Biochemistry and Biophysics, 202*(1), 43-53.

Shrestha, H., Bala, R., & Arora, S. (2014). Lipid-based drug delivery systems. *Journal of pharmaceutics, 2014*.

Silverthorn, D. U., Ober, W. C., Garrison, C. W., Silverthorn, A. C., & Johnson, B. R. (2013). *Human Physiology: An Integrated Approach, 6th Edition*: Pearson Education, Inc.

Souto, E. B., & Muller, R. H. (2007). *Nanoparticulate Drug Delivery Systems* (Vol. 166): Informa Healthcare.

St-Onge, M.-P., Bosarge, A., Goree, L. L. T., & Darnell, B. (2008). Medium chain triglyceride oil consumption as part of a weight loss diet does not lead to an adverse metabolic profile when compared to olive oil. *Journal of the American College of Nutrition, 27*(5), 547-552.

Stavenuiter, A. W., Arcidiacono, M. V., Ferrantelli, E., Keuning, E. D., Vila Cuenca, M., ter Wee, P. M., . . . Dusso, A. S. (2015). A novel rat model of vitamin D deficiency: safe and rapid induction of vitamin D and calcitriol deficiency without hyperparathyroidism. *BioMed research international, 2015*.

Suckow, M. A., Weisbroth, S. H., & Franklin, C. L. (2005). *The laboratory rat*: Elsevier.

Sun, M., Zhai, X., Xue, K., Hu, L., Yang, X., Li, G., & Si, L. (2011). Intestinal absorption and intestinal lymphatic transport of sirolimus from self-microemulsifying drug delivery systems assessed using the single-pass intestinal perfusion (SPIP) technique and a chylomicron flow blocking approach: linear correlation with oral bioavailabilities in rats. *European Journal of Pharmaceutical Sciences, 43*(3), 132-140.

Taylor, P. (1998). Ostwald ripening in emulsions. *Advances in colloid and interface science, 75*(2), 107-163.

Trevaskis, N. L., Charman, W. N., & Porter, C. J. (2008). Lipid-based delivery systems and intestinal lymphatic drug transport: a mechanistic update. *Advanced drug delivery reviews, 60*(6), 702-716.

Tso, P., & Balint, J. (1986). Formation and transport of chylomicrons by enterocytes to the lymphatics. *American Journal of Physiology-Gastrointestinal and Liver Physiology, 250*(6), G715-G726.

The United States Pharmacopoeia-National Formulary (USP 30 NF 25). (2007). In (pp. 2850-2854). Rockville, Md: United States Pharmacopeial Convention.

Urbaniak, G. C., & Plous, S. (2013). Research Randomizer (Version 4.0). Retrieved from https://www.randomizer.org/

Valenzuela, R., & Valenzuela, A. (2013). Overview About Lipid Structure. In *Lipid Metabolism*: InTech.

References

VWR, I. (2014). Safety Data Sheet, Sodium azide. Retrieved from
https://ni.vwr.com/assetsvc/asset/en_NI/id/7668043/contents

Wall, R., & Shani, M. (2008). Are animal models as good as we think? *Theriogenology, 69*(1), 2-9.

Walstra, P. (1983). Formation of emulsions. In *Encyclopedia of emulsion Technology, vol. 1. Basic Theory* (pp. 57-128).

Walstra, P. (1987). Fat crystallization. In *Food structure and behaviour, Vol. 1* (pp. 67-85): Royal Society of Chemistry.

Waters, C. (2017). MassTrak Vitamin D Solution: High-Throughput Vitamin D Analysis Made Simple. Retrieved from https://www.waters.com/webassets/cms/library/docs/720005793en.pdf

Weers, J. G. (1998). Molecular diffusion in emulsions and emulsion mixtures. In *Modern aspects of emulsion science* (pp. 292-327).

Williams, H. D., Sassene, P., Kleberg, K., Bakala-N'Goma, J.-C., Calderone, M., Jannin, V., . . . Jule, E. (2012). Toward the establishment of standardized in vitro tests for lipid-based formulations, part 1: method parameterization and comparison of in vitro digestion profiles across a range of representative formulations. *Journal of pharmaceutical sciences, 101*(9), 3360-3380.

You, Y.-Q. N., Ling, P.-R., Qu, J. Z., & Bistrian, B. R. (2008). Effects of medium-chain triglycerides, long-chain triglycerides, or 2-monododecanoin on fatty acid composition in the portal vein, intestinal lymph, and systemic circulation in rats. *Journal of Parenteral and Enteral Nutrition, 32*(2), 169-175.

Appendices

A FOTS Application

In Section 2.5, the animal experiment methods were described in detail. The FOTS application (numbered 11828) which was prepared to apply for this experiment set is given in this appendix. Although this application contains three steps of experiments intended to be performed, only the first step could be performed due to time constraints. The application includes general information, background and purpose, calculations on the number of animals needed, alternatives/3Rs, method description, information on animals and attachments about the designed experiments. The attachments include a time table for all experiments, a scheme of the animals for experimental groups, a publication about the tail incision method (Fluttert *et al.*, 2000) and the safety sheet of fenofibrate. The time table and the experimental group scheme were not given in this thesis in order to avoid repetition. The safety sheet of fenofibrate also does not take place in the appendix since that step of the experiment set could not be performed yet.

Application 11828: Optimising Emulsions for More Efficient Uptake of Lipophilic Compounds

Applicant and participants

Establishment	102: NTNU - Avdeling for komparativ medisin
Address	Postboks 8905
	7491 Trondheim
Telephone	72573399
E-mail	dyreavdelingen@medisin.ntnu.no
Local persons responsible for overseeing the welfare and care of the animals	Siv Eggen
	Anne Åm
Invoice address	NTNU, Felles Fakturamottak
	0508 Oslo Postboks 50, Økern
Birth date of applicant (for invoicing)	02.10.1984
Applicant	Morten Johnsen Dille - Forsker (Ansvarlig søker/Prosjektansvarlig) (Course in animal experimentation)
Participant 1	Tonje S. Steigedal - Forsker (Ansvarlig søker/Prosjektansvarlig) (Course in animal experimentation)
Participant 2	Tuna Baydin - Forsker (Ansvarlig søker/Prosjektansvarlig) (Course in animal experimentation)
Application date	18.08.2017

Application 11828: Optimising Emulsions for More Efficient Uptake of Lipophilic Compounds

General information

Id	11828
Invoice reference	N1748835
Working title	Optimising Emulsions for More Efficient Uptake of Lipophilic Compounds
Animal species	Pattedyr - gnagere (Rodentia) - Rotte (Rattus norvegicus)
Establishment	102: NTNU - Avdeling for komparativ medisin
Application category	Pilot experiment
Degree of distress for animals	Moderate distress

Reason for degree of distress for animals
Total degree of distress will be mild/moderate.

Rats will be fed with a small volume (1ml) using oral gavage, which will not cause significant distress for the animals[1]. Blood samples will be taken from the tail vein, in low volumes, minimizing pain and distress. The experiment itself will only last for 24 hours. Rats will be kept from solid food for 12 hours before the experiment + 8 hours into the experiment, but will have free access to sugar water for energy. For part 3, the rats may be kept in wire floor cages for the 24 hours of the experiment, to reduce/avoid coprophagia.

1. Turner PV, Vaughn E, Sunohara J, Junkin A, Ovari J, Leri F. Oral gavage in rats: an animal welfare issue? J Am Assoc Lab Anim Sci. 2011 In press.

Previous experience with comparable experiments	Yes
Experiments/procedures funded by	Annen finansieringskilde
Planned start	01.09.2017
Planned end	01.09.2020

Application summary (cf regulations § 8)
Previous experiments have shown that pre-emulsified oil may be digested and its constituents are taken up at a faster rate compared to bulk oil. This rate of digestion is also dependent on emulsion parameters such as droplet size or oil composition. We wish to further examine this link between emulsion parameters and digestion/uptake rate for our simplified emulsion system, and to do this we will perform the following experiment on rats (Sprague-Dawley).

The experiment will be performed in 3 steps:

1. Examination of emulsion droplet size influence on uptake kinetics. Rats will be divided up into 4 groups, with 5 rats in each group. 3 emulsions with different droplet sizes as well as 1 non-emulsified control feed will be prepared, with a lipophilic marker (fat soluble vitamin) in the oil phase. In the beginning of the experiment, the rats in each group will be fed with one of the feeds. Blood samples will be taken at time points (0, 1h, 2h, 4h, 6h, 8h, 24h), and analyzed for marker, giving a view of how quickly the marker is taken up and transported into blood for the different feeds.

2. Similar to part 1, except one droplet size is chosen (based on the results from part 1) and emulsions are prepared with two different oil types. It is known that triglycerides with certain fatty acids may promote or demote e.g. lymphatic transport on behalf of portal vein transport, and this experiment is to see if this difference is relevant for our emulsion system. 2 groups with 5 rats in each.

3. Based on the results in step 1 and 2, an optimized emulsion will be prepared containing a poorly bioavailable lipophilic active pharmaceutical ingredient (API) (Fenofibrate), in an attempt to increase the bioavailability and/or rate of uptake of this drug. This will be compared to a non-emulsified control. 2 groups with 5 rats in each.

For all steps: rat blood samples will be taken from the tail vein, which allows for repeated blood sampling with minimal pain and invasiveness. Blood volumes taken will be small, causing no discomfort for the animals. The feeds given to the animals are not expected to cause any issues, as they will be formulated using food grade ingredients (except for the API).

The results from these experiments may find use in optimizing pharma-/nutraceutical delivery systems or in formulation of improved animal feed.

Application 11828: Optimising Emulsions for More Efficient Uptake of Lipophilic Compounds

Public access

Does the application contain information that should be kept from public access?	Yes
If yes, refer to the act(s) and regulation(s) of relevance (examples: Open files act, article 13, 1st paragraph together with Public administration act, article 13, 1st paragraph, 2nd point).	Offentlighetsloven, § 13, 1. avsnitt og Forvaltningsloven, § 13, 1. avsnitt, 2

If yes, which information do you want to keep from public access?
Pre-clinical trials that may give rise to patent application(s)

Application 11828: Optimising Emulsions for More Efficient Uptake of Lipophilic Compounds

Background and purpose

Give a short presentation of the background and purpose of the experiment. Describe the hypothesis to be tested. If the experiments are required by law by public authorities, please refer to the relevant acts and regulations.
Lipolysis, the digestion of lipids, starts with the interaction of ingested lipids which are triglycerides (TG) with bile salts in the small intestine. Bile salts act as an emulsifier of the lipids. Lipases break down the TGs to free fatty acids (FAs) as well as di- and monoglycerides (MGs). Free FAs and MGs form micelles and these micelles are absorbed by enterocytes and in these intestinal epithelial cells, FAs and MG regenerate TGs. Then the TGs are packaged into lipoproteins called chylomicrons and tranferred to the lymphatic system. From there, TGs end up in the blood stream (Kalepu et al., 2013).

When lipophilic active pharmaceutical ingredients (APIs) are absorbed with long chain triglycerides (LCTs), their transport thorugh the lymphatic system is promoted (Trevaskis et al., 2008). However, when the API is transported thorugh the portal vein, it ends up in the liver and encounters the hepatic first-pass metabolism which may reduce the bioavailability of the drug (Sun et al., 2011). Therefore, delivering APIs through the lymphatic system may be a more efficient system to improve oral bioavailability of lipophilic drugs.

It was previously shown that emulsified omega-3 is taken up more rapidly than non-emulsified omega-3 (Haug et al., 2010).

Medium chain glycerides (MCTs) are degraded by lipolysis at higher rate than LCTs such as olive oil (Liao et al., 1984).

Considering all these previous findings, a novel delivery system of lipophilic APIs is going to be performed. The purpose of the experiment is to optimize the parameters of lipolysis: droplet size of the emulsions and the oil type. These optimized parameters are going to increase the bioavailability of lipophilic APIs. The findings can be used to improve the absorbtion of pharmaceutics and food supplements.

Reference list

Kalepu S., Manthina M. & Padavala V. (2013), 'Oral lipid-based drug delivery systems - an overview' Acta Pharmaceutica Sinica B, 3(6), 361-372.

Trevaskis N. L., Charman W. N. & Porter C. J. H. (2008), 'Lipid-based delivery systems and intestinal lymphatic drug transport: A mechanistic update' Advanced Drug Delivery Reviews, 60, 702-716.

Sun M., Zhai X., Xue K., Hu L., Yang X., Li G. & Si L. (2011), 'Intestinal absorption and intestinal lymphatic transport of sirolimus from self-microemulsifying drug delivery systems assessed using the single-pass intestinal perfusion (SPIP) technique and a chylomicron flow blocking approach: Linear correlation with oral bioavailabilities in rats' European Journal of Pharmaceutical Sciences, 43, 132-140.

Haug I. J., Sagmo L. B., Zeiss D., Olsen I. C., Draget K. I. & Seternes T. (2011), 'Bioavailability of EPA and DHA delivered by gelled emulsions and soft gel capsules' European Journal of Lipid Science and Technology, 113, 137-145.

Liao T. H., Hamosh P. & Hamosh M. (1984), 'Fat digestion by lingual lipase: Mechanism of lipolysis in the stomach and upper small intestine' Pediatric Research, 18, 402-409.

Application 11828: Optimising Emulsions for More Efficient Uptake of Lipophilic Compounds

Calculating number of animals

Give the rationale and justifications for the numbers of animals that will be used. Pilot experiments have to be carried out if any doubts or uncertainties about the number om animals (see § 6). Seek statistical help if you are in doubt
In some of the previous rat feeding studies, 5 animals in each group were chosen. Since this is a pilot study, using similar number of rats as past experiments were preferred.

Describe all experimental groups and group sizes. A table describing the groups and group sizes may be added as an attachment to this application
1. Pharmacokinetics of different droplet sizes
3 droplet sizes + 1 control = 4 groups
5 animal in each group
(5 * 4) = 20 animals

2. Different oil types experiment
2 groups
5 animals in each group
(2 * 5) = 10 animals

3. API experiment
2 group
5 animals
(2 * 5) = 10 animals

Total 40 animals.

Experimental groups divided by cages are shown as an excel table in attachment

Which statistical method has been used   Not applicable

If "Power analysis"/"Resource equation": Which input has been used?
If "Other method": Describe in detail the statistical method used.
If "Not applicable": Describe why statistics can not been applied.
Pilot study

Application 11828: Optimising Emulsions for More Efficient Uptake of Lipophilic Compounds

Alternatives/3Rs

Replacement: Why is it not possible to obtain the aim of this experiment without the use of animals? Which alternatives are considered and why were they rejected?
Lipid metabolism and uptake is a process too complex for in vitro models or simulations, as it is dependent on the interplay between many different organs/body systems.

List the databases and search terms you have used, searching for alternatives
pubmed, norecopa

"rat digestion model" "digestion models"

Reduction: When the use of animals is unavoidable: Which efforts, steps and measures have you taken to minimise the number of animals and still achieve valid scientific results?
Only male rats are going to be used to give less variability between individuals, to improve result quality with a low number of animals.

Refinement: When the use of animals is unavoidable: Which improvements of the husbandry and the procedures have been implemented to minimise the pain, suffering, distress and lasting harm and improve animal welfare, compared to previous comparable experiments? (Keywords: analgesia, anaesthesia, endpoints, environmental enrichment, surgical techniques, sampling techniques etc.).
Before the experiments, the rats will go through the acclimatization phase where they will be played with and handled to make the animals more comfortable and relaxed during the experiment. Before and during the experiment, rats will be given access to standard environmental enrichment. An oral gavage using water may be performed a few days before the experiments, to make the rats get used to the procedure.

The rats will not have access to solid food for 12 hours before and 8 hours into the experiment (total of 20 hours) to minimize interference from solid food particles and compounds on the results. However, the rats will still have access to sugar water for energy. The emulsions/oils given to the rats will also contain digestible energy.

The composition and volume of feed given to the rats is not expected to cause any harm or distress, beyond the discomfort of one oral gavage event for each rat. The highly experienced technical staff of the animal facility is going to perform the gavage on the rats, minimizing risk and discomfort.

The API used for part 3 has a low toxicity. In rats the oral LD50 is >2g/kg and the oral lowest published toxic dose (TDLO) is 9mg/kg. The amount of API given in this experiment will be below 9mg/kg, thus no toxic effects are expected, however the animals will be closely monitored for adverse effects.

Blood sampling will be performed through puncture/incision of tail vein, which provides rapid blood sampling with minimal pain and invasiveness and without the need for anaesthesia, optimal for repeated sampling. Blood volumes withdrawn will be small (total blood taken from each rat < 10% blood volume).

Methods description

Preparation of the animals before the actual experiment/intervention.
For field experiments: Describe any tracking, tracing, capture, resraint, transport, etc.
For lab experiments: Describe any purchase, transport, quarantine/acclimation, housing, environmental enrichment, feeding regime, tagging, weighing etc
The animals will be delivered via Forsøksdyrsentralen and will be acclimatised for at least 7 days before start of the experiment. The animals will be housed (4/cage) with access to environmental enrichment and food/water ad libitum.

For part 3, using cages with wire flooring for the 24 hours of the experiment may be necessary to reduce coprophagia, as some of the API may travel through the intestine and end up in excrement.

Describe the procedures (surgery, administration of test substance, physical treatments etc.) that will be applied to the animals during the experiment. You may also attach drawings, figures, protocols or timelines (activity map) to this application
For all parts:

12 hours before start of the experiments, solid food will be removed from the rats and replaced with access to sugar water.

At the start of the experiment, the animals will each be fed 1 ml of liquid emulsion or liquid non-emulsified oil through oral gavage. Each animal will be marked with a unique identifier, using a permanent marker.

100-200 µl blood will be withdrawn from each rat at specific time points (0h, 1h, 2h, 4h, 6h, 8h, 24h), through puncture/incision of tail vein. This method is described in detail in a research paper (can be found in

Application 11828: Optimising Emulsions for More Efficient Uptake of Lipophilic Compounds

attachments). For blood sampling, rats will be restrained by gently wrapping in a towel and holding. If necessary, a restrain cage will be used.

Solid food will be made available for the rats again 8 hours into the experiments.

Full time table for the experiments is attached.

Which parameters will be measured and which samples will be taken during the experiment?
For all parts:

100-200 µl blood will be withdrawn from each rat at specific time points (0h, 1h, 2h, 4h, 6h, 8h, 24h), through puncture of tail vein. Total amount of blood withdrawn from each rat will be <2 ml, <10 % of total blood volume. During the experiments, general health of the rats is going to be monitored with special focus on complications related to oral gavage and blood sampling.

Describe the follow-up and supervision of the animals during the experiment (before, during and after procedures).
Before: One week prior to the experiment, the rats are going to be pet and played with to lower the stress levels of the rats during the procedures. This also includes handling the animals and getting them used to restrain methods. An oral gavage using water may be performed a few days before the experiments, to make the rats get used to this procedure.

In addition, the researchers are going to attend a special training prior to the experiments. The training is going to include the practises of handling and blood sampling. Three animals are going to be taken from the animal facility for training purposes and these animals are going to be returned to the facility after the training (FOTS 5729).

Under: Monitoring general health. The rats will be observed for bleeding or inflammation around the blood sampling point as well as for adverse reactions to the gavage event or to the API (for part 3).

After: Euthanasia

If animals are to be euthanised:
Which method of euthanasia will be used (cf. regulations § 16, part 2 and appendix C)?
The animals will be put into deep anaesthesia with isoflurane, before bleeding out through aorta blood sampling.

If a method of euthanasia will be used, that is not mentioned in appendix C:
Describe the chosen method of euthanasia.
- - -

Reason for choosing a deviating method of euthanasia (cf. regulations § 16, part 3)
- - -

Criteria for humane endpoints, i.e. setting of clear, predictable and irreversible criteria that allow early termination of the experiments before the animals experience significant harm whilst still meeting the experimental objectives.
Damage of the food pipe or trachea during gavage feeding
- Symptoms: hunched posture, breathing problems (dyspnea/rales), general pain

Damage of the tail due to blood collection
- Inflammation that causes pain to the animal (see general pain symptoms)
- Spreading tail necrosis

Reactions to the emulsion formulations or API
- Symptoms: diarrhea, lethargy, signs of stomach pain (abdominal contractions, stretching/extension of hind limbs, back arch), general pain.

Bleeding: if total blood lost is approaching 10% of total blood volume

General pain symptoms: lethargy, facial expression (pronounced orbital tightening, nose/cheek flattening, curled/angled ear position, whisker tension)

Which actions will be taken if animals reach the humane endpoint (examples: treatment of symptoms, reduced exposure or euthanasia)?
If rats reach the humane endpoints, the animal(s) will be removed from the experiment and euthanasia will be performed.

Application 11828: Optimising Emulsions for More Efficient Uptake of Lipophilic Compounds

Animals (species, medication and pain assessment)

Animal species	Pattedyr - gnagere (Rodentia) - Rotte (Rattus norvegicus)
Strain/line	Sprague Dawley
Sex	Male
Number of animals	40
Weight at start	250 g
Weight at end	250 g
Age	- - -
Number of reused animals (§ 17)	Reuse not applicable
Experience with this species	Yes
Describe the distribution of animals according to sex, weight and age	- - -
Duration for the most affected individual animal (d, h, min)	1, 12, 0

Animals with a deviant phenotype

Do the animals have any congenital or hereditary disease/illness or other abnormalities related to their phenotype that may impair their welfare (examples: diabetes, autoimmun disease, tumors)?
No

No known or described incidents in litterature ☑

Describe wich precautions, efforts and/or treatments the animals will be given in order to safeguard their wellbeing and welfare.
The rats are going to be pet and played with for 1 week prior to the experiment, as well as getting them used to handling and restraint. This is expected to reduce stress for the rats during the experiment.

Such action will not be necessary ☐

Sedation, analgesia and anaesthesia

Indicate medication (product name and generic name), induction dosage and any maintenance dosage, method of administration (and times and any period)
- - -

Medication will be used, that wholly or partly makes the animal incapable of expressing pain, e.g. neuromuscular blockers ☐

Give further description of the sedation or pain treatment that will be used in connection with such medication
- - -

The experiment involves pain, but analgesia cannot be used ☐

Rationale for why analgesia cannot be used
- - -

Rationale for using the chosen animal model

Give the rationales for the choice of animal model (see regulations on animal experimentation, chapter IV). Why the species, strain, sex, age, gene modification etc.?
Due to their large size, rats enable larger volumes of blood sampling (when compared to mice).

The Sprague Dawley (SD) strain is chosen as they are a much used general multipurpose model, are generally calm and easy to handle and have a good size in regards to required blood volumes taken.

Male rats are chosen to minimize variance (and to avoid oestrus cycle).

Application 11828:   Optimising Emulsions for More Efficient Uptake of Lipophilic Compounds

Attachments

Time table for all experiments
Showing time points for all events during the experiments

Document reference: http://asp.gitek.no/fdu/pmws.dll/FDyrDocDownload?_FDLKey=17834

Experimental groups
Showing the experimental groups for all 3 parts, including cage distribution

Document reference: http://asp.gitek.no/fdu/pmws.dll/FDyrDocDownload?_FDLKey=17835

Research paper about the tail incision method
Describing the tail incision method in detail and indicating the refinement level of the method

Document reference: http://asp.gitek.no/fdu/pmws.dll/FDyrDocDownload?_FDLKey=17869

Fenofibrate API MSDS

Document reference: http://asp.gitek.no/fdu/pmws.dll/FDyrDocDownload?_FDLKey=17871

B   Nutritional Values of Rat Food

In Subsection 2.5.1, the rat food given to the rats on a regular basis was mentioned. RM1, Special Diets Services rat foods nutritional values is given in this appendix. It contains vitamin D, cholecalciferol, α-tocopherol and vitamin E. It also contains several fatty acids.

SDS
Special Diets Services

Rat and Mouse No.1 Maintenance

Pelleted, Expanded and Expanded Ground

SUITABLE SPECIES AND APPLICATIONS

Rats and mice for long and short term maintenance.

BENEFITS

- High quality human food grade soya bean concentrate provides a less variable source of protein.

- Low protein level promotes longer life expectancy, reducing obesity and associated problems in the aged animal.

- Low nutrient levels reduce the risk of undesirable side-effects in toxicity trials being masked.

FEEDING GUIDE

Ad-lib feeding is recommended.

AVAILABLE AS

Diet	Form	Product Code
Standard		
RM1 (P)	9.5mm Pelleted	801151
RM1 (E)	Expanded	801002
SQC		
RM1 (E) SQC	Expanded	811002
RM1 (E) FG SQC	Expanded Ground	811004

- All diets are available irradiated and are available in a range of packaging.

- All Standard diets are available with full analysis on request.

INGREDIENTS

Wheat, Barley, Wheatfeed, De-hulled Extracted Toasted Soya, Soya Protein Concentrate, Macro Minerals, Soya Oil, Whey Powder, Amino Acids, Vitamins, Micro Minerals.

Email: info@sdsdiets.com

Catalogue revision 4   0103

Calculated Analysis

Rat and Mouse No.1 Maintenance

NUTRIENTS		Total	Supp (9)
Proximate Analysis			
Moisture (1)	%	10.00	
Crude Oil	%	2.71	
Crude Protein	%	14.38	
Crude Fibre	%	4.65	
Ash	%	6.00	
Nitrogen Free Extract	%	61.73	
Digestibility Co-Efficients (7)			
Digestible Crude Oil	%	2.47	
Digestible Crude Protein	%	12.92	
Carbohydrates, Fibre and Non Starch Polysaccharides (NSP)			
Total Dietary Fibre	%	17.05	
Pectin	%	1.52	
Hemicellulose	%	10.17	
Cellulose	%	4.32	
Lignin	%	1.68	
Starch	%	44.97	
Sugar	%	4.05	
Energy (5)			
Gross Energy	MJ/kg	14.74	
Digestible Energy (15)	MJ/kg	11.90	
Metabolisable Energy (15)	MJ/kg	10.74	
Atwater Fuel Energy (AFE)(8)	MJ/kg	13.75	
AFE from Oil	%	7.42	
AFE from Protein	%	17.49	
AFE from Carbohydrate	%	75.09	
Fatty Acids			
Saturated Fatty Acids			
C12:0 Lauric	%	0.02	
C14:0 Myristic	%	0.14	
C16:0 Palmitic	%	0.31	
C18:0 Stearic	%	0.04	
Monounsaturated Fatty Acids			
C14:1 Myristoleic	%	0.02	
C16:1 Palmitoleic	%	0.09	
C18:1 Oleic	%	0.77	
Polyunsaturated Fatty Acids			
C18:2(ω6) Linoleic	%	0.69	
C18:3(ω3) Linolenic	%	0.06	
C20:4(ω6) Arachidonic	%	0.13	
C22:5(ω3) Clupanodonic	%		
Amino Acids			
Arginine	%	0.91	
Lysine (6)	%	0.66	0.07
Methionine	%	0.22	0.04
Cystine	%	0.24	
Tryptophan	%	0.18	
Histidine	%	0.35	
Threonine	%	0.49	
Isoleucine	%	0.54	
Leucine	%	0.98	
Phenylalanine	%	0.66	
Valine	%	0.69	
Tyrosine	%	0.49	
Taurine	%		
Glycine	%	1.11	
Aspartic Acid	%	0.67	

NUTRIENTS		Total	Supp (9)
Glutamic Acid	%	3.17	
Proline	%	1.20	
Serine	%	0.56	
Hydroxyproline	%		
Hydroxylysine	%		
Alanine	%	0.16	
Macro Minerals			
Calcium	%	0.73	0.63
Total Phosphorus	%	0.52	0.04
Phytate Phosphorus	%	0.24	
Available Phosphorus	%	0.28	0.04
Sodium	%	0.25	0.19
Chloride	%	0.38	0.32
Potassium	%	0.67	
Magnesium	%	0.23	
Micro Minerals			
Iron	mg/kg	159.30	82.50
Copper	mg/kg	11.50	1.94
Manganese	mg/kg	72.44	19.22
Zinc	mg/kg	35.75	
Cobalt	μg/kg	634.10	550.00
Iodine	μg/kg	1202.69	1085.00
Selenium	μg/kg	298.99	100.00
Fluorine	mg/kg	10.49	
Vitamins			
β-Carotene (2)	mg/kg	0.16	
Retinol (2)	μg/kg	2566.38	2400.00
Vitamin A (2)	iu/kg	8554.27	8000.00
Cholecalciferol (3)	μg/kg	15.54	15.00
Vitamin D (3)	iu/kg	621.70	600.00
α-Tocopherol (4)	mg/kg	76.45	56.82
Vitamin E (4)	iu/kg	84.10	62.50
Vitamin B$_1$ (Thiamine)	mg/kg	8.58	1.96
Vitamin B$_2$ (Riboflavin)	mg/kg	4.33	2.94
Vitamin B$_6$ (Pyridoxine)	mg/kg	4.81	0.98
Vitamin B$_{12}$ (Cyanocobalamine)	μg/kg	7.49	6.00
Vitamin C (Ascorbic Acid)	mg/kg	2.59	
Vitamin K (Menadione)	mg/kg	10.17	9.36
Folic Acid (Vitamin B$_9$)	mg/kg	0.79	
Nicotinic Acid (Vitamin PP) (6)	mg/kg	61.32	2.45
Pantothenic Acid (Vitamin B$_{3/5}$)	mg/kg	20.17	5.80
Choline (Vitamin B$_{4/7}$)	mg/kg	1080.14	366.60
Inositol	mg/kg	2369.59	
Biotin (Vitamin H) (6)	μg/kg	277.13	

Notes
1. All values are calculated using a moisture basis of 10%.
   Typical moisture levels will range between 9.5 - 11.5%.
2. a. Vitamin A includes Retinol and the Retinol equivalents of β-carotene
   b. Retinol includes the Retinol equivalents of β-Carotene.
   c. 0.48 μg Retinol = 1 μg β-carotene = 1.6 iu Vitamin A activity
   d. 1 μg Retinol = 3.33* iu Vitamin A activity
   e. 1 iu Vitamin A = 0.3 μg Retinol = 0.6 μg β-carotene
   f. The standard analysis for Vitamin A does not detect β-carotene
3. 1μg Cholecalciferol (D$_3$) = 40.0 iu Vitamin D
4. 1 mg all-rac-α-tocopherol = 1.1 iu Vitamin E activity
   1 mg all-rac-α-tocopherol acetate = 1.0 iu Vitamin E activity
5. 1 MJ = 239.23 Kcalories = 239.23 Calories = 239,230 calories
6. These nutrients coming from natural raw materials such as cereals may have
   low availabilities due to the interactions with other compounds.
7. Based on in-vitro digestibility analysis.
8. AF Energy = Atwater Fuel Energy = ((CO%/100)*9000)+
   ((CP%/100)*4000)+((NFE%/100)*4000)/239.23
9. Supplemented nutrients from manufactured and mined sources.
15. Calculated.

C Blood Sampling Time Points

In Subsection 2.5.3, the blood sampling method and time points were described in detail. In this appendix, the real time points for each blood sampling, rats corresponding to feed type, weight of each rat before feeding as well as additional comments are given. T80 percentages are given as (w/w).

Table 12: Weight measurements of rats. The measurements were taken before each rat was fed with gavage technique.

Cage number	Rat 1	Rat 2	Rat 3	Rat 4
Cage 1	246 g	258 g	250 g	242 g
Cage 2	276 g	278 g	308 g	281 g
Cage 3	276 g	253 g	271 g	279 g
Cage 4	267 g	279 g	265 g	285 g
Cage 5	265 g	286 g	268 g	292 g

In Table 13, time points of blood sampling for rats in cage 1 can be found. During the gavage procedure, rat 1 threw up approximately 10% of the feed.

Table 13: Feed type and blood sampling time points information for cage 1.

Cage 1	Feed	0h	Gavage	1h	2h	4h	6h	8h	24h
Rat 1	2% T80 (No SB)	08:55	09:50	10:50	11:50	14:00	15:50	17:50	10:15
Rat 2	Corn oil	09:10	10:00	11:20	12:00	14:10	16:15	18:10	10:25
Rat 3	0.25% T80	09:20	10:10	11:30	12:10	14:20	16:20	18:20	10:40
Rat 4	2% T80	09:35	10:20	11:40	12:20	14:30	16:30	18:40	10:50

In Table 14, time points of blood sampling for rats in cage 2 can be found. For all rats in this cage, the removal of plasma was postponed until 09:45 due to misplaced micropipette. Also, the rats in this cage seized the foam filter of the cage during the removal of the solid rat food stage (approximately 12 hours before gavage feeding) and ate it. The leftover particles from the foam filter was found in the cage approximately at 6h time point.

Table 14: Feed type and blood sampling time points information for cage 2.

Cage 2	Feed	0h	Gavage	1h	2h	4h	6h	8h	24h
Rat 1	2% T80 (No SB)	08:50	08:53	09:50	10:50	12:51	14:52	16:50	09:05
Rat 2	2% T80	09:02	09:05	10:05	11:06	13:05	15:06	17:03	09:15
Rat 3	Corn oil	09:15	09:19	10:21	11:21	13:20	15:21	17:20	09:25
Rat 4	0.25% T80	09:32	09:35	10:36	11:36	13:36	15:35	17:38	09:35

In Table 15, time points of blood sampling for rats in cage 3 can be found.

Table 15: Feed type and blood sampling time points information for cage 3.

Cage 3	Feed	0h	Gavage	1h	2h	4h	6h	8h	24h
Rat 1	0.25% T80	08:45	08:50	09:55	10:55	12:50	14:55	16:55	09:00
Rat 2	2% T80	09:00	09:05	10:15	11:15	13:10	15:10	17:15	09:10
Rat 3	Corn oil	09:12	09:20	10:30	11:25	13:25	15:30	17:35	09:20
Rat 4	2% T80 (No SB)	09:30	09:35	10:40	11:40	13:45	15:45	17:45	09:30

In Table 16, time points of blood sampling for rats in cage 4 can be found. In this cage, rat 2 threw up 2-3 drops of feed after the gavage feeding.

Table 16: Feed type and blood sampling time points information for cage 4.

Cage 4	Feed	0h	Gavage	1h	2h	4h	6h	8h	24h
Rat 1	2% T80	08:50	08:55	10:00	11:00	13:00	14:57	16:58	09:02
Rat 2	2% T80 (No SB)	09:05	09:10	10:17	11:17	13:11	15:16	17:10	09:14
Rat 3	0.25% T80	09:20	09:25	10:30	11:30	13:25	15:28	17:26	09:24
Rat 4	Corn oil	09:40	09:45	10:45	11:50	13:43	15:47	17:45	09:35

In Table 17, time points of blood sampling for rats in cage 5 can be found. In this cage, the feed of rat 4 came slightly out of the nose after gavage feeding. Also, the plasma of rat 1 and rat 2 got mixed during the collection stage after centrifugation at 24h time point. These samples were removed from the UHPLC – MS/MS analyses of vitamin D_3 and 25-OH-vitamin D_3.

Table 17: Feed type and blood sampling time points information for cage 5.

Cage 5	Feed	0h	Gavage	1h	2h	4h	6h	8h	24h
Rat 1	2% T80	08:45	08:50	09:51	10:52	12:52	14:53	16:52	08:56
Rat 2	2% T80 (No SB)	09:00	09:05	10:07	11:05	13:06	15:07	17:06	09:05
Rat 3	Corn oil	09:15	09:20	10:22	11:21	13:22	15:26	17:22	09:15
Rat 4	0.25% T80	09:32	09:35	10:37	11:35	13:36	15:37	17:39	09:30

D Droplet Size Graphs

In Section 2.2, the droplet size measurement method was described in detail. After the droplet sizes were measured with Mastersizer 3000 machine, Malvern software calculated the droplet size parameters. The results were plotted using MATLAB® R2017a. In Figure 22, the droplet size graph of 20% (w/w) olive oil emulsions with T80 percentage ranging from 2 to 0.25 is given. In Figure 23, the droplet size graph of 20% (w/w) coconut oil emulsions with T80 percentage ranging from 2 to 0.25 can be found. In Figure 24, the droplet size graph of 20% (w/w) corn oil emulsions with T80 percentage ranging from 2 to 0.25 is given. These emulsions were used in *in vivo* experiments and they contain 0.125% (w/w) vitamin D_3 and 10% (w/w) vitamin E. In Section 3.1, the results of droplet size measurements of these emulsions as well as other emulsions were given in Table 4.
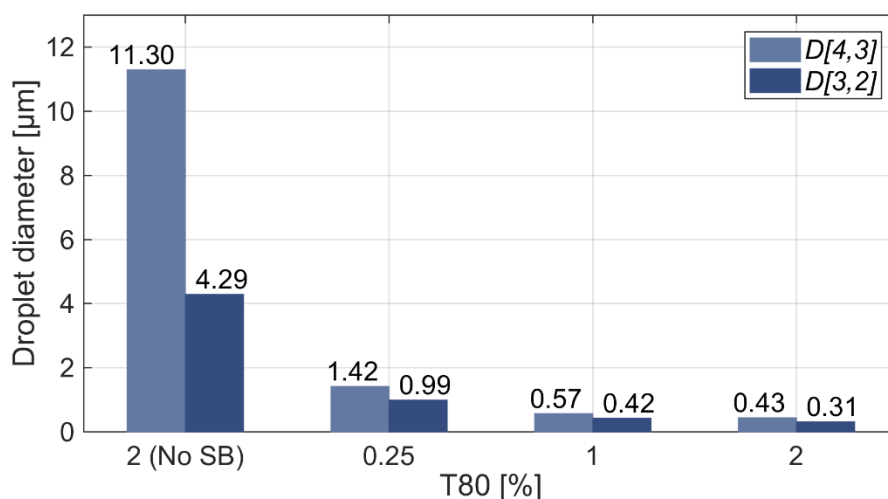
Figure 22: Droplet size plot of 20% (w/w) olive oil emulsions with T80 percentage ranging from 2 to 0.25. The non-starbursted emulsion is generated by the VDI 12 Homogeniser and the other emulsions are generated with a combination of the VDI 12 Homogeniser and the Star Burst Mini. The *D[4,3]* volume mean and *D[3,2]* surface mean of each emulsion are shown in separate bars.
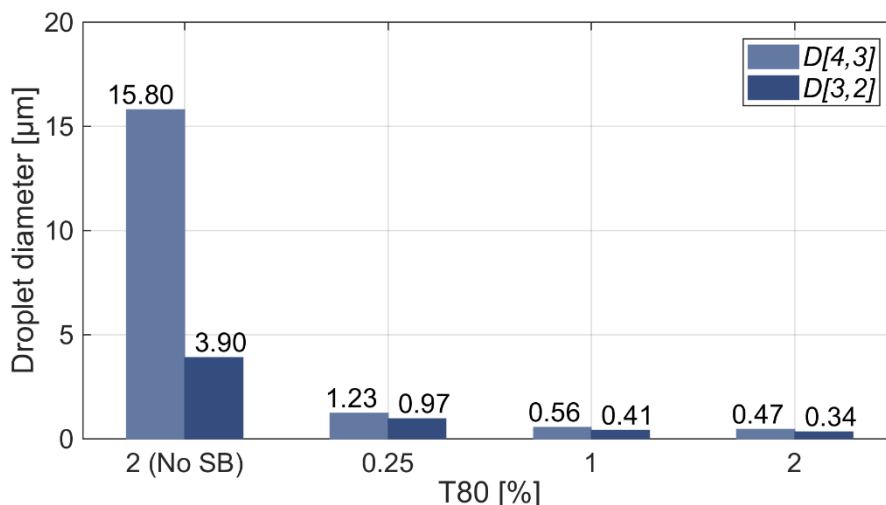
Figure 23: Droplet size plot of 20% (w/w) coconut oil emulsions with T80 percentage ranging from 2 to 0.25. The non-starbursted emulsion is generated by the VDI 12 Homogeniser and the other emulsions are generated with a combination of the VDI 12 Homogeniser and the Star Burst Mini. The $D[4,3]$ volume mean and $D[3,2]$ surface mean of each emulsion are shown in separate bars.
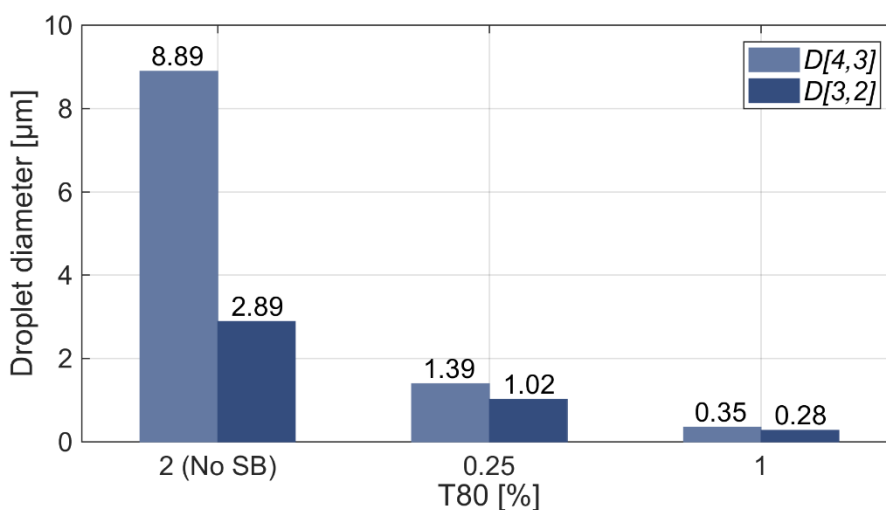
Figure 24: Droplet size plot of 20% (w/w) corn oil emulsions with T80 percentage ranging from 2 to 0.25. Emulsions contain 0.125% (w/w) vitamin D_3 and 10% (w/w) vitamin E. The non-starbursted emulsion is generated by the VDI 12 Homogeniser and the other emulsions are generated with a combination of the VDI 12 Homogeniser and the Star Burst Mini. The $D[4,3]$ volume mean and $D[3,2]$ surface mean of each emulsion are shown in separate bars.

E Droplet Size Distribution Chromatograms

Droplet size distribution data was obtained from the Mastersizer software and the chromatograms were plotted using MATLAB® R2017a. The size classes on the x-axis are plotted on a logarithmic scale. Droplet size distribution chromatograms of all corn oil emulsions can be found below from Figure 25 to Figure 27.
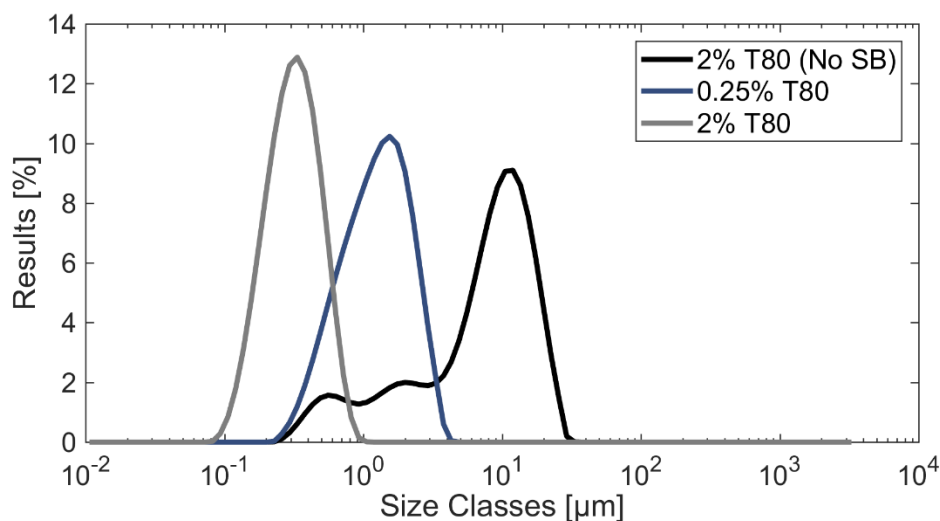
Figure 25: Size distribution chromatogram of 20% (w/w) corn oil emulsions with T80 percentage ranging from 2 to 0.25. Emulsions contain 0.125% (w/w) vitamin D_3 and 10% (w/w) vitamin E. The non-starbursted emulsion is generated by the VDI 12 Homogeniser and the other emulsions are generated with a combination of the VDI 12 Homogeniser and the Star Burst Mini.
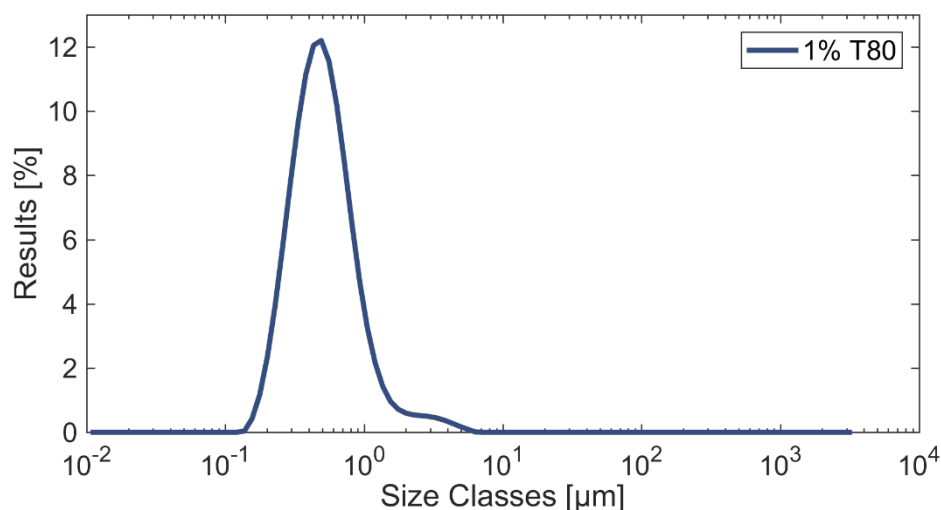
Figure 26: Size distribution chromatogram of 20% (w/w) corn oil emulsion with 1% T80. The emulsion contains 0.025% (w/w) vitamin D_3 and 0.011% (w/w) vitamin K_3. The emulsion is generated with a combination of the VDI 12 Homogeniser and the Star Burst Mini.
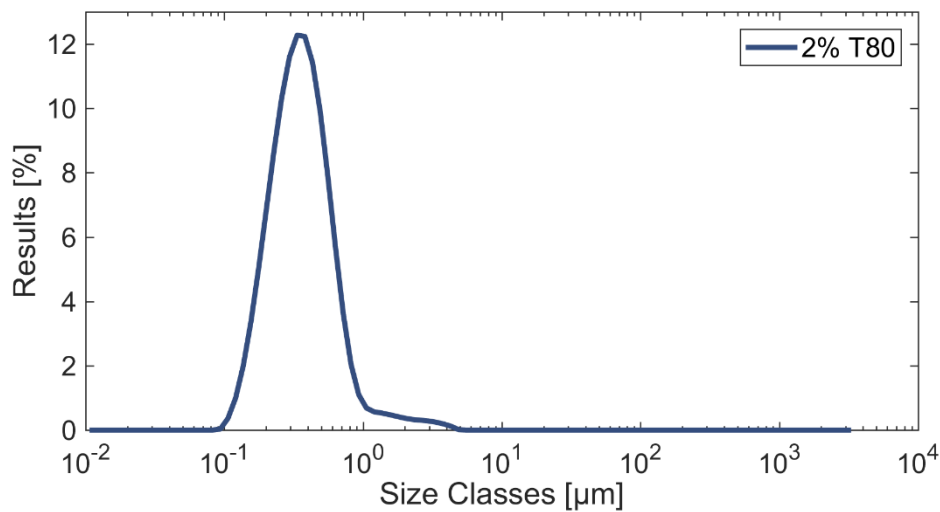
Figure 27: Size distribution chromatogram of 20% (w/w) corn oil emulsion with 2% T80. The emulsion contains 0.025% (w/w) vitamin D_3 and 0.011% (w/w) vitamin K_3. The emulsion is generated with a combination of the VDI 12 Homogeniser and the Star Burst Mini.

Droplet size distribution of olive oil emulsions can be found in Figure 28.
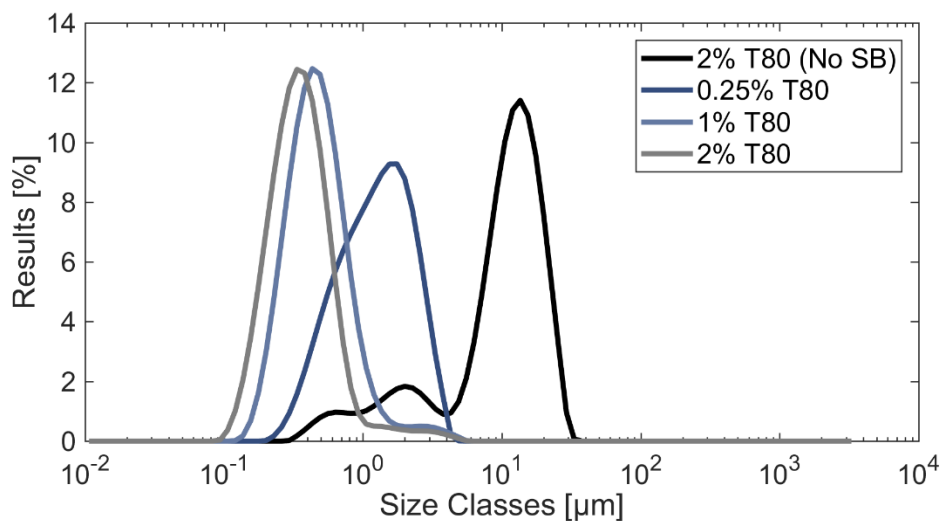
Figure 28: Size distribution chromatogram of 20% (w/w) olive oil emulsions with T80 percentage ranging from 2 to 0.5. The non-starbursted emulsion is generated by the VDI 12 Homogeniser and the other emulsions are generated with a combination of the VDI 12 Homogeniser and the Star Burst Mini.

Droplet size distribution of coconut oil emulsions can be found in Figure 29.
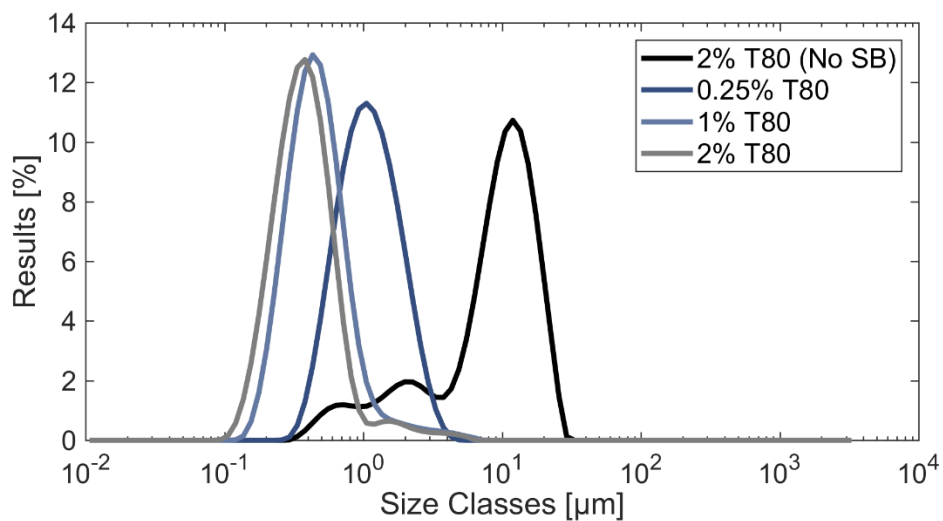
Figure 29: Size distribution chromatogram of 20% (w/w) coconut oil emulsions with T80 percentage ranging from 2 to 0.5. The non-starbursted emulsion is generated by the VDI 12 Homogeniser and the other emulsions are generated with a combination of the VDI 12 Homogeniser and the Star Burst Mini.

F Stability Chromatograms

In Section 3.2, the stability of the emulsions was discussed. In this appendix, droplet size chromatogram of each emulsion was plotted in a comparative manner regarding time. The exact date of each measurement can be found in Table 18. In the chromatograms, "m" indicates months after preparation and "w" indicates weeks after preparation. Given months and weeks are approximate values. The plots were generated using MATLAB® R2017a. The size classes on the x-axis are plotted on a logarithmic scale.

Table 18: Timetable of droplet size measurements for the stability analyses of emulsions. T80 percentages are given as (w/w).

Emulsion	Vitamins	1st Measurement Date	2nd Measurement Date	3rd Measurement Date
20% (w/w) corn oil	-	26.05.2017	06.09.2017	12.03.2018
	Vit D_3 and K_3 (1% T80)	25.10.2017	01.11.2017	13.03.2018
	Vit D_3 and K_3 (2% T80)	02.11.2017	13.03.2018	-
	Vit D_3 and E	15.01.2018	13.03.2018	-
20% (w/w) olive oil	-	04.10.2017	12.03.2018	-
20% (w/w) coconut oil	-	11.10.2017	13.03.2018	-
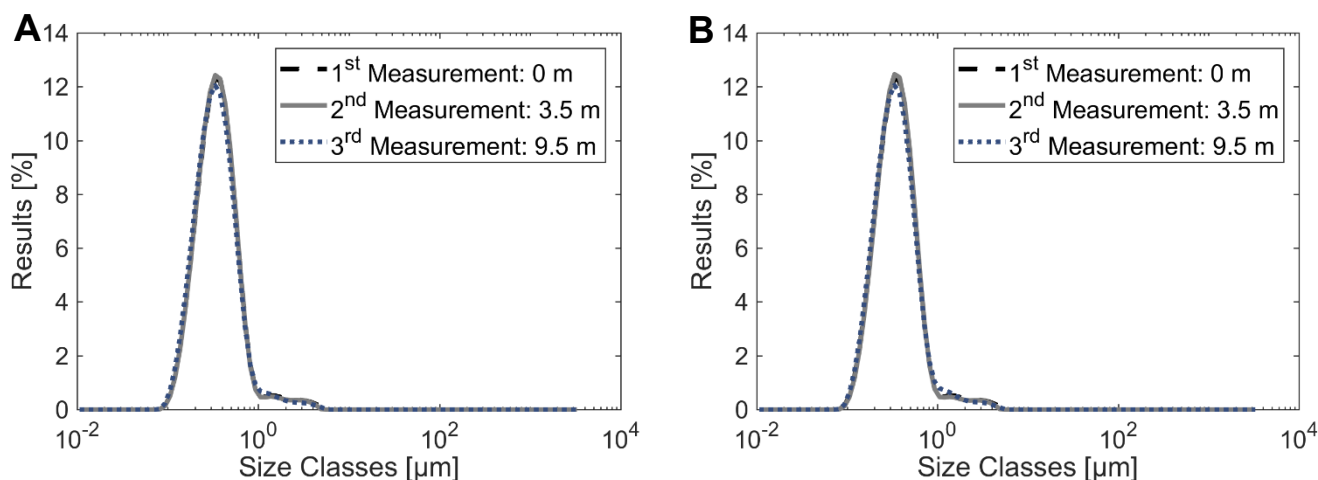
Figure 30: Stability chromatogram of the 20% (w/w) corn oil emulsion with 2% T80. The second and the third measurements were performed on the emulsions that were stored at **A)** +4°C and **B)** room temperature.
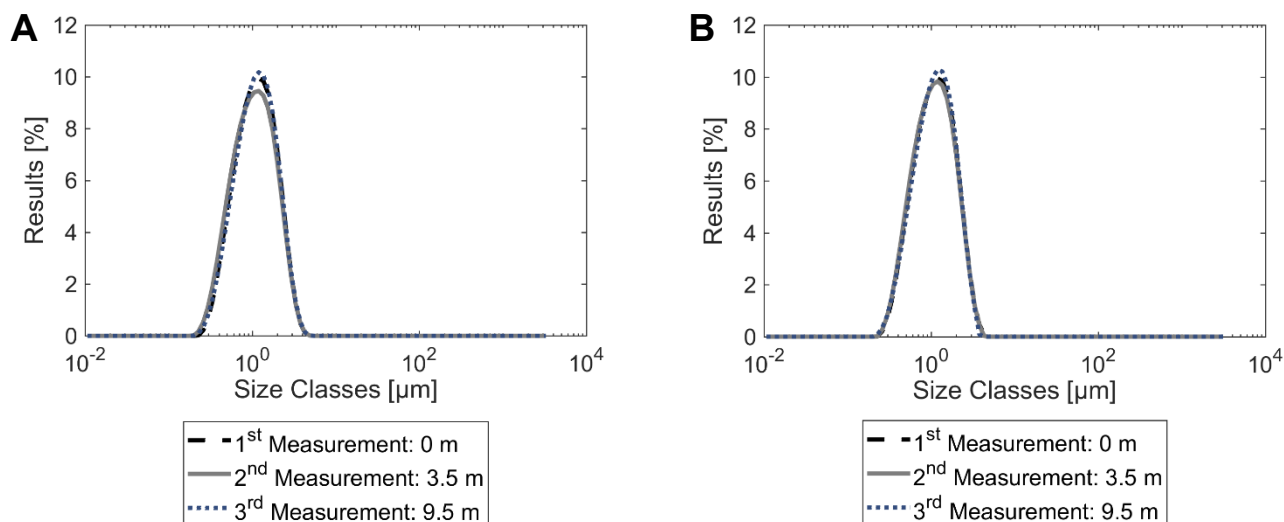
Figure 31: Stability chromatogram of the 20% (w/w) corn oil emulsion with 0.25% T80. The second and the third measurement was performed on the emulsions that were stored at **A)** +4°C and **B)** room temperature.
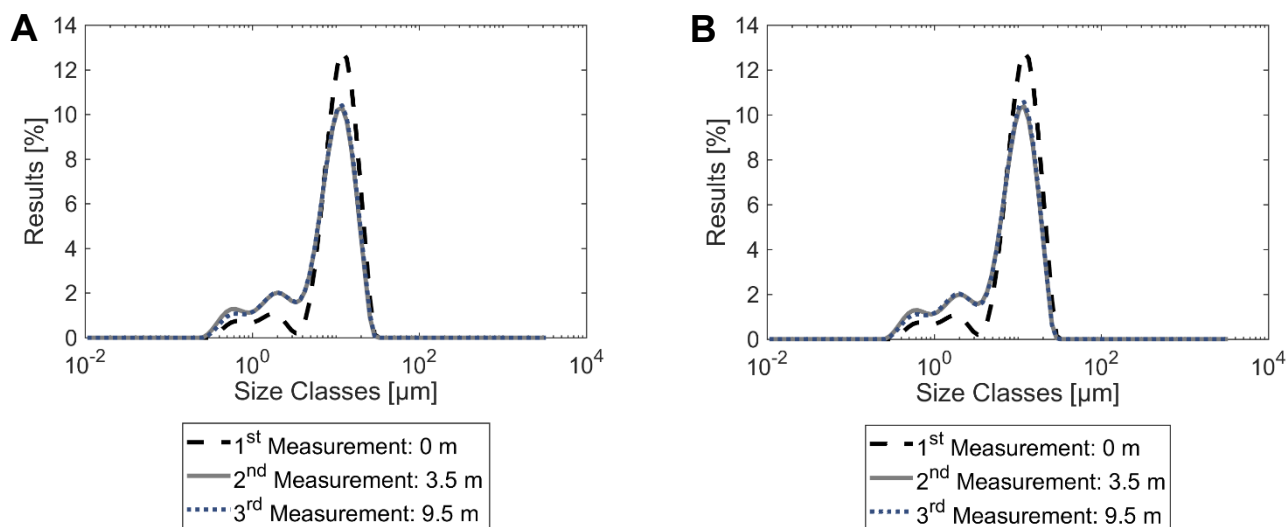
Figure 32: Stability chromatogram of the 20% (w/w) corn oil emulsion with 2% T80 (non-starbursted). The second and the third measurement was performed on the emulsions that were stored at **A)** +4°C and **B)** room temperature.
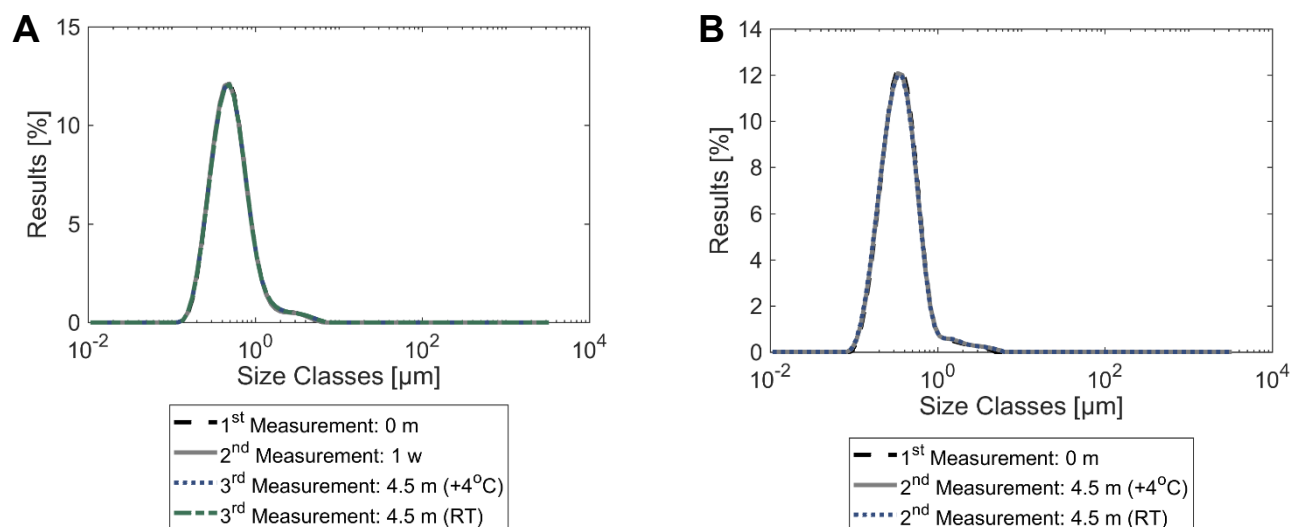
Figure 33: Stability chromatogram of the 20% (w/w) corn oil emulsions with **A)** 1% T80 and **B)** 2% T80. Emulsion contains 0.025% (w/w) vitamin D_3 and 0.011% (w/w) vitamin K_3. The second measurements were performed on the emulsions that were stored at +4°C. The third measurement was performed on the emulsions that were stored at +4°C and at room temperature.
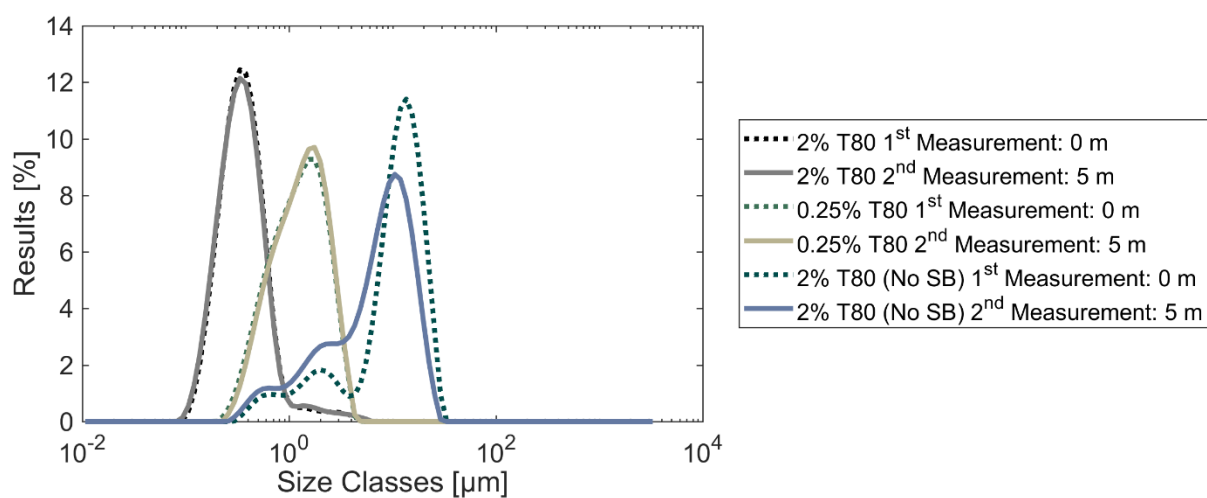
Figure 34: Stability chromatogram of the 20% (w/w) olive oil emulsions with 2% T80, 0.25% T80 and 2% T80 (non-starbursted). The second measurement was performed on the emulsions that were stored at +4°C.
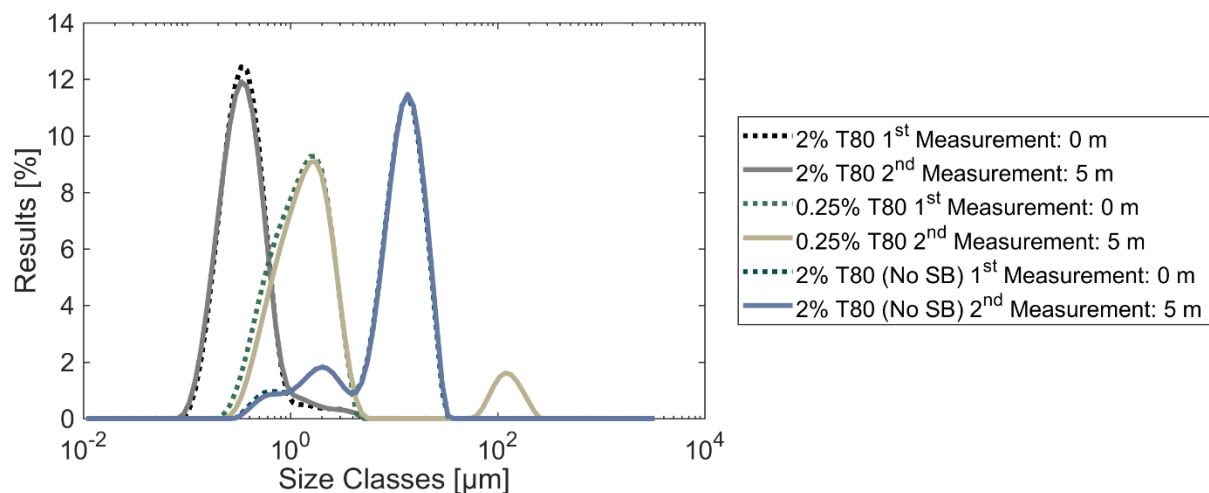
Figure 35: Stability chromatogram of the 20% (w/w) olive oil emulsions with 2% T80, 0.25% T80 and 2% T80 (non-starbursted). The second measurement was performed on the emulsions that were stored at room temperature.
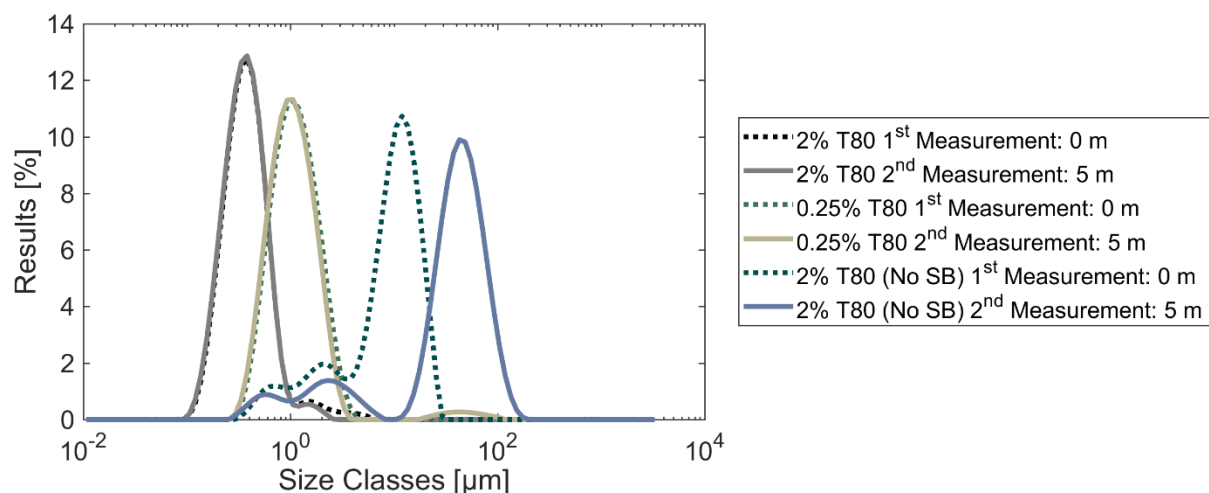
Figure 36: Stability chromatogram of the 20% (w/w) coconut oil emulsions with 2% T80, 0.25% T80 and 2% T80 (non-starbursted). The second measurement was performed on the emulsions that were stored at +4°C.
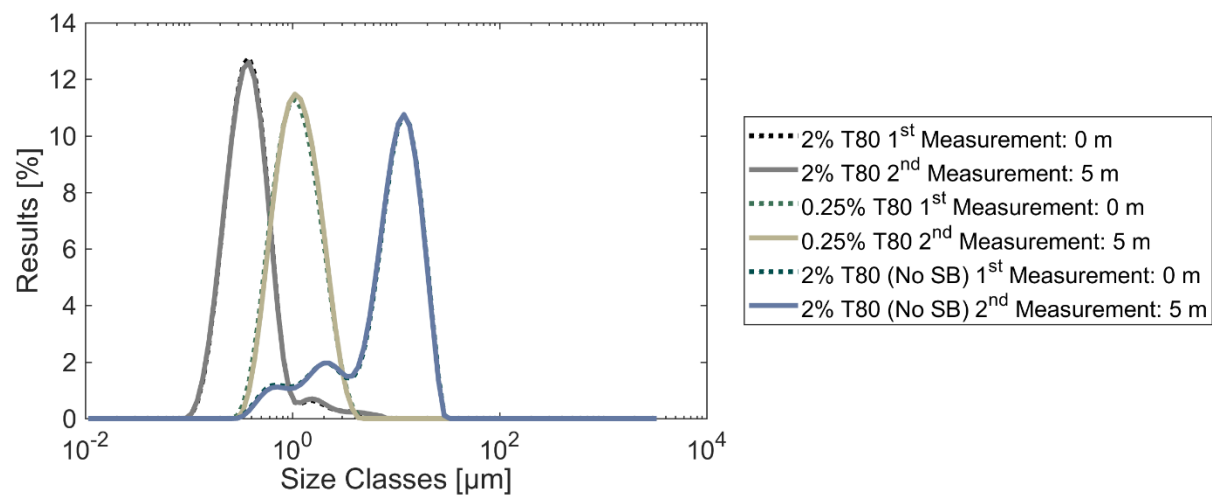
Figure 37: Stability chromatogram of the 20% (w/w) coconut oil emulsions with 2% T80, 0.25% T80 and 2% T80 (non-starbursted). The second measurement was performed on the emulsions that were stored at room temperature.

G Complete *In Vitro* Lipolysis Plots

In Section 3.3, *in vitro* lipolysis method development and results were discussed in detail. This appendix provides complete *in vitro* lipolysis plots of the experiments which do not have the traditional curve. The plots were generated using MATLAB® R2017a.
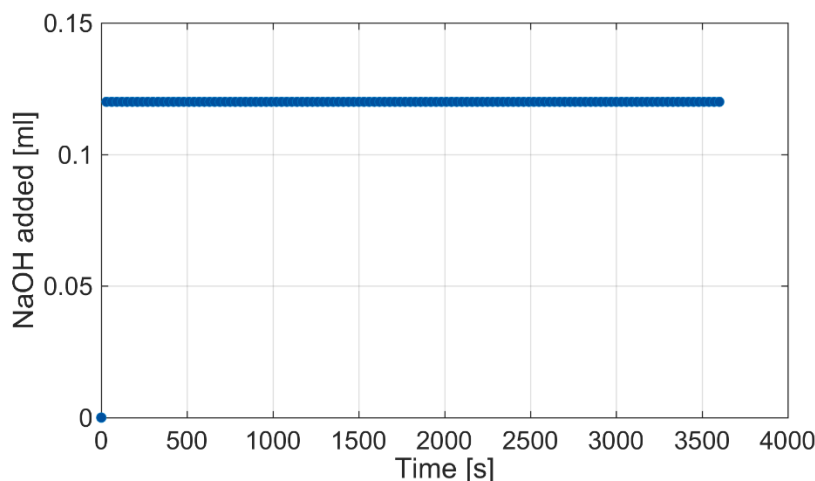
Figure 38: *In vitro* lipolysis of MQ-water. 0.4 mg/ml pancreatin was used in the experiment. In total, 0.12 ml NaOH was titrated throughout the *in vitro* lipolysis reaction.
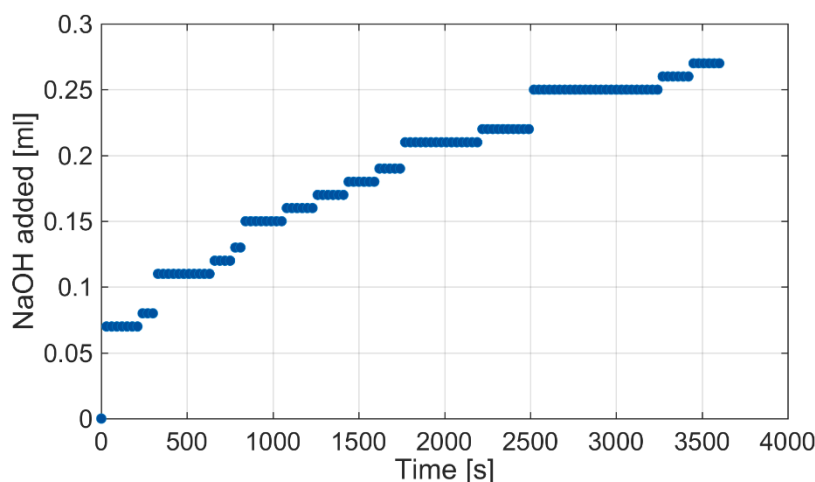
Figure 39: *In vitro* lipolysis of T80. 2 ml T80 was substituted with emulsion in the *in vitro* lipolysis protocol. 0.4 mg/ml pancreatin was used in the experiment. In total, 0.27 ml NaOH was titrated throughout the reaction. *In vitro* lipolysis was performed with Method 1.
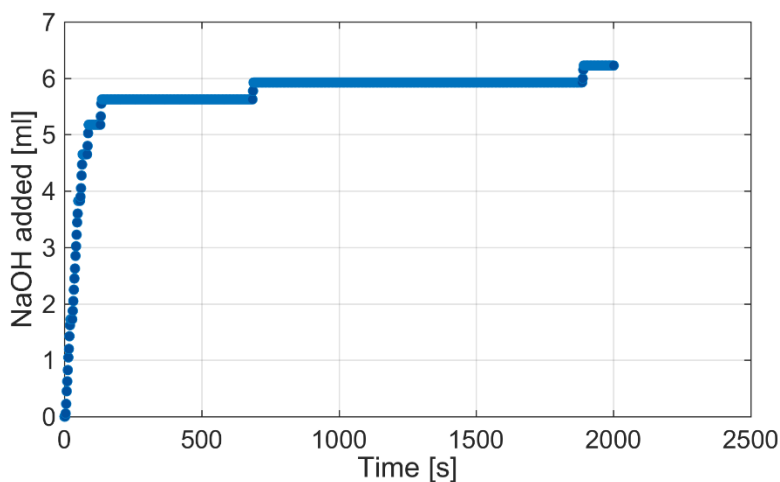
Figure 40: *In vitro* lipolysis of 20% (w/w) corn oil emulsion with 2% T80. 1.2 mg/ml pancreatin and 1.2 mg/ml lipase were used in the experiment. *In vitro* lipolysis was performed with Method 2.
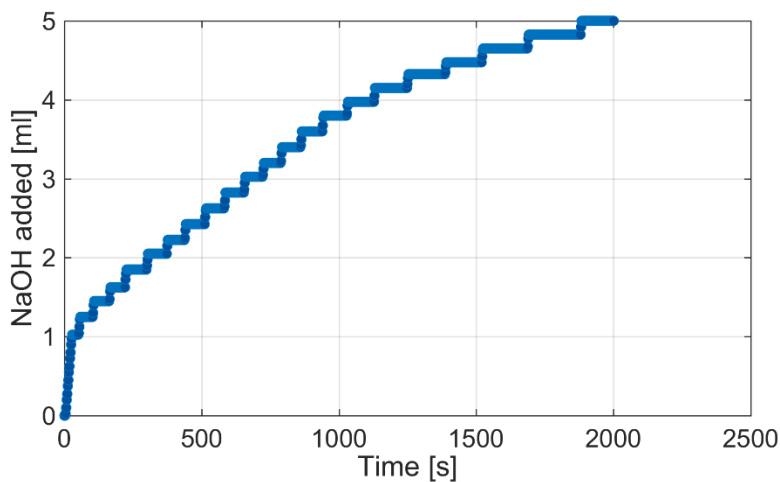
Figure 41: *In vitro* lipolysis of 20% (w/w) corn oil emulsion with 2% T80 (non-starbursted). 1.2 mg/ml pancreatin and 1.2 mg/ml lipase were used in the experiment. *In vitro* lipolysis was performed with Method 2.
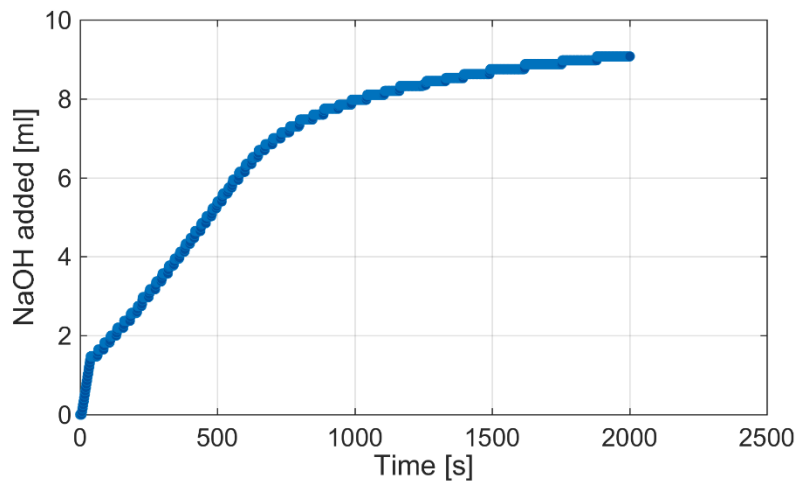
Figure 42: *In vitro* lipolysis of 20% (w/w) coconut oil emulsion with 2% T80 (non-starbursted). The emulsion has been kept in room temperature. 1.2 mg/ml pancreatin and 1.2 mg/ml lipase were used in the reaction. *In vitro* lipolysis was performed with Method 2.

H Initial *In Vitro* Lipolysis Plots

In Subsection 3.3.2 and 3.3.3, *in vitro* lipolysis results were discussed in detail. This appendix gives comparative graphs of initial *in vitro* lipolysis data for all *in vitro* lipolysis experiments. These graphs were plotted by selecting initial slope time points of the data collected from the titrator. The plots were generated using MATLAB® R2017a. Later in the appendix, Table 19 presents the initial rates and time required to reach the plateau for all *in vitro* lipolysis plots.
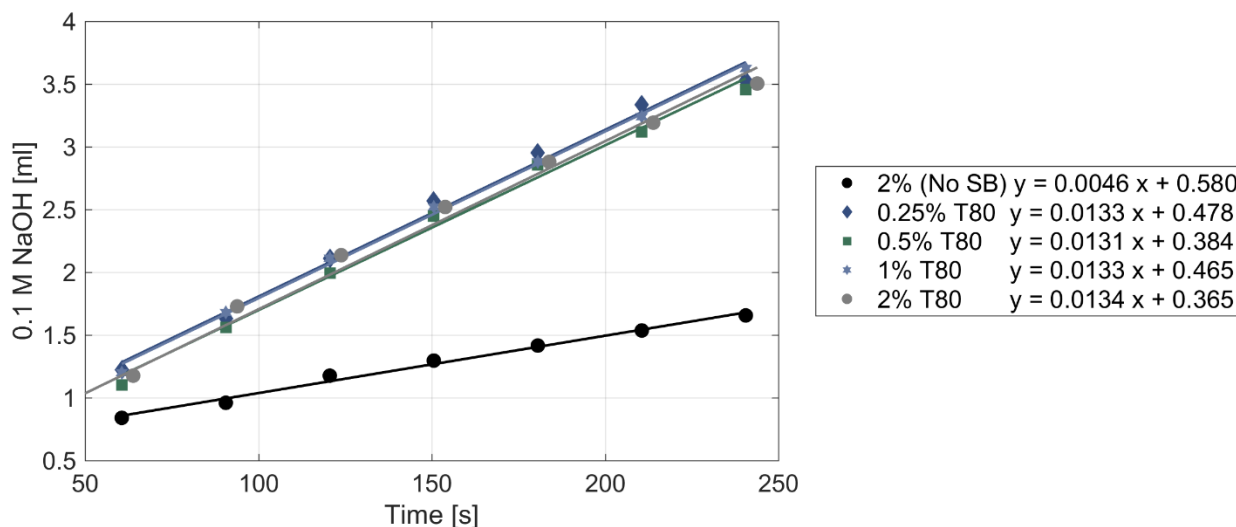
Figure 43: *In vitro* lipolysis of the 20% (w/w) corn oil emulsions with T80 percentage ranging from 2 to 0.25. 0.4 mg/ml pancreatin was used in the experiment. *In vitro* lipolysis was performed with Method 1.
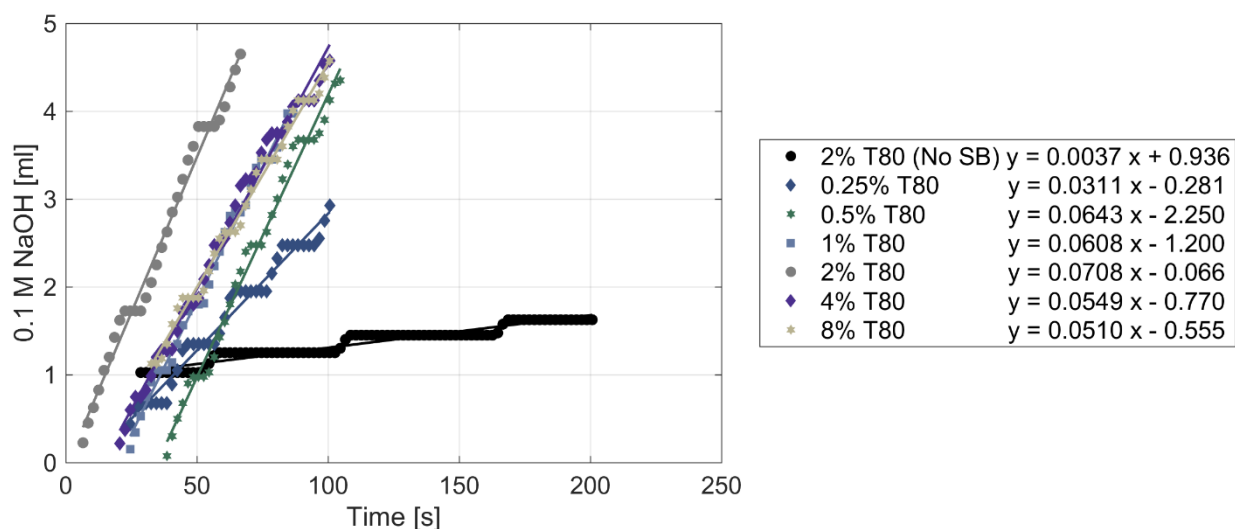
Figure 44: *In vitro* lipolysis of the 20% (w/w) corn oil emulsions with T80 percentage ranging from 8 to 0.25. 1.2 mg/ml pancreatin and 1.2 mg/ml lipase were used in the experiment. *In vitro* lipolysis was performed with Method 2.
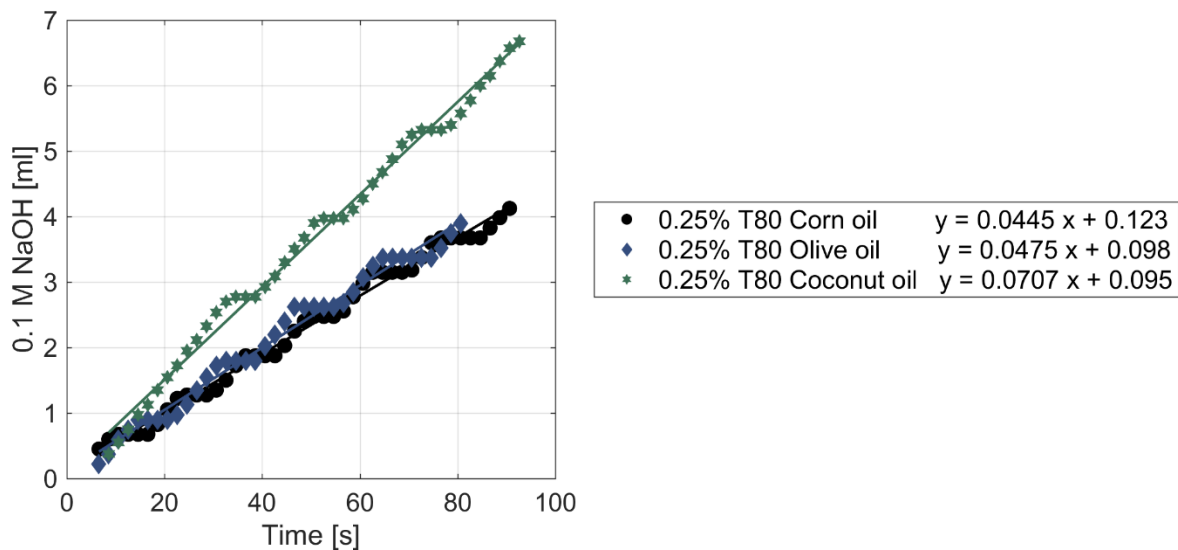
Figure 45: *In vitro* lipolysis of 20% (w/w) oil emulsions with different oil types (corn oil, olive oil and coconut oil). All emulsions contained 0.25% T80. 1.2 mg/ml pancreatin and 1.2 mg/ml lipase were used in the experiment. *In vitro* lipolysis was performed with Method 2.
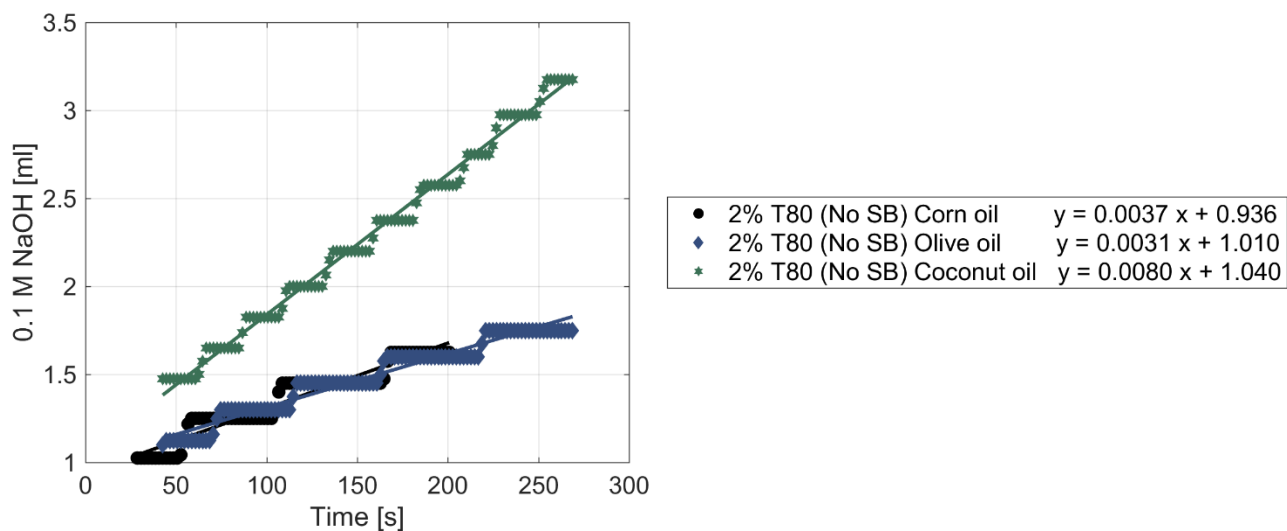
Figure 46: *In vitro* lipolysis of 20% (w/w) oil emulsions with different oil types (corn oil, olive oil and coconut oil). All emulsions contained 2% T80. The emulsions did not go through the starburst process. 1.2 mg/ml pancreatin and 1.2 mg/ml lipase were used in the experiment. *In vitro* lipolysis was performed with Method 2.

Table 19: Initial *in vitro* lipolysis rate of emulsions (in mmol FA/min) with different pancreatin and lipase concentrations. "P" stands for pancreatin and "L" stands for lipase.

Emulsion		Enzyme									
Oil Type	T80 [%] (w/w)	0.4 mg/ml P	t [s] until plateau	0.8 mg/ml P and L	t [s] until plateau	1.2 mg/ml P and L	t [s] until plateau	2.4 mg/ml P and L	t [s] until plateau	3.6 mg/ml P and L	t [s] until plateau
Corn oil	8	-	-	-	-	0.0510	182.73	-	-	-	-
	4	-	-	-	-	0.0549	170.71	-	-	-	-
	2	0.0134	993.93	-	-	0.0708	142.71	0.0818	124.67	0.0888	128.68
	1	0.0133	750.63	-	-	0.0608	220.76	-	-	-	-
	0.5	0.0131	660.62	-	-	0.0643	228.78	-	-	-	-
	0.25	0.0133	690.62	-	-	0.0378 ± 0.0067	224.74	-	-	-	-
	2 (No SB)	0.0046 (M1) 0.0032 (M2)	2010.69	0.0055	1965.78	0.0037	≥ 2000	-	-	-	-
Olive oil	2	-	-	-	-	0.0651	170.70	-	-	-	-
	0.25	-	-	-	-	0.0475	276.80	-	-	-	-
	2 (No SB)	-	-	-	-	0.0031	≥ 2000	-	-	-	-
Coco-nut oil	2	-	-	-	-	0.0981	100.67	-	-	-	-
	0.25	-	-	-	-	0.0707	142.69	-	-	-	-
	2 (No SB)	-	-	-	-	0.0080	1501.76	-	-	-	-

I UHPLC – MS/MS Analysis Tables

The UHPLC – MS/MS analyses were performed by Kåre A. Kristiansen, Senior Engineer, Department of Biotechnology and Food Science, NTNU. The SPE protocol and the analyses of the results were performed by Tuna Baydin.

At the end of each UHPLC – MS/MS analysis, the MassLynx software provided data for individual plates which contained plasma samples obtained from the rats in the *in vivo* experiments. The data was processed and presented as tables in this appendix, from Table 20 to Table 34. Each table shows results of a single cage and a single analyte. Response is the analyte area divided by the IS area. Since QCs give crucial information about the precision of the assay, they were included in the plate sequence. It should be noted that in the tables QC locations were shown in a way that facilitates easy tracking of the analyte results. Since the plates were shared amongst different cage results, the analyte results were carried to individual tables, resulting in sequentially observed QC results. Standard curve for each analyzed compound in individual plates was prepared by plotting response versus concentration of the standard solutions at 50 nM, 125 nM, 250 nM, 500 nM, 1000 nM and 5000 nM (from Figure 47 to Figure 57). The plots were generated using MATLAB® R2017a.

There were empty cells reported by the MassLynx software. These empty cells imply that the integrator did not find a peak to integrate. There were instances where the integrator integrated noise and reported a very low concentration, which is usually out of the standard curve range. These very low values were considered as noise and reported as N/A.
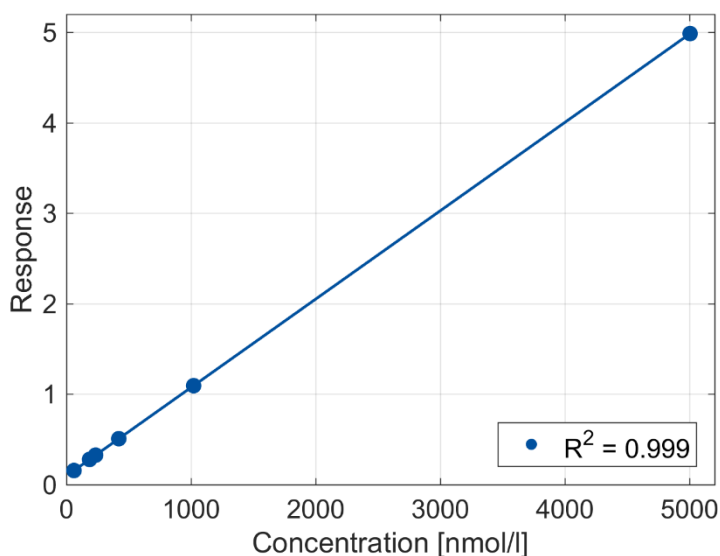
Figure 47: Standard curve of Vitamin D_3 for the plasma samples obtained from rats in cage 1.

Table 20: UHPLC – MS/MS data for vitamin D_3 compound analyzed on plasma samples from the rats in cage 1.

Sample Name	Sample Type	RT	Area	IS Area	Response	Concentration (nmol/l)	Standard Deviation (nmol/l)
Blank1	Blank	2.45	1453.647	10029.675	0.145	49.18	
Blank2	Blank	2.45	1555.116	9718.674	0.160	64.61	
Blank3	Blank	2.45	1386.969	9783.623	0.142	45.93	
50 nM standard	Standard	2.44	2028.414	12976.014	0.156	60.83	21.7
125 nM standard	Standard	2.57	2190.323	7862.925	0.279	185.93	48.7
250 nM standard	Standard	2.56	3519.445	10806.798	0.326	234.14	-6.3
500 nM standard	Standard	2.56	6501.856	12808.452	0.508	420.35	-15.9
1000 nM standard	Standard	2.56	13498.901	12335.159	1.094	1020.78	2.1
5000 nM standard	Standard	2.56	63822.996	12801.580	4.986	5002.97	0.1
Rat 1 0h	Analyte	2.46	1732.649	6572.854	0.264	170.63	
Rat 1 1h	Analyte	2.56	2348.175	5784.953	0.406	316.26	
Rat 1 2h	Analyte	2.56	3582.200	3870.951	0.925	847.90	
Rat 1 4h	Analyte	2.56	6148.036	5825.308	1.055	980.93	
Rat 1 6h	Analyte	2.56	9580.335	7857.675	1.219	1148.59	
Rat 1 8h	Analyte	2.56	6363.042	3827.506	1.662	1602.17	
Rat 1 24h	Analyte	2.56	5733.880	5018.090	1.143	1070.21	
1000 nM QC1	QC	2.56	11263.579	10740.171	1.049	974.11	-2.6
Rat 2 0h	Analyte	N/A	N/A	6473.611	N/A	N/A	
Rat 2 1h	Analyte	2.56	3201.280	7284.074	0.439	350.62	
Rat 2 2h	Analyte	2.56	5073.492	6625.713	0.766	684.49	
Rat 2 4h	Analyte	2.56	7870.096	4629.733	1.700	1640.50	
Rat 2 6h	Analyte	2.56	10761.211	5756.406	1.869	1813.99	
Rat 2 8h	Analyte	2.56	11182.737	5388.915	2.075	2024.51	
Rat 2 24h	Analyte	2.56	7742.308	6272.356	1.234	1164.07	
1000 nM QC2	QC	2.56	10876.446	10273.437	1.059	984.30	-1.6
Rat 3 0h	Analyte	2.46	2115.773	3519.752	0.601	516.02	

Rat 3 1h	Analyte	2.56	4071.405	4141.148	0.983	907.00	
Rat 3 2h	Analyte	2.56	6408.350	4854.299	1.320	1251.86	
Rat 3 4h	Analyte	2.56	7930.057	3233.145	2.453	2410.94	
Rat 3 6h	Analyte	2.56	11090.197	4018.671	2.760	2725.04	
Rat 3 8h	Analyte	2.56	9868.589	3520.488	2.803	2769.58	
Rat 3 24h	Analyte	2.56	6129.475	3727.931	1.644	1583.50	
1000 nM QC3	QC	2.56	10650.044	10723.799	0.993	917.20	-8.3
Rat 4 0h	Analyte	N/A	N/A	4019.562	N/A	N/A	
Rat 4 1h	Analyte	2.56	2897.880	3109.409	0.932	854.62	
Rat 4 2h	Analyte	2.56	6449.418	3558.573	1.812	1755.59	
Rat 4 4h	Analyte	2.56	9078.210	3213.775	2.825	2791.68	
Rat 4 6h	Analyte	2.56	11794.450	3097.343	3.808	3797.81	
Rat 4 8h	Analyte	2.56	7727.615	1600.858	4.827	4840.88	
Rat 4 24h	Analyte	2.56	6808.253	2600.065	2.618	2580.57	
1000 nM QC4	QC	2.56	8019.246	8009.588	1.001	925.47	-7.5
Blank4	Blank	2.46	1689.875	10205.148	0.166	70.32	
Blank5	Blank	2.46	1213.426	10386.901	0.117	20.41	
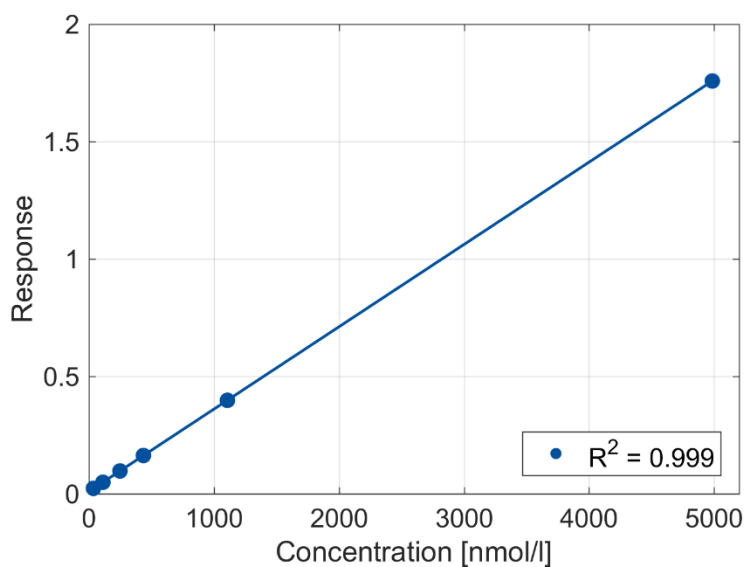
Figure 48: Standard curve of 25-OH-Vitamin D$_3$ for the plasma samples obtained from rats in cage 1.

Table 21: UHPLC – MS/MS data for 25-OH-vitamin D_3 compound analyzed on plasma samples from the rats in cage 1.

Sample Name	Sample Type	RT	Area	IS Area	Response	Concentration (nmol/l)	Standard Deviation (nmol/l)
Blank1	Blank	1.68	162.147	15713.344	0.010	0.96	
Blank2	Blank	N/A	N/A	15521.884	N/A	N/A	
Blank3	Blank	N/A	N/A	15393.947	N/A	N/A	
50 nM standard	Standard	1.69	384.961	17032.061	0.023	35.98	-28.0
125 nM standard	Standard	1.69	702.346	14260.604	0.049	111.97	-10.4
250 nM standard	Standard	1.69	1335.419	13763.311	0.097	248.21	-0.7
500 nM standard	Standard	1.69	2715.426	16678.467	0.163	435.79	-12.8
1000 nM standard	Standard	1.69	6690.014	16792.268	0.398	1107.59	10.8
5000 nM standard	Standard	1.69	33196.844	18879.965	1.758	4985.46	-0.3
Rat 1 0h	Analyte	1.67	422.243	9205.570	0.046	102.33	
Rat 1 1h	Analyte	1.67	1104.835	7889.260	0.140	370.87	
Rat 1 2h	Analyte	1.67	1235.710	7375.884	0.168	449.26	
Rat 1 4h	Analyte	1.68	1485.058	10267.563	0.145	383.97	
Rat 1 6h	Analyte	1.68	1514.647	10324.240	0.147	389.88	
Rat 1 8h	Analyte	1.68	1312.406	7184.591	0.183	492.42	
Rat 1 24h	Analyte	1.68	1303.804	8776.406	0.149	395.15	
1000 nM QC1	QC	1.69	5904.901	15907.544	0.371	1030.03	3.0
Rat 2 0h	Analyte	1.67	1319.594	8317.793	0.159	423.92	
Rat 2 1h	Analyte	1.67	1510.230	9088.049	0.166	445.39	
Rat 2 2h	Analyte	1.67	606.764	10059.202	0.060	143.53	
Rat 2 4h	Analyte	1.68	1382.432	9143.990	0.151	402.64	
Rat 2 6h	Analyte	1.68	1183.594	10149.168	0.117	304.08	
Rat 2 8h	Analyte	1.68	1369.523	9964.974	0.137	363.43	
Rat 2 24h	Analyte	1.68	1049.290	8821.822	0.119	310.70	
1000 nM QC2	QC	1.69	4876.257	16526.900	0.295	812.88	-18.7
Rat 3 0h	Analyte	1.67	1406.079	7234.327	0.194	525.76	

Rat 3 1h	Analyte	1.67	1476.785	9294.313	0.159	424.62	
Rat 3 2h	Analyte	1.67	1201.534	9594.624	0.125	328.63	
Rat 3 4h	Analyte	1.68	1338.578	9436.698	0.142	376.02	
Rat 3 6h	Analyte	1.68	1356.416	9090.623	0.149	397.01	
Rat 3 8h	Analyte	1.68	1272.511	8180.810	0.156	415.08	
Rat 3 24h	Analyte	1.68	1281.301	8835.806	0.145	385.04	
1000 nM QC3	QC	1.69	5359.637	15519.763	0.345	956.30	-4.4
Rat 4 0h	Analyte	1.67	1297.468	8175.774	0.159	424.06	
Rat 4 1h	Analyte	1.67	1351.695	8582.304	0.157	420.64	
Rat 4 2h	Analyte	1.67	1292.295	8454.357	0.153	407.41	
Rat 4 4h	Analyte	1.68	1121.805	9436.299	0.119	310.53	
Rat 4 6h	Analyte	1.68	1097.258	9040.277	0.121	317.64	
Rat 4 8h	Analyte	1.68	1234.507	8179.845	0.151	401.89	
Rat 4 24h	Analyte	1.68	874.792	6795.657	0.129	338.61	
1000 nM QC4	QC	1.69	4034.643	11381.814	0.354	982.36	-1.8
Blank4	Blank	1.68	81.681	16804.367	0.005	N/A	
Blank5	Blank	1.76	28.700	17006.088	0.002	N/A	
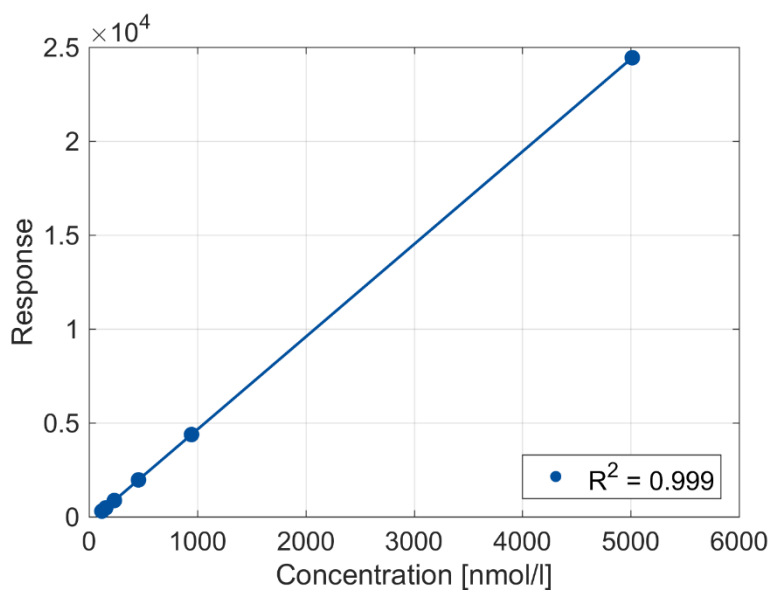
Figure 49: Standard curve of Vitamin E for the plasma samples obtained from rats in cage 1 and cage 2.

Table 22: UHPLC – MS/MS data for vitamin E compound analyzed on plasma samples from the rats in cage 1. 25x dilution was performed on the plasma samples.

Sample Name	Sample Type	RT	Area	IS Area	Response	Concentration (nmol/l)	Standard Deviation (nmol/l)
Blank1	Blank	2.76	296.342	10522.462	70.407	72.76	
Blank2	Blank	2.77	443.141	13470.301	82.244	75.16	
Blank3	Blank	2.77	544.068	16494.643	82.461	75.20	
50 nM standard	Standard	2.77	1247.522	10417.782	299.373	119.19	138.4
125 nM standard	Standard	2.77	2411.193	12741.887	473.084	154.42	23.5
250 nM standard	Standard	2.76	8206.870	23657.018	867.276	234.36	-6.3
500 nM standard	Standard	2.76	18164.252	23135.521	1962.810	456.53	-8.7
1000 nM standard	Standard	2.76	21948.105	12537.520	4376.485	946.00	-5.4
5000 nM standard	Standard	2.76	173434.781	17741.678	24438.892	5014.50	0.3
1000 nM QC1	QC	2.75	58807.316	22952.529	6405.320	1357.43	35.7
1000 nM QC2	QC	2.75	76998.477	22173.287	8681.446	1819.01	81.9
1000 nM QC3	QC	2.75	69921.727	17383.982	10055.482	2097.66	109.8
1000 nM QC4	QC	2.74	80239.648	16172.783	12403.500	2573.82	157.4
Rat 1 0h	Analyte	2.74	635.414	53.540	29670.060	6075.34	
Rat 1 1h	Analyte	2.74	579.382	N/A	N/A	N/A	
Rat 1 2h	Analyte	2.74	395.452	N/A	N/A	N/A	
Rat 1 4h	Analyte	2.74	919.069	N/A	N/A	N/A	
Rat 1 6h	Analyte	2.74	629.783	N/A	N/A	N/A	
Rat 1 8h	Analyte	2.74	196208.453	12563.819	39042.359	7975.97	
Rat 1 24h	Analyte	2.74	4196.432	409.450	25622.371	5254.50	
Rat 2 0h	Analyte	2.74	391.133	N/A	N/A	N/A	
Rat 2 1h	Analyte	2.74	631.518	103.415	15266.596	3154.43	
Rat 2 2h	Analyte	2.74	4621.773	300.748	38418.984	7849.56	
Rat 2 4h	Analyte	2.74	417.775	N/A	N/A	N/A	
Rat 2 6h	Analyte	2.74	2054.282	N/A	N/A	N/A	

Rat 2 8h	Analyte	2.74	690.548	49.995	34530.853	7061.07	
Rat 2 24h	Analyte	2.74	4501.283	947.742	11873.703	2466.38	
Rat 3 0h	Analyte	2.74	229.040	N/A	N/A	N/A	
Rat 3 1h	Analyte	2.74	377.839	47.714	19797.072	4073.18	
Rat 3 2h	Analyte	2.74	661.067	N/A	N/A	N/A	
Rat 3 4h	Analyte	2.74	656.132	N/A	N/A	N/A	
Rat 3 6h	Analyte	2.74	69629.891	4316.227	40330.299	8237.16	
Rat 3 8h	Analyte	2.74	570.283	N/A	N/A	N/A	
Rat 3 24h	Analyte	2.73	316.474	141.765	5580.961	1190.26	
Rat 4 0h	Analyte	2.74	488.637	N/A	N/A	N/A	
Rat 4 1h	Analyte	2.74	548.092	N/A	N/A	N/A	
Rat 4 2h	Analyte	2.74	629.858	N/A	N/A	N/A	
Rat 4 4h	Analyte	2.73	747.336	95.857	19490.908	4011.09	
Rat 4 6h	Analyte	2.74	645.267	N/A	N/A	N/A	
Rat 4 8h	Analyte	2.73	610.604	46.739	32660.305	6681.74	
Rat 4 24h	Analyte	2.74	1347.853	333.267	10110.910	2108.90	
1000 nM QC5	QC	2.74	86220.867	18061.895	11934.084	2478.62	147.9
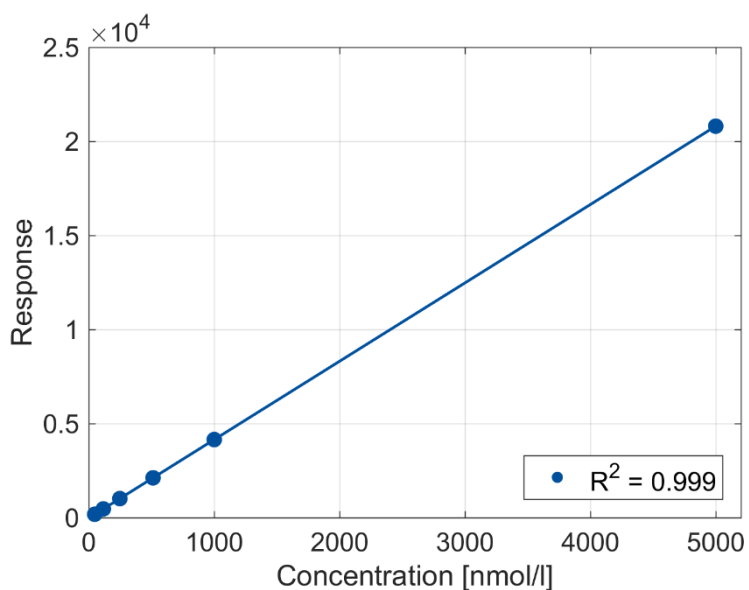
Figure 50: Standard curve of Vitamin D_3 for the plasma samples obtained from rats in cage 2.

Table 23: UHPLC – MS/MS data for vitamin D_3 compound analyzed on plasma samples from the rats in cage 2.

Sample Name	Sample Type	RT	Area	IS Area	Response	Concentration (nmol/l)	Standard Deviation (nmol/l)
Blank1	Blank	2.59	3.003	26167.533	0.287	5.07	
Blank2	Blank	2.57	29.526	36114.820	2.044	5.49	
Blank3	Blank	N/A	N/A	42648.266	N/A	N/A	
50 nM standard	Standard	2.62	1502.333	21032.867	178.570	47.86	-4.3
125 nM standard	Standard	2.62	4215.966	22707.633	464.157	116.41	-6.9
250 nM standard	Standard	2.62	10761.393	26543.209	1013.573	248.29	-0.7
500 nM standard	Standard	2.61	25862.221	30561.553	2115.585	512.81	2.6
1000 nM standard	Standard	2.61	39609.488	23871.199	4148.251	1000.72	0.1
5000 nM standard	Standard	2.61	237931.313	28590.846	20804.851	4998.90	-0.0
Rat 1 0h	Analyte	2.59	418.922	10484.213	99.894	28.98	
Rat 1 1h	Analyte	2.61	1745.620	10668.161	409.072	103.19	
Rat 1 2h	Analyte	2.61	6317.438	9102.435	1735.096	421.48	
Rat 1 4h	Analyte	2.61	10137.382	4547.307	5573.289	1342.78	
Rat 1 6h	Analyte	2.61	38836.688	11199.837	8669.030	2085.87	
Rat 1 8h	Analyte	2.61	30427.961	10384.020	7325.670	1763.42	
Rat 1 24h	Analyte	2.61	19987.811	12248.509	4079.642	984.26	
1000 nM QC1	QC	2.60	53047.289	37285.637	3556.818	858.76	-14.1
Rat 2 0h	Analyte	2.58	347.021	10484.102	82.749	24.86	
Rat 2 1h	Analyte	2.60	2487.663	12897.687	482.192	120.74	
Rat 2 2h	Analyte	2.61	7295.853	10895.582	1674.039	406.83	
Rat 2 4h	Analyte	2.61	20375.275	9808.237	5193.409	1251.60	
Rat 2 6h	Analyte	2.61	26330.504	10549.611	6239.686	1502.74	
Rat 2 8h	Analyte	2.60	27804.721	10065.700	6905.809	1662.64	
Rat 2 24h	Analyte	2.60	15942.494	8895.063	4480.714	1080.53	
1000 nM QC2	QC	2.60	66841.648	50560.277	3305.048	798.33	-20.2
Rat 3 0h	Analyte	2.59	197.564	10542.768	46.848	16.24	

Rat 3 1h	Analyte	2.59	495.332	12848.979	96.376	28.13	
Rat 3 2h	Analyte	2.60	916.715	9498.356	241.283	62.92	
Rat 3 4h	Analyte	2.60	7546.201	9179.613	2055.152	498.31	
Rat 3 6h	Analyte	2.60	19835.375	8943.081	5544.894	1335.97	
Rat 3 8h	Analyte	2.60	27756.188	8132.806	8532.168	2053.02	
Rat 3 24h	Analyte	2.60	26065.895	11568.994	5632.706	1357.05	
1000 nM QC3	QC	2.60	60635.383	50098.961	3025.780	731.29	-26.9
Rat 4 0h	Analyte	2.59	540.346	10238.401	131.941	36.67	
Rat 4 1h	Analyte	2.60	2447.796	9463.063	646.671	160.22	
Rat 4 2h	Analyte	2.60	9778.898	12335.922	1981.793	480.70	
Rat 4 4h	Analyte	2.60	21135.096	7657.611	6900.029	1661.25	
Rat 4 6h	Analyte	2.60	41511.852	6938.598	14956.859	3595.17	
Rat 4 8h	Analyte	2.60	45802.637	5443.821	21034.232	5053.95	
Rat 4 24h	Analyte	2.60	11335.940	2945.189	9622.422	2314.72	
1000 nM QC4	QC	2.60	70513.109	56123.617	3140.973	758.94	-24.1
1000 nM QC5	QC	2.59	82446.930	70856.609	2908.936	703.25	-29.7
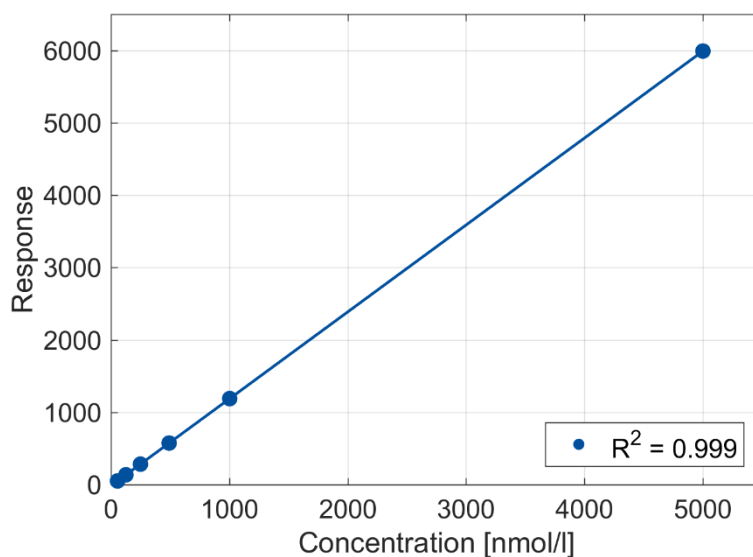
Figure 51: Standard curve of 25-OH-Vitamin D_3 for the plasma samples obtained from rats in cage 2.

Table 24: UHPLC – MS/MS data for 25-OH-vitamin D$_3$ compound analyzed on plasma samples from the rats in cage 2.

Sample Name	Sample Type	RT	Area	IS Area	Response	Concentration (nmol/l)	Standard Deviation (nmol/l)
Blank1	Blank	N/A	N/A	64170.137	N/A	N/A	
Blank2	Blank	N/A	N/A	80265.008	N/A	N/A	
Blank3	Blank	N/A	N/A	90048.336	N/A	N/A	
50 nM standard	Standard	1.75	893.516	43836.363	50.957	55.51	11.0
125 nM standard	Standard	1.74	2526.547	46460.445	135.952	126.27	1.0
250 nM standard	Standard	1.74	5766.618	50925.098	283.093	248.75	-0.5
500 nM standard	Standard	1.74	13146.887	57200.535	574.596	491.40	-1.7
1000 nM standard	Standard	1.74	22692.074	47715.484	1188.926	1002.79	0.3
5000 nM standard	Standard	1.74	135157.297	56398.672	5991.156	5000.28	0.0
Rat 1 0h	Analyte	1.73	1390.476	28060.555	123.882	116.22	
Rat 1 1h	Analyte	1.73	1298.552	32460.014	100.012	96.35	
Rat 1 2h	Analyte	1.73	1363.208	31869.143	106.938	102.11	
Rat 1 4h	Analyte	1.73	743.033	10181.569	182.446	164.97	
Rat 1 6h	Analyte	1.73	2041.635	23064.549	221.296	197.31	
Rat 1 8h	Analyte	1.73	2989.001	29552.791	252.853	223.58	
Rat 1 24h	Analyte	1.73	3644.155	28105.234	324.153	282.93	
1000 nM QC1	QC	1.73	25845.607	55038.496	1173.979	990.34	-1.0
Rat 2 0h	Analyte	1.73	718.388	27205.611	66.015	68.05	
Rat 2 1h	Analyte	1.73	780.164	34227.816	56.983	60.53	
Rat 2 2h	Analyte	1.73	924.400	26918.574	85.852	84.56	
Rat 2 4h	Analyte	1.73	1317.073	30055.596	109.553	104.29	
Rat 2 6h	Analyte	1.73	1937.776	27570.275	175.712	159.36	
Rat 2 8h	Analyte	1.73	2829.474	31344.668	225.674	200.95	
Rat 2 24h	Analyte	1.73	2347.114	22371.461	262.289	231.43	
1000 nM QC2	QC	1.73	31627.084	65930.156	1199.265	1011.39	1.1
Rat 3 0h	Analyte	1.72	790.808	29948.371	66.014	68.05	

Rat 3 1h	Analyte	1.72	727.122	30905.402	58.818	62.06	
Rat 3 2h	Analyte	1.72	706.768	31296.947	56.457	60.09	
Rat 3 4h	Analyte	1.72	957.788	29459.383	81.280	80.76	
Rat 3 6h	Analyte	1.72	1430.399	30796.385	116.117	109.76	
Rat 3 8h	Analyte	1.72	2174.988	33816.531	160.793	146.94	
Rat 3 24h	Analyte	1.73	2480.156	22873.477	271.073	238.74	
1000 nM QC3	QC	1.73	29127.338	59911.711	1215.428	1024.85	2.5
Rat 4 0h	Analyte	1.72	833.639	31230.168	66.733	68.65	
Rat 4 1h	Analyte	1.72	790.614	34644.453	57.052	60.59	
Rat 4 2h	Analyte	1.72	747.690	26396.074	70.815	72.04	
Rat 4 4h	Analyte	1.72	1521.212	34247.563	111.045	105.53	
Rat 4 6h	Analyte	1.72	2508.587	39580.457	158.449	144.99	
Rat 4 8h	Analyte	1.72	2102.621	26525.459	198.170	178.06	
Rat 4 24h	Analyte	1.73	1022.489	12166.338	210.106	187.99	
1000 nM QC4	QC	1.72	32035.770	67491.727	1186.655	1000.90	0.1
1000 nM QC5	QC	1.72	38654.777	78576.508	1229.845	1036.85	3.7

The standard curve of vitamin E for the plasma samples obtained from rats in cage 2 can be found in Figure 49. Plasma samples obtained from cage 2 and cage 1 were analyzed for vitamin E in the same analysis plate. Therefore, samples from cage 1 and cage 2 have the same standard curve for vitamin E compound.

Table 25: UHPLC – MS/MS data for vitamin E compound analyzed on plasma samples from the rats in cage 2. 25x dilution was performed on the plasma samples.

Sample Name	Sample Type	RT	Area	IS Area	Response	Concentration (nmol/l)	Standard Deviation (nmol/l)
Blank1	Blank	2.76	296.342	10522.462	70.407	72.76	
Blank2	Blank	2.77	443.141	13470.301	82.244	75.16	
Blank3	Blank	2.77	544.068	16494.643	82.461	75.20	
50 nM standard	Standard	2.77	1247.522	10417.782	299.373	119.19	138.4
125 nM standard	Standard	2.77	2411.193	12741.887	473.084	154.42	23.5
250 nM standard	Standard	2.76	8206.870	23657.018	867.276	234.36	-6.3

500 nM standard	Standard	2.76	18164.252	23135.521	1962.810	456.53	-8.7
1000 nM standard	Standard	2.76	21948.105	12537.520	4376.485	946.00	-5.4
5000 nM standard	Standard	2.76	173434.781	17741.678	24438.892	5014.50	0.3
Rat 1 0h	Analyte	2.76	3466.195	995.129	8707.904	1824.38	
Rat 1 1h	Analyte	2.76	19060.986	1517.640	31399.057	6425.97	
Rat 1 2h	Analyte	2.76	82098.781	3181.083	64521.093	13142.86	
Rat 1 4h	Analyte	2.76	64303.262	1308.160	122888.756	24979.38	
Rat 1 6h	Analyte	2.75	2006.995	115.366	43491.908	8878.31	
Rat 1 8h	Analyte	2.75	87418.055	4342.666	50325.108	10264.03	
Rat 1 24h	Analyte	2.75	31298.984	1732.570	45162.654	9217.12	
1000 nM QC1	QC	2.75	58807.316	22952.529	6405.320	1357.43	35.7
Rat 2 0h	Analyte	2.75	30266.926	1274.014	59392.844	12102.90	
Rat 2 1h	Analyte	2.75	776.055	N/A	N/A	N/A	
Rat 2 2h	Analyte	2.75	480.221	N/A	N/A	N/A	
Rat 2 4h	Analyte	2.75	60598.867	4131.300	36670.580	7494.99	
Rat 2 6h	Analyte	2.75	1290.447	116.089	27790.036	5694.09	
Rat 2 8h	Analyte	2.75	61710.750	3001.141	51406.074	10483.24	
Rat 2 24h	Analyte	2.75	56109.266	3120.305	44954.953	9175.00	
1000 nM QC2	QC	2.75	76998.477	22173.287	8681.446	1819.01	81.9
Rat 3 0h	Analyte	2.75	10308.210	303.383	84943.866	17284.45	
Rat 3 1h	Analyte	2.75	2040.803	191.626	26624.819	5457.79	
Rat 3 2h	Analyte	2.75	752.046	62.448	30106.889	6163.93	
Rat 3 4h	Analyte	2.75	871.768	N/A	N/A	N/A	
Rat 3 6h	Analyte	2.75	4786.754	88.962	134516.816	27337.46	
Rat 3 8h	Analyte	2.75	33685.477	1156.609	72810.857	14823.97	
Rat 3 24h	Analyte	2.75	61265.418	1476.375	103742.982	21096.76	
1000 nM QC3	QC	2.75	69921.727	17383.982	10055.482	2097.66	109.8
Rat 4 0h	Analyte	2.75	13399.170	1142.167	29328.395	6006.06	
Rat 4 1h	Analyte	2.75	1185.944	77.728	38144.041	7793.80	
Rat 4 2h	Analyte	2.75	36459.527	77.317	1178897.493	239129.84	

Rat 4 4h	Analyte	2.75	544.111	26.760	50832.493	10366.92	
Rat 4 6h	Analyte	2.74	113171.523	45.789	6178968.912	1253105.93	
Rat 4 8h	Analyte	2.74	696.930	N/A	N/A	N/A	
Rat 4 24h	Analyte	2.74	91992.836	632.432	363647.143	73803.33	
1000 nM QC4	QC	2.74	80239.648	16172.783	12403.500	2573.82	157.4
1000 nM QC5	QC	2.74	86220.867	18061.895	11934.084	2478.62	147.9
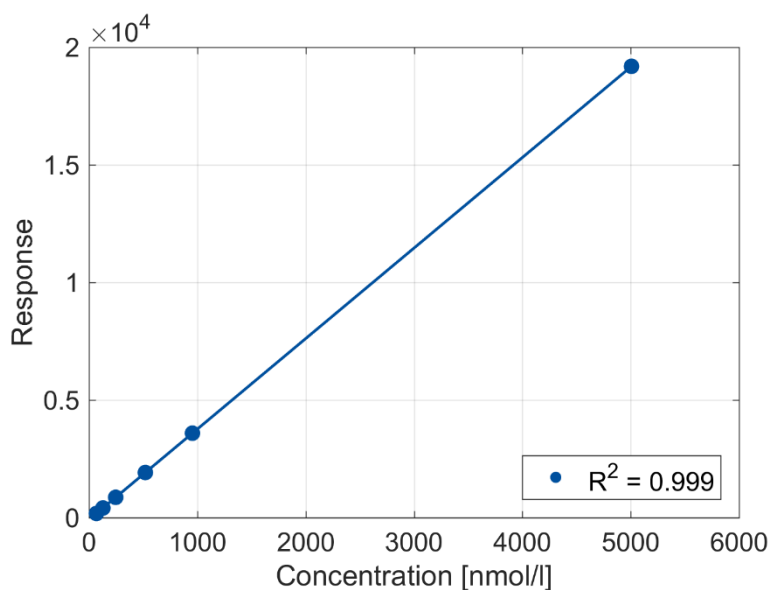
Figure 52: Standard curve of Vitamin D_3 for the plasma samples obtained from rats in cage 3.

Table 26: UHPLC – MS/MS data for vitamin D_3 compound analyzed on plasma samples from the rats in cage 3.

Sample Name	Sample Type	RT	Area	IS Area	Response	Concentration (nmol/l)	Standard Deviation (nmol/l)
Blank1	Blank	N/A	N/A	10025.533	N/A	N/A	
Blank2	Blank	N/A	N/A	10787.681	N/A	N/A	
Blank3	Blank	N/A	N/A	11811.590	N/A	N/A	
50 nM standard	Standard	2.59	597.562	8382.449	178.218	68.29	36.6
125 nM standard	Standard	2.59	1512.796	9235.864	409.490	128.37	2.7
250 nM standard	Standard	2.59	2521.143	7294.438	864.063	246.48	-1.4
500 nM standard	Standard	2.59	6217.748	8107.531	1917.275	520.11	4.0

1000 nM standard	Standard	2.59	17090.619	11899.925	3590.489	954.82	-4.5
5000 nM standard	Standard	2.59	125004.164	16287.531	19187.095	5006.93	0.1
Rat 1 0h	Analyte	2.58	246.273	5597.865	109.985	50.56	
Rat 1 1h	Analyte	2.59	2154.283	6493.832	829.357	237.46	
Rat 1 2h	Analyte	2.59	4032.855	5018.665	2008.928	543.92	
Rat 1 4h	Analyte	2.59	6934.616	4126.978	4200.783	1113.38	
Rat 1 6h	Analyte	2.59	12949.898	4628.933	6993.997	1839.08	
Rat 1 8h	Analyte	2.59	13976.947	4791.556	7292.489	1916.63	
Rat 1 24h	Analyte	2.59	7461.402	3483.660	5354.571	1413.14	
1000 nM QC1	QC	2.59	12069.802	7109.747	4244.104	1124.63	12.5
Rat 2 0h	Analyte	2.58	179.881	3301.743	136.202	57.37	
Rat 2 1h	Analyte	2.59	3025.871	7262.586	1041.596	292.60	
Rat 2 2h	Analyte	2.59	4001.703	5103.754	1960.176	531.25	
Rat 2 4h	Analyte	2.59	21143.674	8436.682	6265.400	1649.78	
Rat 2 6h	Analyte	2.59	28629.137	9490.525	7541.505	1981.32	
Rat 2 8h	Analyte	2.59	19180.781	4930.377	9725.819	2548.82	
Rat 2 24h	Analyte	2.59	15554.905	8169.765	4759.900	1258.64	
1000 nM QC2	QC	2.59	13580.592	7586.602	4475.189	1184.67	18.5
Rat 3 0h	Analyte	2.58	325.264	7562.778	107.521	49.92	
Rat 3 1h	Analyte	2.59	1975.892	9000.919	548.803	164.57	
Rat 3 2h	Analyte	2.59	5401.901	10231.478	1319.922	364.91	
Rat 3 4h	Analyte	2.59	60040.121	26209.033	5727.045	1509.91	
Rat 3 6h	Analyte	2.59	18899.971	5024.953	9403.059	2464.97	
Rat 3 8h	Analyte	2.60	21851.225	5353.189	10204.770	2673.26	
Rat 3 24h	Analyte	2.59	17854.764	6277.666	7110.431	1869.33	
1000 nM QC3	QC	2.59	14111.390	9908.507	3560.423	947.01	-5.3
Rat 4 0h	Analyte	2.58	197.681	7376.863	66.994	39.39	
Rat 4 1h	Analyte	2.59	3559.194	10921.899	814.692	233.65	
Rat 4 2h	Analyte	2.59	8230.523	5901.244	3486.775	927.88	
Rat 4 4h	Analyte	2.59	17103.447	4894.226	8736.543	2291.80	
Rat 4 6h	Analyte	2.59	28627.541	5752.628	12441.071	3254.27	

Rat 4 8h	Analyte	2.59	34224.375	6895.523	12408.187	3245.72	
Rat 4 24h	Analyte	2.59	15586.051	4949.474	7872.579	2067.34	
1000 nM QC4	QC	2.59	12914.768	8378.370	3853.604	1023.18	2.3
1000 nM QC5	QC	2.59	13998.808	7448.413	4698.587	1242.71	24.3
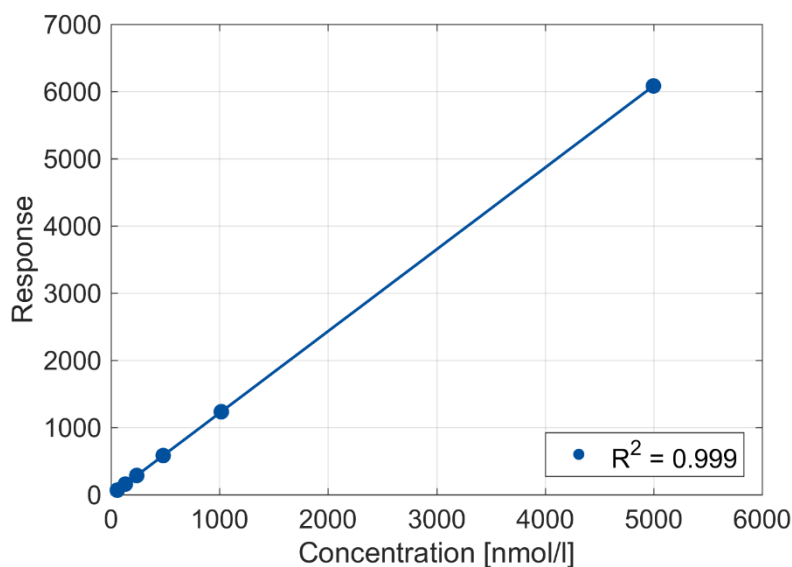
Figure 53: Standard curve of 25-OH-Vitamin D_3 for the plasma samples obtained from rats in cage 3.

Table 27: UHPLC – MS/MS data for 25-OH-vitamin D_3 compound analyzed on plasma samples from the rats in cage 3.

Sample Name	Sample Type	RT	Area	IS Area	Response	Concentration (nmol/l)	Standard Deviation (nmol/l)
Blank1	Blank	N/A	N/A	31218.719	N/A	N/A	
Blank2	Blank	N/A	N/A	37508.574	N/A	N/A	
Blank3	Blank	N/A	N/A	41927.141	N/A	N/A	
50 nM standard	Standard	1.72	361.978	13543.404	66.818	58.32	16.6
125 nM standard	Standard	1.72	2069.032	32974.590	156.866	132.28	5.8
250 nM standard	Standard	1.72	3496.446	30655.111	285.144	237.65	-4.9
500 nM standard	Standard	1.72	9026.882	38806.633	581.530	481.10	-3.8
1000 nM standard	Standard	1.72	20110.963	40754.211	1233.674	1016.77	1.7

5000 nM standard	Standard	1.72	98816.109	40620.563	6081.656	4998.89	-0.0
Rat 1 0h	Analyte	1.72	571.339	16962.070	84.208	72.60	
Rat 1 1h	Analyte	1.71	649.172	17299.281	93.815	80.49	
Rat 1 2h	Analyte	1.72	444.029	10843.422	102.373	87.52	
Rat 1 4h	Analyte	1.72	544.578	10838.136	125.616	106.61	
Rat 1 6h	Analyte	1.72	1047.858	12854.302	203.795	170.83	
Rat 1 8h	Analyte	1.72	1102.787	12681.779	217.396	182.00	
Rat 1 24h	Analyte	1.72	1538.425	9868.654	389.725	323.55	
1000 nM QC1	QC	1.72	16605.150	32154.350	1291.050	1063.90	6.4
Rat 2 0h	Analyte	1.72	216.042	5925.095	91.156	78.31	
Rat 2 1h	Analyte	1.71	668.858	27936.822	59.855	52.60	
Rat 2 2h	Analyte	1.72	186.373	9940.416	46.873	41.93	
Rat 2 4h	Analyte	1.71	961.222	21791.730	110.274	94.01	
Rat 2 6h	Analyte	1.71	1699.049	28428.381	149.415	126.16	
Rat 2 8h	Analyte	1.71	2476.266	29218.686	211.873	177.46	
Rat 2 24h	Analyte	1.71	1965.535	20455.018	240.227	200.75	
1000 nM QC2	QC	1.72	20795.168	42999.387	1209.039	996.53	-0.3
Rat 3 0h	Analyte	1.71	559.871	26457.502	52.903	46.89	
Rat 3 1h	Analyte	1.71	741.991	30752.914	60.319	52.98	
Rat 3 2h	Analyte	1.71	796.694	31228.688	63.779	55.82	
Rat 3 4h	Analyte	1.71	1677.340	40207.246	104.293	89.10	
Rat 3 6h	Analyte	1.72	1866.616	29577.232	157.775	133.03	
Rat 3 8h	Analyte	1.72	2871.034	34358.535	208.903	175.02	
Rat 3 24h	Analyte	1.72	3190.589	30824.977	258.767	215.98	
1000 nM QC3	QC	1.72	20480.551	44146.836	1159.797	956.09	-4.4
Rat 4 0h	Analyte	1.71	463.261	33495.418	34.576	31.83	
Rat 4 1h	Analyte	1.71	695.246	33383.215	52.066	46.20	
Rat 4 2h	Analyte	1.71	794.406	35594.613	55.795	49.26	
Rat 4 4h	Analyte	1.72	892.228	22852.373	97.608	83.61	
Rat 4 6h	Analyte	1.71	2195.118	36186.176	151.654	128.00	
Rat 4 8h	Analyte	1.71	2688.989	37102.035	181.189	152.26	

Rat 4 24h	Analyte	1.71	2491.346	34018.566	183.087	153.82	
1000 nM QC4	QC	1.71	18735.947	43205.199	1084.126	893.93	-10.6
1000 nM QC5	QC	1.71	26132.861	50228.543	1300.698	1071.82	7.2
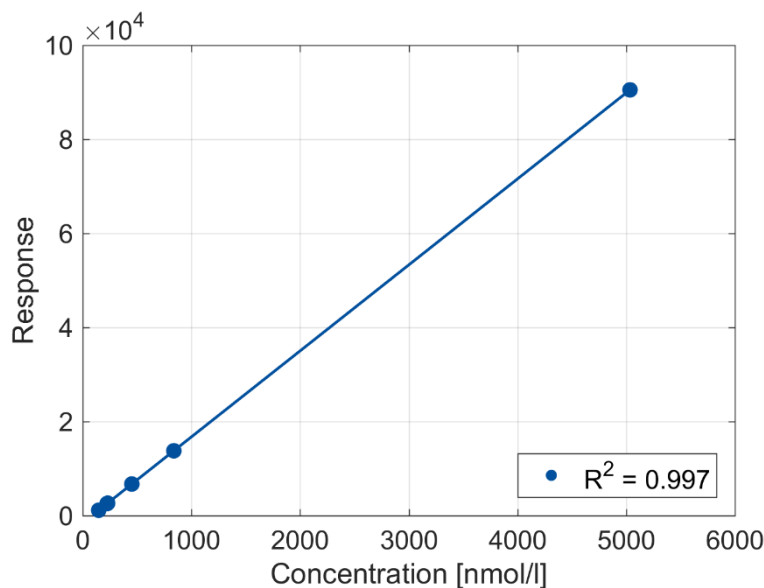
Figure 54: Standard curve of Vitamin E for the plasma samples obtained from rats in cage 3 and cage 4.

Table 28: UHPLC – MS/MS data for vitamin E compound analyzed on plasma samples from the rats in cage 3. 25x dilution was performed on the plasma samples.

Sample Name	Sample Type	RT	Area	IS Area	Response	Concentration (nmol/l)	Standard Deviation (nmol/l)
Blank1	Blank	N/A	N/A	787.486	N/A	N/A	
Blank2	Blank	2.73	278.508	1423.527	489.116	110.79	
Blank3	Blank	2.73	225.776	1254.571	449.907	108.65	
50 nM standard	Standard	2.74	422.645	920.047	1148.433	146.85	193.7
125 nM standard	Standard	2.74	709.899	690.375	2570.701	224.65	79.7
250 nM standard	Standard	2.74	1021.947	963.691	2651.127	229.05	-8.4
500 nM standard	Standard	2.74	2026.475	753.783	6721.016	451.66	-9.7
1000 nM standard	Standard	2.74	4915.348	891.514	13783.710	837.96	-16.2
5000 nM standard	Standard	2.74	70954.836	1959.787	90513.454	5034.83	0.7

Rat 1 0h	Analyte	2.74	41200.934	1497.764	68770.738	3845.57	
Rat 1 1h	Analyte	2.74	29175.918	1444.448	50496.657	2846.04	
Rat 1 2h	Analyte	2.74	91924.633	1327.522	173113.201	9552.77	
Rat 1 4h	Analyte	2.74	84404.031	1820.403	115913.936	6424.15	
Rat 1 6h	Analyte	2.74	98028.617	1671.152	146648.266	8105.22	
Rat 1 8h	Analyte	2.74	122762.484	2063.465	148733.422	8219.27	
Rat 1 24h	Analyte	2.74	77295.539	1518.316	127271.825	7045.39	
1000 nM QC1	QC	2.74	5412.458	512.523	26401.049	1528.09	52.8
Rat 2 0h	Analyte	2.74	33794.645	889.124	95022.306	5281.45	
Rat 2 1h	Analyte	2.74	93501.781	1943.495	120275.304	6662.71	
Rat 2 2h	Analyte	2.74	84570.336	1546.093	136748.462	7563.73	
Rat 2 4h	Analyte	2.74	74090.008	800.993	231244.243	12732.34	
Rat 2 6h	Analyte	2.74	124682.234	1264.292	246545.565	13569.28	
Rat 2 8h	Analyte	2.73	102070.047	883.763	288737.045	15877.01	
Rat 2 24h	Analyte	2.73	31920.945	624.479	127790.306	7073.75	
1000 nM QC2	QC	2.73	4462.301	479.806	23250.548	1355.77	35.6
Rat 3 0h	Analyte	2.74	28790.652	665.620	108134.717	5998.66	
Rat 3 1h	Analyte	2.73	31134.973	762.082	102137.870	5670.65	
Rat 3 2h	Analyte	2.74	23092.605	490.588	117678.199	6520.65	
Rat 3 4h	Analyte	2.74	49160.879	262.282	468587.999	25714.27	
Rat 3 6h	Analyte	2.74	56771.492	320.353	443038.554	24316.80	
Rat 3 8h	Analyte	2.74	66018.438	206.935	797574.577	43708.76	
Rat 3 24h	Analyte	2.74	38754.551	382.555	253261.302	13936.61	
1000 nM QC3	QC	2.74	5991.136	760.898	19684.426	1160.71	16.1
Rat 4 0h	Analyte	2.74	20384.178	232.913	218796.053	12051.47	
Rat 4 1h	Analyte	2.74	28024.527	276.025	253822.362	13967.29	
Rat 4 2h	Analyte	2.74	43366.215	611.646	177252.099	9779.15	
Rat 4 4h	Analyte	2.74	41896.676	106.372	984673.504	53942.46	
Rat 4 6h	Analyte	2.74	49620.730	97.307	1274849.959	69814.17	
Rat 4 8h	Analyte	2.73	133441.391	377.895	882794.103	48369.99	
Rat 4 24h	Analyte	2.73	43047.434	99.525	1081322.130	59228.83	

| 1000 nM QC4 | QC | 2.73 | 4106.292 | 975.868 | 10519.589 | 659.43 | -34.1 |
| 1000 nM QC5 | QC | 2.73 | 8116.966 | 593.520 | 34189.943 | 1954.12 | 95.4 |
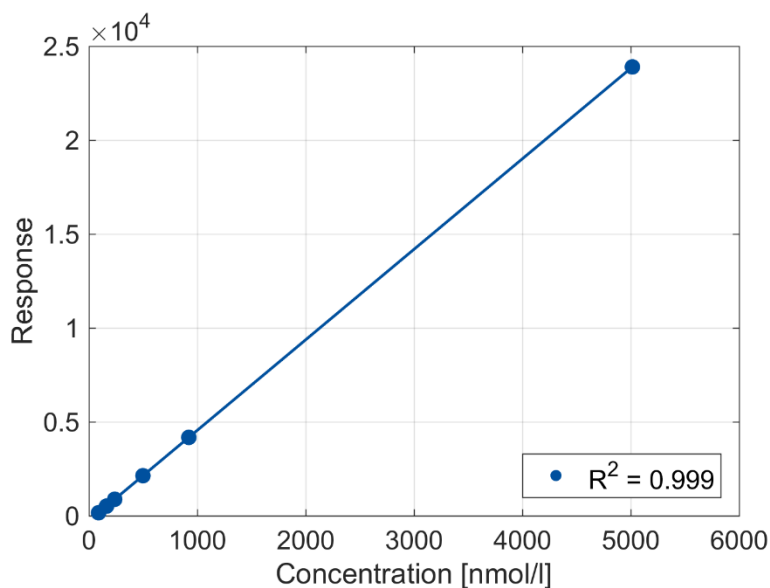
Figure 55: Standard curve of Vitamin D$_3$ for the plasma samples obtained from rats in cage 4 and cage 5.

Table 29: UHPLC – MS/MS data for vitamin D$_3$ compound analyzed on plasma samples from the rats in cage 4.

Sample Name	Sample Type	RT	Area	IS Area	Response	Concentration (nmol/l)	Standard Deviation (nmol/l)
Blank1	Blank	N/A	N/A	1939.700	N/A	N/A	
Blank2	Blank	N/A	N/A	3738.148	N/A	N/A	
Blank3	Blank	N/A	N/A	6180.148	N/A	N/A	
50 nM standard	Standard	2.57	428.037	6611.530	161.852	89.28	78.6
125 nM standard	Standard	2.57	1125.331	5476.444	513.714	162.31	29.8
250 nM standard	Standard	2.57	2091.903	5952.761	878.543	238.02	-4.8
500 nM standard	Standard	2.57	6073.533	7117.508	2133.307	498.44	-0.3
1000 nM standard	Standard	2.57	6548.935	3922.773	4173.664	921.90	-7.8
5000 nM standard	Standard	2.57	48663.043	5091.199	23895.669	5015.05	0.3
1000 nM QC1	QC	2.57	4096.333	1967.941	5203.831	1135.70	13.6

1000 nM QC2	QC	2.57	7668.844	4789.295	4003.117	886.50	-11.3
1000 nM QC3	QC	2.57	8879.156	5578.208	3979.394	881.58	-11.8
1000 nM QC4	QC	2.57	14538.113	7693.103	4724.398	1036.20	3.6
Rat 1 0h	Analyte	2.58	18.464	1258.542	36.677	63.30	
Rat 1 1h	Analyte	2.57	1431.255	2748.799	1301.709	325.85	
Rat 1 2h	Analyte	2.57	3086.378	1832.243	4211.202	929.69	
Rat 1 4h	Analyte	2.57	18493.643	2070.487	22330.064	4690.12	
Rat 1 6h	Analyte	2.57	31104.492	3079.642	25250.088	5296.15	
Rat 1 8h	Analyte	2.58	34876.426	2431.846	35853.860	7496.88	
Rat 1 24h	Analyte	2.58	8459.861	1686.718	12538.938	2658.05	
Rat 2 0h	Analyte	N/A	N/A	1247.071	N/A	N/A	
Rat 2 1h	Analyte	2.58	631.755	2847.494	554.659	170.80	
Rat 2 2h	Analyte	2.58	2000.401	831.873	6011.738	1303.38	
Rat 2 4h	Analyte	2.58	12726.919	1426.861	22298.807	4683.63	
Rat 2 6h	Analyte	2.58	12537.525	1655.104	18937.669	3986.05	
Rat 2 8h	Analyte	2.58	31503.951	2594.950	30351.212	6354.85	
Rat 2 24h	Analyte	2.58	7930.385	1078.138	18389.077	3872.20	
Rat 3 0h	Analyte	2.59	5.724	618.508	23.136	60.49	
Rat 3 1h	Analyte	2.58	1033.702	2093.359	1234.502	311.90	
Rat 3 2h	Analyte	2.58	5982.451	3784.212	3952.244	875.95	
Rat 3 4h	Analyte	2.58	27187.213	3483.189	19513.162	4105.49	
Rat 3 6h	Analyte	2.58	20396.965	1836.387	27767.792	5818.68	
Rat 3 8h	Analyte	2.58	24671.363	1905.741	32364.528	6772.69	
Rat 3 24h	Analyte	2.58	22712.711	2338.277	24283.597	5095.56	
Rat 4 0h	Analyte	2.57	37.100	1408.194	65.865	69.36	
Rat 4 1h	Analyte	2.58	821.031	1280.804	1602.570	388.29	
Rat 4 2h	Analyte	2.58	1303.328	1031.755	3158.037	711.11	
Rat 4 4h	Analyte	2.58	13472.207	1802.100	18689.594	3934.57	
Rat 4 6h	Analyte	2.58	19660.922	823.743	59669.466	12439.62	
Rat 4 8h	Analyte	2.58	14667.783	655.010	55983.050	11674.54	
Rat 4 24h	Analyte	2.58	19730.355	1582.445	31170.680	6524.92	

1000 nM QC5	QC	2.58	10026.028	5669.364	4421.143	973.26	-2.7
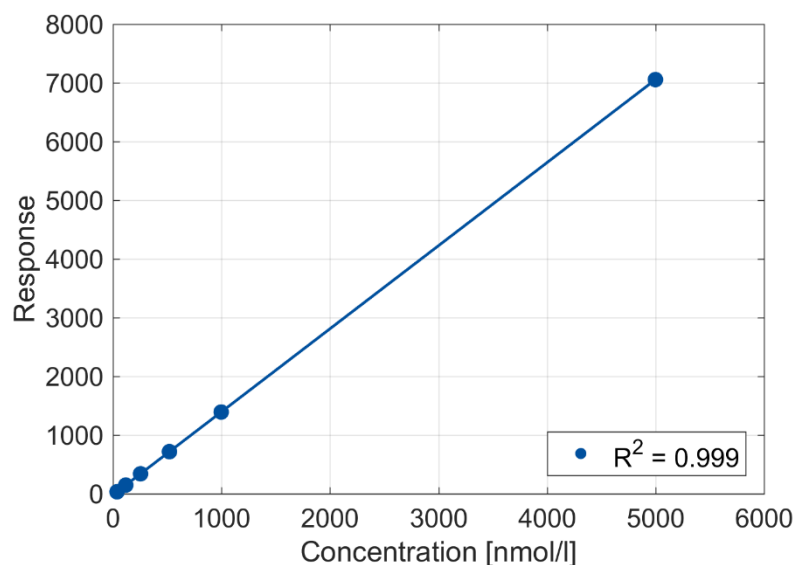
Figure 56: Standard curve of 25-OH-Vitamin D_3 for the plasma samples obtained from rats in cage 4 and cage 5.

Table 30: UHPLC – MS/MS data for 25-OH-vitamin D_3 compound analyzed on plasma samples from the rats in cage 4.

Sample Name	Sample Type	RT	Area	IS Area	Response	Concentration (nmol/l)	Standard Deviation (nmol/l)
Blank1	Blank	N/A	N/A	15462.592	N/A	N/A	
Blank2	Blank	N/A	N/A	21820.156	N/A	N/A	
Blank3	Blank	N/A	N/A	29821.336	N/A	N/A	
50 nM standard	Standard	1.70	94.019	6973.563	33.706	37.28	-25.4
125 nM standard	Standard	1.70	674.041	11428.907	147.442	117.65	-5.9
250 nM standard	Standard	1.70	558.820	4104.607	340.361	253.96	1.6
500 nM standard	Standard	1.70	3215.376	11207.497	717.238	520.26	4.1
1000 nM standard	Standard	1.70	10473.611	18807.115	1392.241	997.20	-0.3
5000 nM standard	Standard	1.70	17023.723	6032.211	7055.341	4998.65	-0.0
1000 nM QC1	QC	1.70	5616.417	9735.153	1442.303	1032.57	3.3
1000 nM QC2	QC	1.70	17588.365	29775.174	1476.764	1056.92	5.7

1000 nM QC3	QC	1.70	16668.148	29267.213	1423.790	1019.49	1.9
1000 nM QC4	QC	1.70	18641.381	36444.371	1278.756	917.01	-8.3
Rat 1 0h	Analyte	1.70	192.595	12727.758	37.830	40.20	
Rat 1 1h	Analyte	1.70	416.019	20147.844	51.621	49.94	
Rat 1 2h	Analyte	1.70	240.465	12245.527	49.092	48.16	
Rat 1 4h	Analyte	1.70	719.994	18507.219	97.259	82.19	
Rat 1 6h	Analyte	1.70	1976.242	28082.707	175.931	137.78	
Rat 1 8h	Analyte	1.70	1876.708	17702.404	265.036	200.74	
Rat 1 24h	Analyte	1.71	1706.417	13911.774	306.650	230.14	
Rat 2 0h	Analyte	1.70	177.049	11743.154	37.692	40.10	
Rat 2 1h	Analyte	1.70	471.445	24636.170	47.841	47.27	
Rat 2 2h	Analyte	1.71	324.713	11683.107	69.483	62.56	
Rat 2 4h	Analyte	1.71	685.623	16423.877	104.364	87.21	
Rat 2 6h	Analyte	1.71	1069.455	16436.617	162.663	128.40	
Rat 2 8h	Analyte	1.70	2642.811	31041.771	212.843	163.86	
Rat 2 24h	Analyte	1.71	1321.782	14172.869	233.154	178.21	
Rat 3 0h	Analyte	1.71	187.076	11242.287	41.601	42.86	
Rat 3 1h	Analyte	1.71	459.936	22747.346	50.548	49.19	
Rat 3 2h	Analyte	1.70	499.335	33092.703	37.722	40.12	
Rat 3 4h	Analyte	1.70	1145.460	26523.525	107.966	89.76	
Rat 3 6h	Analyte	1.70	1803.679	29761.807	151.510	120.52	
Rat 3 8h	Analyte	1.70	2820.871	33575.453	210.040	161.88	
Rat 3 24h	Analyte	1.70	2839.155	28450.150	249.485	189.75	
Rat 4 0h	Analyte	1.71	218.653	12668.382	43.149	43.96	
Rat 4 1h	Analyte	1.70	435.466	22396.328	48.609	47.82	
Rat 4 2h	Analyte	1.70	294.837	16366.086	45.038	45.29	
Rat 4 4h	Analyte	1.70	904.234	33776.719	66.927	60.76	
Rat 4 6h	Analyte	1.70	1431.829	27720.281	129.132	104.71	
Rat 4 8h	Analyte	1.70	2334.054	25845.338	225.771	172.99	
Rat 4 24h	Analyte	1.70	2852.905	28320.840	251.838	191.41	
1000 nM QC5	QC	1.71	24536.953	53455.996	1147.530	824.29	-17.6

The standard curve of vitamin E for the plasma samples obtained from rats in cage 4 can be found in Figure 54. Plasma samples obtained from cage 4 and cage 3 were analyzed for vitamin E in the same analysis plate. Therefore, samples from cage 3 and cage 4 have the same standard curve for vitamin E compound.

Table 31: UHPLC – MS/MS data for vitamin E compound analyzed on plasma samples from the rats in cage 4. 25x dilution was performed on the plasma samples.

Sample Name	Sample Type	RT	Area	IS Area	Response	Concentration (nmol/l)	Standard Deviation (nmol/l)
Blank1	Blank	N/A	N/A	787.486	N/A	N/A	
Blank2	Blank	2.73	278.508	1423.527	489.116	110.79	
Blank3	Blank	2.73	225.776	1254.571	449.907	108.65	
50 nM standard	Standard	2.74	422.645	920.047	1148.433	146.85	193.7
125 nM standard	Standard	2.74	709.899	690.375	2570.701	224.65	79.7
250 nM standard	Standard	2.74	1021.947	963.691	2651.127	229.05	-8.4
500 nM standard	Standard	2.74	2026.475	753.783	6721.016	451.66	-9.7
1000 nM standard	Standard	2.74	4915.348	891.514	13783.710	837.96	-16.2
5000 nM standard	Standard	2.74	70954.836	1959.787	90513.454	5034.83	0.7
1000 nM QC1	QC	2.74	5412.458	512.523	26401.049	1528.09	52.8
1000 nM QC2	QC	2.73	4462.301	479.806	23250.548	1355.77	35.6
1000 nM QC3	QC	2.74	5991.136	760.898	19684.426	1160.71	16.1
1000 nM QC4	QC	2.73	4106.292	975.868	10519.589	659.43	-34.1
Rat 1 0h	Analyte	2.73	24479.367	164.367	372327.885	20449.16	
Rat 1 1h	Analyte	2.73	27514.361	84.286	816101.162	44722.11	
Rat 1 2h	Analyte	2.73	36330.402	240.388	377830.861	20750.15	
Rat 1 4h	Analyte	2.73	71022.320	142.281	1247923.475	68341.38	
Rat 1 6h	Analyte	2.73	45976.945	77.453	1484027.249	81255.48	
Rat 1 8h	Analyte	2.73	66125.461	214.371	771156.791	42263.80	
Rat 1 24h	Analyte	2.73	36496.910	90.090	1012790.265	55480.36	
Rat 2 0h	Analyte	2.73	19486.748	107.055	455063.939	24974.55	
Rat 2 1h	Analyte	2.73	19250.934	N/A	N/A	N/A	

Rat 2 2h	Analyte	2.73	34138.648	45.020	1895749.000	103775.32	
Rat 2 4h	Analyte	2.73	53505.977	152.509	877095.401	48058.29	
Rat 2 6h	Analyte	2.73	53291.531	210.790	632045.294	34654.85	
Rat 2 8h	Analyte	2.73	67627.172	841.028	201025.329	11079.47	
Rat 2 24h	Analyte	2.73	54575.738	120.491	1132361.297	62020.50	
Rat 3 0h	Analyte	2.73	24164.143	113.130	533990.608	29291.58	
Rat 3 1h	Analyte	2.73	30798.197	81.831	940908.610	51548.67	
Rat 3 2h	Analyte	2.73	45316.227	69.619	1627293.806	89091.69	
Rat 3 4h	Analyte	2.73	197759.797	321.700	1536833.984	84143.84	
Rat 3 6h	Analyte	2.74	75695.313	44.085	4292577.577	234874.01	
Rat 3 8h	Analyte	2.73	93688.445	140.034	1672601.743	91569.89	
Rat 3 24h	Analyte	2.73	56670.395	64.422	2199186.419	120372.35	
Rat 4 0h	Analyte	2.73	35623.730	193.277	460785.945	25287.53	
Rat 4 1h	Analyte	2.73	41153.926	321.943	319574.630	17563.73	
Rat 4 2h	Analyte	2.73	40874.461	174.278	586339.943	32154.92	
Rat 4 4h	Analyte	2.73	79558.547	282.658	703664.384	38572.18	
Rat 4 6h	Analyte	2.73	161278.922	211.263	1908508.849	104473.24	
Rat 4 8h	Analyte	2.73	88428.195	254.619	868240.341	47573.95	
Rat 4 24h	Analyte	2.73	78328.125	212.941	919598.915	50383.10	
1000 nM QC5	QC	2.73	8116.966	593.520	34189.943	1954.12	95.4

The standard curve of vitamin D_3 for the plasma samples obtained from rats in cage 5 can be found in Figure 55. Plasma samples obtained from cage 4 and cage 5 were analyzed for vitamin D_3 in the same analysis plate. Therefore, samples from cage 4 and cage 5 have the same standard curve for vitamin D_3 compound.

Table 32: UHPLC – MS/MS data for vitamin D_3 compound analyzed on plasma samples from the rats in cage 5.

Sample Name	Sample Type	RT	Area	IS Area	Response	Concentra tion (nmol/l)	Standard Deviation (nmol/l)
Blank1	Blank	N/A	N/A	1939.700	N/A	N/A	
Blank2	Blank	N/A	N/A	3738.148	N/A	N/A	
Blank3	Blank	N/A	N/A	6180.148	N/A	N/A	

50 nM standard	Standard	2.57	428.037	6611.530	161.852	89.28	78.6
125 nM standard	Standard	2.57	1125.331	5476.444	513.714	162.31	29.8
250 nM standard	Standard	2.57	2091.903	5952.761	878.543	238.02	-4.8
500 nM standard	Standard	2.57	6073.533	7117.508	2133.307	498.44	-0.3
1000 nM standard	Standard	2.57	6548.935	3922.773	4173.664	921.90	-7.8
5000 nM standard	Standard	2.57	48663.043	5091.199	23895.669	5015.05	0.3
Rat 1 0h	Analyte	N/A	N/A	4468.889	N/A	N/A	
Rat 1 1h	Analyte	2.57	229.883	1635.181	351.464	128.63	
Rat 1 2h	Analyte	2.57	4295.566	5255.302	2043.444	479.79	
Rat 1 4h	Analyte	2.57	9458.005	3502.669	6750.570	1456.72	
Rat 1 6h	Analyte	2.57	23891.877	5493.484	10872.825	2312.26	
Rat 1 8h	Analyte	2.57	11173.701	3378.667	8267.832	1771.61	
Rat 1 24h	Analyte	2.57	14185.097	6173.878	5743.998	1247.81	
1000 nM QC1	QC	2.57	4096.333	1967.941	5203.831	1135.70	13.6
Rat 2 0h	Analyte	2.57	122.652	2215.152	138.424	84.42	
Rat 2 1h	Analyte	2.57	1220.875	7216.135	422.967	143.47	
Rat 2 2h	Analyte	2.57	2085.459	2864.744	1819.935	433.40	
Rat 2 4h	Analyte	2.57	6169.129	2011.580	7667.019	1646.92	
Rat 2 6h	Analyte	2.57	13914.696	4486.766	7753.188	1664.80	
Rat 2 8h	Analyte	2.57	19827.346	4904.016	10107.709	2153.47	
Rat 2 24h	Analyte	2.57	10158.129	4288.161	5922.194	1284.79	
1000 nM QC2	QC	2.57	7668.844	4789.295	4003.117	886.50	-11.3
Rat 3 0h	Analyte	N/A	N/A	3701.183	N/A	N/A	
Rat 3 1h	Analyte	2.58	757.352	5576.264	339.543	126.16	
Rat 3 2h	Analyte	2.57	1645.629	3203.746	1284.144	322.20	
Rat 3 4h	Analyte	2.57	9353.327	3207.967	7289.139	1568.49	
Rat 3 6h	Analyte	2.57	12376.161	2755.269	11229.540	2386.29	
Rat 3 8h	Analyte	2.57	11645.319	3005.039	9688.160	2066.39	
Rat 3 24h	Analyte	2.57	6505.034	3375.542	4817.770	1055.58	
1000 nM QC3	QC	2.57	8879.156	5578.208	3979.394	881.58	-11.8

Rat 4 0h	Analyte	N/A	N/A	3376.236	N/A	N/A	
Rat 4 1h	Analyte	2.57	621.843	3131.487	496.444	158.72	
Rat 4 2h	Analyte	2.57	6358.029	4646.365	3420.969	765.68	
Rat 4 4h	Analyte	2.57	34957.520	7230.251	12087.243	2564.30	
Rat 4 6h	Analyte	2.57	32791.914	4035.129	20316.521	4272.22	
Rat 4 8h	Analyte	2.57	33644.133	5186.962	16215.722	3421.14	
Rat 4 24h	Analyte	2.57	20802.820	3626.985	14338.921	3031.62	
1000 nM QC4	QC	2.57	14538.113	7693.103	4724.398	1036.20	3.6
1000 nM QC5	QC	2.58	10026.028	5669.364	4421.143	973.26	-2.7

The standard curve of 25-OH-Vitamin D_3 for the plasma samples obtained from rats in cage 5 can be found in Figure 56. Plasma samples obtained from cage 4 and cage 5 were analyzed for 25-OH-Vitamin D_3 in the same analysis plate. Therefore, samples from cage 4 and cage 5 have the same standard curve for 25-OH-Vitamin D_3 compound.

Table 33: UHPLC – MS/MS data for 25-OH-vitamin D_3 compound analyzed on plasma samples from the rats in cage 5.

Sample Name	Sample Type	RT	Area	IS Area	Response	Concentration (nmol/l)	Standard Deviation (nmol/l)
Blank1	Blank	N/A	N/A	15462.592	N/A	N/A	
Blank2	Blank	N/A	N/A	21820.156	N/A	N/A	
Blank3	Blank	N/A	N/A	29821.336	N/A	N/A	
50 nM standard	Standard	1.70	94.019	6973.563	33.706	37.28	-25.4
125 nM standard	Standard	1.70	674.041	11428.907	147.442	117.65	-5.9
250 nM standard	Standard	1.70	558.820	4104.607	340.361	253.96	1.6
500 nM standard	Standard	1.70	3215.376	11207.497	717.238	520.26	4.1
1000 nM standard	Standard	1.70	10473.611	18807.115	1392.241	997.20	-0.3
5000 nM standard	Standard	1.70	17023.723	6032.211	7055.341	4998.65	-0.0
Rat 1 0h	Analyte	N/A	N/A	2629.705	N/A	N/A	
Rat 1 1h	Analyte	N/A	N/A	2575.885	N/A	N/A	
Rat 1 2h	Analyte	1.70	248.607	10643.893	58.392	54.73	
Rat 1 4h	Analyte	1.70	234.958	5809.914	101.102	84.91	

Rat 1 6h	Analyte	1.70	894.009	10843.322	206.120	159.11	
Rat 1 8h	Analyte	1.70	203.481	2626.065	193.713	150.34	
Rat 1 24h	Analyte	1.70	1678.012	15141.265	277.059	209.23	
1000 nM QC1	QC	1.70	5616.417	9735.153	1442.303	1032.57	3.3
Rat 2 0h	Analyte	1.70	213.156	8393.663	63.487	58.33	
Rat 2 1h	Analyte	1.69	252.013	12190.778	51.681	49.99	
Rat 2 2h	Analyte	1.70	66.316	3904.327	42.463	43.47	
Rat 2 4h	Analyte	1.69	214.343	3474.465	154.227	122.44	
Rat 2 6h	Analyte	1.70	404.288	5894.424	171.471	134.63	
Rat 2 8h	Analyte	1.70	980.519	9854.611	248.746	189.23	
Rat 2 24h	Analyte	1.70	1261.789	9037.461	349.044	260.10	
1000 nM QC2	QC	1.70	17588.365	29775.174	1476.764	1056.92	5.7
Rat 3 0h	Analyte	1.70	215.884	8893.972	60.683	56.35	
Rat 3 1h	Analyte	1.70	214.873	12339.487	43.534	44.23	
Rat 3 2h	Analyte	1.70	162.378	5378.046	75.482	66.80	
Rat 3 4h	Analyte	1.70	345.325	9614.862	89.789	76.91	
Rat 3 6h	Analyte	1.70	497.723	9622.835	129.308	104.84	
Rat 3 8h	Analyte	1.70	686.122	9626.240	178.191	139.38	
Rat 3 24h	Analyte	1.70	782.159	7147.390	273.582	206.78	
1000 nM QC3	QC	1.70	16668.148	29267.213	1423.790	1019.49	1.9
Rat 4 0h	Analyte	1.69	195.126	10468.871	46.597	46.39	
Rat 4 1h	Analyte	1.70	98.214	5278.719	46.514	46.33	
Rat 4 2h	Analyte	1.69	445.544	15575.956	71.512	64.00	
Rat 4 4h	Analyte	1.69	1297.801	26564.277	122.138	99.77	
Rat 4 6h	Analyte	1.69	1343.667	17898.221	187.682	146.08	
Rat 4 8h	Analyte	1.69	1681.058	17598.602	238.806	182.20	
Rat 4 24h	Analyte	1.69	1921.514	16798.758	285.961	215.52	
1000 nM QC4	QC	1.70	18641.381	36444.371	1278.756	917.01	-8.3
1000 nM QC5	QC	1.71	24536.953	53455.996	1147.530	824.29	-17.6
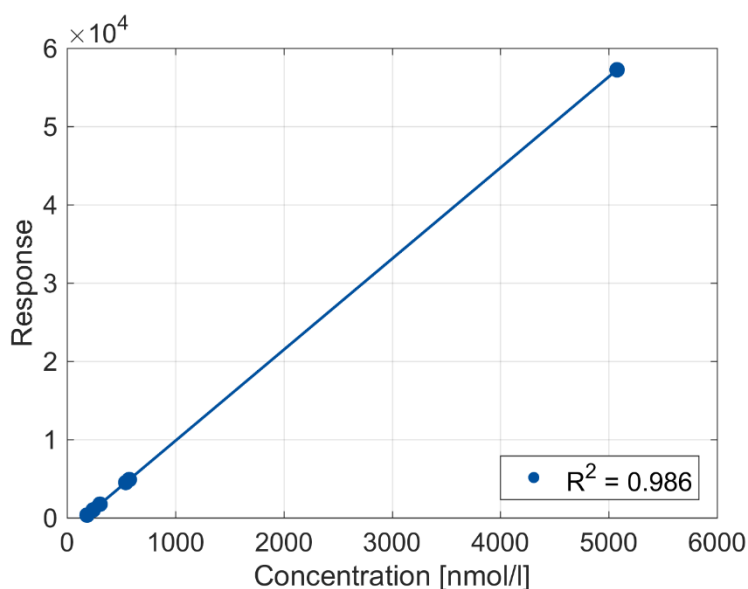
Figure 57: Standard curve of Vitamin E for the plasma samples obtained from rats in cage 5.

Table 34: UHPLC – MS/MS data for vitamin E compound analyzed on plasma samples from the rats in cage 5. 25x dilution was performed on the plasma samples.

Sample Name	Sample Type	RT	Area	IS Area	Response	Concentration (nmol/l)	Standard Deviation (nmol/l)
Blank1	Blank	N/A	N/A	273.774	N/A	N/A	
Blank2	Blank	2.72	195.269	920.160	530.530	200.88	
Blank3	Blank	2.71	216.575	831.953	650.803	211.22	
50 nM standard	Standard	2.71	246.444	1784.435	345.269	184.95	269.9
125 nM standard	Standard	2.72	588.003	1469.765	1000.165	241.26	93.0
250 nM standard	Standard	2.71	1005.211	1450.532	1732.487	304.24	21.7
500 nM standard	Standard	2.72	2582.217	1322.766	4880.336	574.92	15.0
1000 nM standard	Standard	2.72	1791.561	994.269	4504.719	542.62	-45.7
5000 nM standard	Standard	2.71	39936.188	1744.347	57236.588	5077.02	1.5
Rat 1 0h	Analyte	2.72	19555.867	854.388	57221.856	5075.75	
Rat 1 1h	Analyte	2.72	35731.527	1819.481	49095.768	4376.99	
Rat 1 2h	Analyte	2.71	20757.105	952.942	54455.321	4837.86	
Rat 1 4h	Analyte	2.72	34912.766	600.517	145344.620	12653.40	
Rat 1 6h	Analyte	2.71	48421.523	1044.038	115947.703	10125.57	

Rat 1 8h	Analyte	2.72	50210.266	1333.655	94121.542	8248.74	
Rat 1 24h	Analyte	2.71	43642.113	1777.698	61374.476	5432.83	
1000 nM QC1	QC	2.72	1174.040	148.417	19776.036	1855.79	85.6
Rat 2 0h	Analyte	2.71	45173.891	3394.542	33269.504	3016.09	
Rat 2 1h	Analyte	2.71	5824.710	199.976	72817.613	6416.82	
Rat 2 2h	Analyte	2.71	50162.543	1068.070	117413.987	10251.65	
Rat 2 4h	Analyte	2.71	25578.713	539.688	118488.428	10344.04	
Rat 2 6h	Analyte	2.71	97755.125	1506.169	162257.896	14107.77	
Rat 2 8h	Analyte	2.71	116367.578	826.941	351801.332	30406.55	
Rat 2 24h	Analyte	2.71	62382.969	787.668	197998.932	17181.13	
1000 nM QC2	QC	2.71	3292.253	1154.226	7130.867	768.44	-23.2
Rat 3 0h	Analyte	2.71	26092.148	1031.220	63255.532	5594.58	
Rat 3 1h	Analyte	2.71	22270.252	174.477	319100.111	27594.58	
Rat 3 2h	Analyte	2.71	27845.328	326.259	213368.275	18502.74	
Rat 3 4h	Analyte	2.71	70870.313	464.519	381417.730	32953.26	
Rat 3 6h	Analyte	2.71	53158.145	394.749	336657.883	29104.37	
Rat 3 8h	Analyte	2.71	42807.695	193.420	553299.749	47733.34	
Rat 3 24h	Analyte	2.71	69622.094	1037.620	167744.680	14579.58	
1000 nM QC3	QC	2.71	3666.682	774.984	11828.251	1172.37	17.2
Rat 4 0h	Analyte	2.71	31101.854	879.076	88450.413	7761.08	
Rat 4 1h	Analyte	2.71	27548.291	263.479	261389.817	22632.09	
Rat 4 2h	Analyte	2.71	97139.930	299.608	810558.547	69854.95	
Rat 4 4h	Analyte	2.71	69883.828	469.100	372435.664	32180.89	
Rat 4 6h	Analyte	2.71	74546.523	258.683	720442.810	62105.93	
Rat 4 8h	Analyte	2.71	53058.254	84.046	1578250.422	135868.55	
Rat 4 24h	Analyte	2.71	49006.719	130.805	936636.960	80696.40	
1000 nM QC4	QC	2.71	3664.560	1060.578	8638.120	898.05	-10.2
1000 nM QC5	QC	2.72	1329.464	384.295	8648.720	898.96	-10.1